Human Adenovirus Type 5 E4orf4 Interacts with the Nucleopore Component Nup 205 to Regulate Viral Gene Expression and Replication

Lü, YiQing
B.Sc. Honours Biochemistry

Department of Biochemistry and McGill Cancer Centre
McGill University
Montréal, Québec, Canada

July 2012

A thesis submitted to McGill University in partial fulfillment of
the requirements of the degree of Master of Science

List of Content

Abstract

The Adenovirus type 5 E4orf4 protein (E4orf4) is a multifunctional protein that regulates viral transcription and splicing. Much of the activity of E4orf4 is thought to be mediated through binding of the Protein Phosphatase 2A (PP2A). E4orf4 recruits target phosphoproteins into complexes with PP2A resulting in dephosphorylation of host factors, such as SR splicing factors and the AP-1 transcription factor. However, the full complement of cellular factors that interact with E4orf4, and the molecular mechanisms that E4orf4 utilizes during replication to regulate gene expression remain poorly understood. In the following study, we utilized immunoprecipitation followed by mass spectrometry to identify novel interacting proteins with E4orf4. Interestingly, we identified a nucleoporin, Nup 205, a component of the nuclear pore complex as an interacting partner. We show that the Arginine Rich Motif (ARM) of E4orf4 is required for interaction with Nup 205 and for nuclear localization of E4orf4. ARMs are commonly found on many viral nuclear proteins. Interestingly, we observed that Nup 205 interacts with three different viral nuclear proteins containing ARMs. In each case, viral ARM proteins also bound to the same region on Nup 205. Point mutations of the ARM sequence on each of the three viral proteins resulted in loss of interaction with Nup 205 and loss of nuclear localization of the viral protein. Nup 205 may therefore represent a common cellular target for viruses encoding ARM containing proteins.

We have further tested the role of E4orf4 and Nup 205 in adenovirus replication and gene expression. Previous studies have shown that compared to wild type adenovirus, E4orf4 deficient adenovirus (Orf4$^-$) have elevated E1A and E4orf6 expressions and reduced late protein production. Such effects are phenotypically copied by the loss of Nup 205, where wild type adenovirus infecting H1299 cells with reduced level of Nup 205 also results in elevated E1A and E4orf6 and reduced late protein production. Furthermore, knockdown of Nup 205 resulted in reduced cytopathic effect and a more than four-fold reduction in the replication of wild type adenovirus.

Taken together, these data suggest Nup 205 is required by adenovirus for proper regulation of gene expressions and viral replication, and that interaction with E4orf4 may mediate these effects. Since E4orf4 is known to deregulate phosphorylation of its target proteins, our future studies will focus on identifying phosphorylation sites on Nup 205 and determining the effect of E4orf4 on such sites and nucleopore structure and function.

La protéine E4orf4 de l'adénovirus humain de type 5 interagit avec le facteur Nup 205 du pore nucléaire pour réguler l'expression des gènes viraux et la réplication virale

Résumé

La protéine multifonctionnelle E4orf4 de l'adénovirus de type 5 régule la transcription et l'épissage viral. L'activité de E4orf4 est assurée par son interaction avec la protéine phosphatase 2A (PP2A). Le complexe E4orf4/PP2A déphosphoryle certaines phosphoprotéines, comme le facteur d'épissage SR (riche en arginines et en sérines) et le facteur de transcription AP1. Cependant, les mécanismes de régulation d'expression génique pendant la réplication virale qui sont contrôlés par E4orf4 et ses partenaires restent inconnus. Au cours de cette étude, l'utilisation de la technique d'immunoprécipitation et de spectrométrie de masse nous a permis d'identifier des nouvelles protéines qui interagissent avec E4orf4, en particulier le composé du pore nucléaire Nup 205. Nous avons démontré que le motif riche en arginine (ARM – arginine rich motif), présent dans la protéine E4orf4 et autres protéines nucléaire virales, est nécessaire pour son interaction avec Nup 205 et la translocation nucléaire d' E4orf4. De plus, nous avons constaté qu'il y a trois autres protéines nucléaires virales qui interagissent avec la même région de Nup 205 via leur motif ARM. Des mutations ponctuelles du motif ARM sur ces trois protéines virales abolissent leur interaction avec Nup 205 et leur translocation nucléaire. Ceci suggère que Nup 205 est une cible commune pour les virus comportant des protéines ayant un motif ARM.

Nous avons étudié ensuite le rôle de E4orf4 et Nup 205 dans l'expression génique et la réplication adénovirale. Précédemment, des travaux avaient démontré que, comparés aux adénovirus de type sauvage, les adénovirus privés de la protéine E4orf4 (Orf4-) expriment à des niveaux élevés les protéines virales E1A et E4orf6, mais présentent une faible production des protéines virales tardives. Nous avons observé que la suppression de Nup 205 donne le même effet que celui observé par la perte de E4orf4. Ainsi, l'infection des cellules H1299, présentant une faible expression de Nup 205, par des adénovirus de type sauvages, nous permet d'observer une augmentation du niveau d'expression de E1A et de E4orf6 et une diminution de la production des protéines virales tardives. De plus, la diminution de l'expression de Nup 205 réduit l'effet cytopathique et diminue de plus de quatre fois la réplication de l'adénovirus de type sauvage.

En conclusion, nos résultats démontrent que l'interaction entre Nup 205 et E4orf4 favorise la réplication de l'adénovirus et l'expression des gènes viraux. Comme E4orf4 dérégule la phosphorylation de protéines cibles grâce à son interaction avec PP2A, nos prochaines études porteront sur l'identification des sites de phosphorylation potentiels sur Nup 205, ainsi que sur l'analyse de l'effet de E4orf4 sur chaque site. Nous sommes aussi intéressés par la fonction et la structure du pore nucléaire lorsqu'en complexe avec E4orf4.

Acknowledgement

This thesis summarizes my research work carried out at Professor Jose Teodoro's laboratory as part of my Master's study. Any part of this would have not been possible without the supports from many people and organizations, whether listed below or not, and I want to take this opportunity to express my deepest appreciation to every one of them.

I want to thank Professor Jose Teodoro, an extraordinarily gifted and passionate scientist and extremely kind person for serving as my research supervisor during both my undergraduate and graduate studies at McGill University; it is Joe who lights up my budding interest in biochemistry and molecular biology, and offers me this unique opportunity to pursue biochemistry research since my sophomore year at McGill University. I also want to thank the members of our laboratory, Dr. Wissal El-Assaad, Sarah Assadian, Isabelle Gamache, Michael P. Hell, Thomas Kucharski, Karen Lefebvre, Paul Minshall, Amro Mohammed, Mohamed Moustafa, Pavel Pertchenko, Linda Smolders, Simon Sun, Russell Towers, Jay Yang, Anthony Yu, Dr. Rachid Zagani and Lisa Zhang; it is the courage, loves and countless helps from all of you every day that make me enjoy the every moment I have in our lab. I am honoured to be a colleague of every one of you, and no matter how long this paragraph goes on, I would never be able to express enough my gratefulness.

I also want to thank Professor Phil Branton and members of Phil's laboratory, Drs. Paola Blanchette, Theresa ChiYing Cheng, Frédéric Dallaire, Zarina D'Costa, Timra Gilson, SuiYang Li, Melissa Mui, and Neera Sriskandarajah, as well as Professor Thomas Dobner and members of his laboratory, Drs. Sabrina Schreiner and Peter Wimmer. I shall forever miss the great scientific advices, and the spectacular fun time we have had together during the annual retreats, the DNA Tumour Virus Meeting, and the Friday afternoon fun chats. I am very very touched for all the great helps from Mel, Mel's brother Brennan, Theresa and all of you during the days and nights I spent at the hospital following my terrible accident. Indeed, I can never thank the protein E4orf4 enough for introducing you all as my best friends. My thanks also go to my friend Alexei Gorelik, who helped me a lot with the protein structure and gel filtration studies. I am grateful and honoured to have so many good friends, from Beijing to Montréal, and I owe you all big thanks!

The Résumé was translated by Drs. Tommy Alain, Rachid Zagani and Isabelle Gamache. I am also grateful for the critical readings by Dr. Jose Teodoro, Linda Smolders, Dr. Melissa Mui, Dr. Wissal El-Assaad and Thomas Kucharski.

Along my journey, I also owe special thanks to my middle school math teacher Professor XiYong Wang, to my McGill Professors John Silvius and Timothy E. Kennedy, and to my mentors at McGill Cancer Centre, Drs. Magdalena Maslowska, Tommy Alain, RuiFeng Cao, Bruno Foncecca and Colin Lister. My daily research would have not been possible without the hard work of our support and secretary staff at McGill Cancer Centre and the Biochemistry department, Louis Blais, Leah Donnelly-Singer, Johanne Lamoureux, Christine Laberge, Diana Lee, Raffaele Notarmaso, Duncan Robertson, Anthony Sharpe and Patel Steele; thank you all!

I am grateful and honoured to be the recipients of the following scholarships that support my undergraduate and graduate studies at McGill University – Masters' Scholarships from Canadian Institute of Health Research (CIHR) and Fonds de recherche en santé du Québec (FRSQ), McGill Cancer Centre Undergraduate Summer Research Scholarships, McGill Work Study Funds, Provost and Recruitment awards from Faculty of Medicine, and the Alma Mater Scholarships for International Students from McGill University. The research work carried out in this project is supported by two CIHR operating grants to Professor Jose Teodoro.

I want to thank my family, Professors Kuang JieRen, Lü KuangYi, Liu QingXian, Lü KuangHui and Jerry McBride for providing their unconditional supports from Beijing for my study at Montréal. I am also grateful and honoured to be friends of so many lovely individuals from Beijing to Montréal, and all over the world.

Finally, I want to thank my motherland P. R. China, and the beautiful city that I call my second home, Montréal, Québec, Canada, for welcoming me as an International Student and offering me the marvellous opportunity to pursue my research at its finest institution, McGill University. Scientific research is a collaborative global effort, and I wish some of my work from this thesis will be useful in advancing our understanding of the nature.

Preface

In compliance with the Guidelines concerning Thesis Preparation of the Faculty of Graduate and Postdoctoral Studies of McGill University, although this is not a manuscript based thesis, part of this thesis will eventually be submitted for publications. The author performed all of the work presented in this thesis, with the following exceptions: Dr. Jose Teodoro, my thesis advisor, performed the E4orf4 proteomics profiling and identified Nup 205 as the interacting partner of E4orf4 (Figure II-1 and Table II-1); Dr. Paola Blanchette, Research Associate from Dr. Phil Branton's lab, discovered the effect of E4orf4 on viral gene expression (Figure II-4.1.); Dr. Douglass Forbes, our lab's collaborator, provided us with Nup 205 rabbit polyclonal antibody and Nup 205 cDNA; Dr. Thomas Dobner, our lab and Dr. Phil Branton labs' major collaborator in Germany, provided adenoviruses NOAH and E4orf4^{-}; and Dr. Phil Branton, our lab's major collaborator at McGill University, provided E4orf4 mutant constructs (Figure I-3) and general adenovirus reagents (antibodies), together with his insightful advises on my project.

List of Figures

Introduction

Results

Discussion

List of Tables

Results

Materials and Methods

Appendix I

Appendix II

List of Abbreviations

Abbreviation	Full Name
× g	times gravity
2D	Two-dimensional electrophoresis
aa	Amino Acid
Ab	Antibody
Ad5	Human Adenovirus Type 5
Amino Acid Code	Amino Acids are abbreviated as single or triple letter codes
APC/C	Anaphase Promoting Complex/Cyclosome
ARM	Arginine Rich Motif
BrdU	Bromodeoxyuridine
BSA	Bovine Serum Albumin
c. elegan	Caenorhabditis elegans
CAV	Chicken Anemia Virus
Cdc	Cell Division Cycle
cDNA	complementary DNA
CMV	Cytomegalovirus
Co-IP	Co-Immuno Precipitation
CPE	Cytopathic Effect
Ct	Threshold Cycle Value
D. melanogaster	Drosophila melanogaster
DABCO	1,4-diazabicyclo[2.2.2]octane
DAPI	4’,6-diamidino-2-phenylindole
DBP	72-kDa DNA binding protein (E2A)
ddH2O	Distilled and deionized water
DMEM	Dulbecco's Modification Eagle's Medium
DNA	Deoxyribonucleic Acid
ds/ssDNA	Double/Single-Stranded DNA
DTT	Dithiothreitol
E1A	Early Region 1A, in this research, specifically referring to Adenovirus
E1B	Early Region 1B, in this research, specifically referring to Adenovirus
E2A	Early Region 2A, in this research, specifically referring to Adenovirus
E3	Early Region 3, in this research, specifically referring to Adenovirus
E4	Early Region 4, in this research, specifically referring to Adenovirus
E4orf4	Adenovirus Early Region 4, Open Reading Frame 4
E4orf4 Point Mutants	E4orf4 point mutants are named as Original Amino Acid + Position Number + Mutant Amino Acid
E4orf6	Adenovirus Early Region 6, Open Reading Frame 4

ECL	Enhanced Chemiluminescence
EDTA	Ethylenediaminetetraacetic Acid
FACS	Fluorescent-Activated Cell Sorting
FBS	Fetal Bovine Serum
FFU	Fluorescent Focus Unit (FFU)
FL	Full Length
FLAG	FLAG octapeptide tag
g	grams
G418	Geneticin
GAP	GTPase Activating Protein
GEF	GDP/GTP nucleotide Exchange Factor
GFP	Green Fluorescent Protein
h	Hours
HA	Hemagglutinin
HAdV	Human Adenovirus
His	Histidine
HIV	Human Immunodeficiency Virus
HRP	Horseradish Peroxidase
IgG	Immunoglobulin G
IP	Immunoprecipitation
IPG	Immobilized pH Gradient
kb	kilo bases
KD	Knock Down (by siRNA and shRNA)
kDa	kilo Daltons
L	Litres
LacZ	β-galactosidase
LT	Large T antigen
min	Minutes
MLP	Major Late Promoter
MLP	The Major Late Promoter
MOI	Multiplicity of Infection
mRNA	messenger RNA
Mut	Mutant/Mutation
myc	V-myc myelocytomatosis viral oncogene homolog (avian)
N/C, Nuc/Cyt	Nuclear/Cytoplasmic
N/C-terminal	Amino/Carboxy-terminal
NES	Nuclear Export Signal
NF-κb	Nuclear Factor Kappa-light-chain-enhancer of activated B cells
NLS	Nuclear Localization Signal
NPC	Nuclear Pore Complex

NS	Non-Silencing Control (siRNA and shRNA)
Nup	Nucleoporin
Nup 205	Nuclear pore complex protein Nup 205 (nucleoporin 205kDa)
Nup 205 Truncation Mutants	Nup 205 truncation mutants are named as Position + Length relative to the Full Length
OA	Okadaic Acid
orf	open reading frame
p.i.	Post-Infection
p53	tumor protein 53
PBS	Phosphate Buffered Saline
PCR	Polymerase Chain Reaction
PFU	Plaque Forming Unit
PP2A	Protein Phosphatase 2A
PP2A-B55α	B55α containing form of PP2A
pRb	retinoblastoma tumour suppressor protein
qPCR	quantitative Polymerase Chain Reaction
RNA	Ribonucleic Acid
RNAi	RNA interference
rpm	revolutions per minute
rRNA	ribosomal Ribonucleic Acid
RT-PCR	Reverse Transcription - Polymerase Chain Reaction
S. cerevisiae	Saccharomyces cerevisiae
SCF	SKP1/CUL1/F-box
SDS	Sodium Dodecyl Sulfate
SDS-PAGE	SDS-polyacrylamide Gel Electrophoresis
sec	Seconds
SH3	Src-homology 3
shRNA	small hairpin RNA
siRNA	small interfering RNA
Smad1	Mothers against decapentaplegic homolog 1
TCID50	50% Tissue Culture Infective Dose
TGF-β	Transforming Growth Factor Beta
TPL	Tri-Partite Leader Sequence
Tris-HCl	Tris (hydroxymethyl) aminomethane Hydrochloride
WCE	Whole Cell Extract
WD40	Tryptophan Aspartic acid 40 repeat
WT	Wild Type

Introduction

1. Human adenoviruses.

Adenoviruses are non-enveloped viruses containing double-stranded linear DNA genome. They are a frequent cause for many acute infections of the human upper respiratory tract (URT), enteric and ocular systems [1, 2]. The natural targets of adenoviruses are terminally differentiated and non-dividing epithelial cells. In 1953, they were first isolated by Wallace Rowe and his colleagues from adenoid cell culture, and hence the family of viruses were named Adenoviridae [1]. Although in 1962, Trentin and colleagues have shown that Adenoviruses could transform hamster cells, to date, there has been no evidence that adenoviruses are oncogenic in humans [3].

There are more than 51 serotypes of human adenoviruses identified to date [1]. They are classified into six different species or subgroups, A to F, based on their hemagglutination patterns, oncogenic potential, DNA sequence similarity, etc. [1, 2]. Within each species, they are further sub-divided into different types. Two of the best studied types of human adenoviruses are Type 2 and Type 5, both belonging to Species C [1, 2]. Over the past six decades, adenoviruses have made significant contributions to advancing the field of molecular biology, such as the discovery of messenger RNA splicing, and the applications of adenoviral vectors and adenoviral gene therapy; moreover, adenovirus also serves as the model for virologist to study many other viruses [1]. Over the course of evolution, adenoviruses have adopted to utilize host machinery and pathways to most effectively carry out infection and replication. Therefore, the study of adenoviruses and their host interacting partners will continue to provide insights into molecular and cell biology.

1.1. Adenovirus morphology.

Adenoviruses from all species have similar morphology: icosahedral symmetry, non-enveloped, 60-90nm diameter in size, and 150 MDa in weight [1, 2]. Their structures have been characterized by cryo-electron microscopy [1, 2], and a schematic diagram of the human adenovirus is shown in Figure I-1 [2]. There are at least ten proteins inside the human adenovirus capsid, listed in Figure I-1, and all of which are late structural proteins [1, 2].

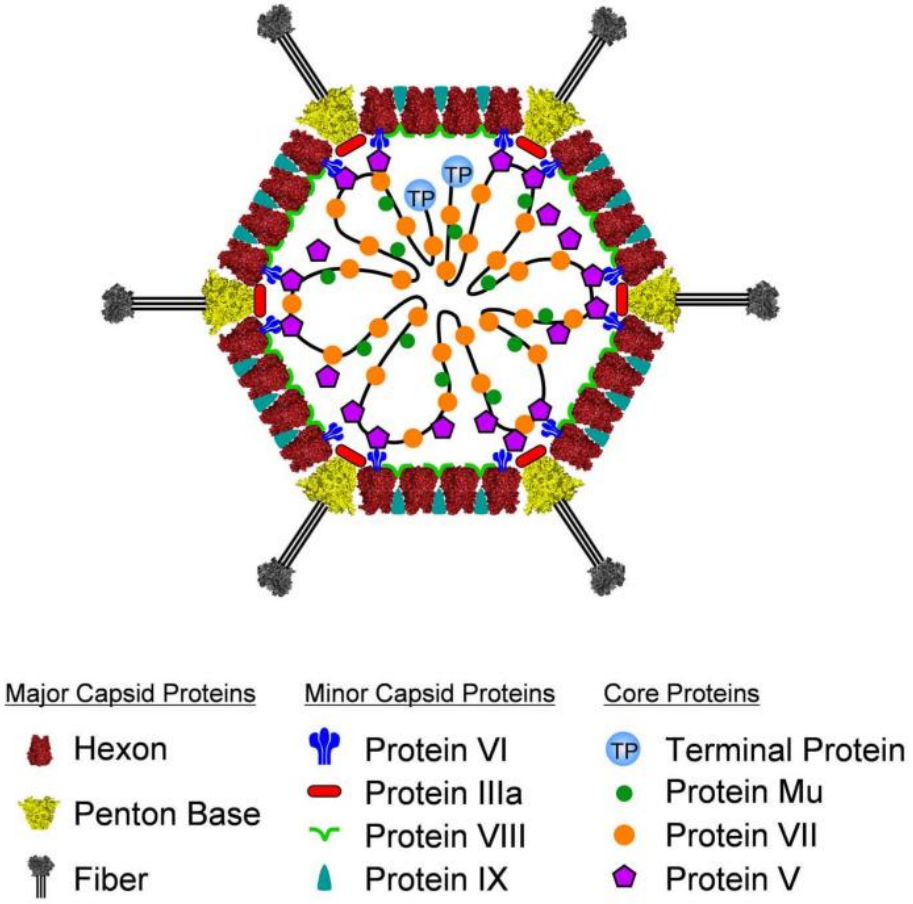

Figure I-1. Schematic diagram of human adenovirus (HAdV) showing the eleven structural proteins in the virion.

The icosahedral capsid of adenovirus is made up of the major capsid proteins, hexon, penton base and the fiber. Minor capsid proteins include pIX, pIIIa, pVI and pVIII. Adapted from [2].

1.2. Adenovirus genome and gene expression.

Adenovirus has a linear, non-segmented and double-stranded DNA genome of 30-38 kbps in size [1]. Upon intake of an adenovirus into the host cell through phagocytosis, the viral genome is uncoated, and the viral DNA enters the host nucleus through the nuclear pore complex [2]. Replication of the adenovirus then occurs in the host nucleus [1].

The genome of adenovirus is arranged in a set of transcription units. Figure I-2 summarizes the transcription units of an adenovirus. These transcription units are further classified as early, delayed early (also known as intermediate) and late regions, depending on the timing at which they are being transcribed. The transcription of early units is before and independent of the viral DNA replication, and it takes place before the transcription of intermediate and late units [1]. There are eight transcriptional promoters and twelve polyadenylation sites on the adenoviral genome. The cellular RNA Polymerase II is used to begin the transcription of viral genome, and the origin of replication is served by the inverted terminal repeats present on each end of the adenoviral genome [1, 2].

There are six early transcription units in adenoviral genome; they are E1A, E1B, E2A, E3 and E4. Three intermediate units are E2 Late, IX and IVa2. Finally, there is only one late transcription unit, and it uses a single promoter termed Major Late Promoter which includes a Tripartite Leader Sequence (TPL) that is present on the mRNAs of all late viral products. Following this single promoter, there are five different polyadenylation sites; through alternative splicing, it is processed into five different late viral mRNAs, L1 to L5 [1, 2]. Products of the early units are largely responsible for regulating the expression of the late products, and it is known that the early product can hijack the host splicing machinery to enhance the alternative splicing of the late viral messengers. A well characterized example is that the early protein E4orf4 can activate the

cellular SR splicing factor proteins by causing its hypo-phosphorylation, and hence enhance the splicing activity of adenoviral late messengers [4].

Adenovirus has evolved a series of sophisticated steps to ensure effective viral replication and gene expression. First, by adenoviral E1A and E4 products, the host cells are induced to enter S phase, which is optimal for viral replication. Second, by actions of adenovirus associated RNA (VA-RNA), which is encoded in the adenoviral genomes, adenovirus can inhibit the activity of the interferon based host-defense system. Finally, by expressing the multifunctional adenoviral E1A protein, adenovirus can effectively induce the activation of all early viral transcription, and hence promote the viral growth cycle (discussed more in detail in Section 1.2.1.).

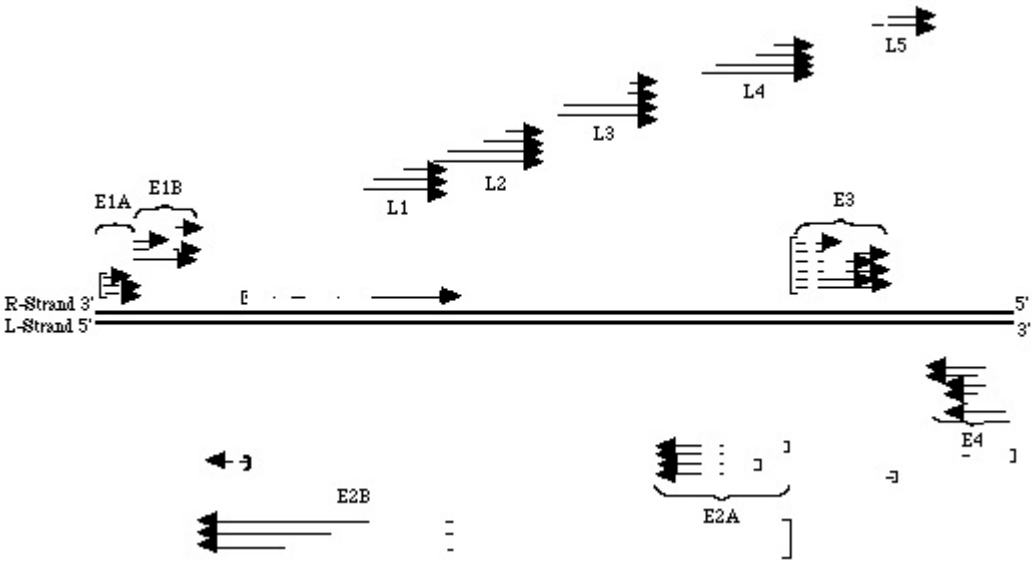

Figure I-2. Transcriptional map of human adenovirus.

The expression of adenoviral genes is controlled at the transcriptional level. Adenovirus genome is divided into multiple transcriptional units as shown in the figure. They are classified into three categories, Early, Intermediate and Late transcription units. Adapted from [1].

1.2.1. The Adenovirus E1A Gene.

The Adenovirus E1A gene, encoded in the adenovirus Early Region 1A (E1A) transcription unit, is the first viral gene to be transcribed upon infection [5]. The transcription of the E1A gene requires only host transcription factors. Through alterative splicing, the primary E1A transcript can yield five distinct mRNAs with sedimentation coefficients of 13S, 12S, 9S, 11S and 10S, with 13S and 12S being the most abundant products. The 12S and 13S mRNAs encode proteins of 243 and 289 amino acids in length, respectively, and they are named 243R and 289R [6-8]. 243R and 289R have the same sequence, except for that a 46 aa region is removed from the 243R due to alternative splicing [6]. Among all serotypes of adenoviruses, there are five highly conserved regions (CRs) within E1A, the N-terminal region, CR1, CR2, CR3 and CR4. While CR1, CR2 and CR4 are all present in the 243R form of E1A, CR3 domain is not [9, 10].

Both 243R and 289R forms of E1A proteins are important transcriptional activators. They can activate the transcription of a variety of both viral and cellular genes in trans [11, 12]. E1A can activate the transcription of all early viral genes. In addition, E1A can also regulate the expression of cellular factors that are required for transcriptional regulation, cell cycle progression, apoptosis, and protein degradation [3, 11-13]. Mutations in E1A gene result in significantly impaired production of other early gene products, reduced synthesis of adenoviral DNA, and ultimately, lowered production of progeny virions [3].

The level and the expression of E1A are tightly regulated. E1A induced transcriptional activation is also targeted by many viral genes to autoregulate their own expressions at the transcriptional level. For example, E4orf4 proteins can negatively regulate the expression of E4 products by inhibiting E1A induced transcriptional activation of the E4 transcription unit [14].

In addition to transcriptional regulation of the expression of viral and host genes, E1A proteins can also induce host cells to enter S phase. Since the natural targets of adenoviruses are non-dividing epithelial cells, by inducing non-dividing cells into S phase, E1A ensures this optimal synthesis environment for adenoviral replication [1]. One of the best characterized mechanisms by which E1A induces cells to enter S phase is that E1A proteins can bind to and hence inhibit the function of the retinoblastoma (Rb) family of transcriptional inhibitor proteins [15-17]. Specifically, the Rb family proteins bind and inhibit the cellular transcription factor, E2F, whose targets include genes that are required for activating viral and cellular DNA synthesis, and cellular genes that are required for cells to enter S-phase of cell cycle. E1A proteins can bind to Rb family proteins, and hence release E2F from the Rb, liberating it to activate transcription of E2F-dependent genes [15-17]. This process also renders E1A oncogenic, and E1A is required for adenoviral transformation of primary rodent cells [3].

1.2.2. The E4 transcription unit.

The Early Region 4 (E4) of human adenovirus encodes seven different polypeptides E4orf1, E4orf2, E4orf3, E4orf3/4, E4orf4, E4orf6 and E4orf6/7. Unlike E1A, the functions of E4 protein products are more heterogeneous. E4 proteins have been shown to be essential for a variety of biological processes, including efficient viral replication, transcriptional control, posttranscriptional modifications, nuclear-cytoplasmic transport of viral late mRNAs, apoptosis, cell cycle control, DNA repair, and inhibition of cellular protein synthesis (termed host shut-off) [18-22]. Among the 51 different known human serotypes of adenoviruses, the E4 transcription units are highly homologous. The E4 regions from the closely related serotypes 2 and 5 (Ad2 and Ad5) have been most widely examined. Among the seven E4 proteins, E4orf3, E4orf4 and E4orf6 are best characterized [1].

The expression of E4 genes are regulated at both transcriptional and post-transcriptional levels. The rate of transcription of the E4 unit peaks at 4 hours post-infection, and it decreases and continues into the late phase of infection [23]. Similar to all other early transcription units, the transcription of E4 genes is activated by E1A protein [24].

The E1A-dependent expression of the E4 transcriptional unit is subject to the feedback regulation of E4 products. Most notably, E4orf4 can down-regulate the expression of E4 genes, including E4orf6 [14, 25]. Specifically, E4orf4 inhibits the E1A-mediated transactivation of E4 promoter through the cellular serine/threonine protein phosphatase 2A (PP2A) [26] (discussed in detail in 1.3.2.2.).

1.2.3. Late gene expression.

More than half of the adenovirus genome encodes late viral products [1]. Unlike early genes, all 18 late adenovirus mRNAs are produced from a single primary transcript, the Major Late Transcription Unit. This transcription unit is sub-divided into five sub-regions, L1 to L5, each defined by a unique polyadenylation site. The transcription is driven by the highly active Major Late Promoter, which becomes fully activated after viral DNA replication, where only minimum activity can be observed in early phase of viral gene expression. All of the 18 mRNAs contain a non-coding 200-nt TPL at their 5' ends. This TPL ensures efficient nuclear export and the translation of late mRNAs [27]; however, the host factors that are required by TPL for this process remain unclear.

Alternative splicing is essential in viral gene expression, and it allows the production of 18 different late viral products encoding mRNAs [1]. Adenovirus has adopted mechanisms to enhance this splicing activity, and one best characterized example is achieved through the early viral product, E4orf4 [4, 14, 26] (discussed in detail in 1.3.2.3.).

The functions of late adenovirus proteins include structural and scaffolding proteins, a protease, and other products required for virus progeny packaging [1].

1.2.4. Host Shut-off.

During an infection, adenovirus has evolved to control cells to preferentially express viral products over most cellular proteins, and this is termed Host Cell Shut-off. This can be observed at post-transcriptional and translational levels. At translational level, viral mRNAs are preferentially translated over cellular products at late stage of infection [28]. One well characterized mechanism at the post-transcriptional processes is by controlling the host to selectively export the newly synthesized late viral mRNAs over cellular messengers, blocking the host mRNAs from entering the cytoplasm. This process is dependent upon the early viral products E1B-55K and E4orf6 [29-32]; however, the host factors that are required for this process, especially the one in the nuclear pore complex and the mRNA export carriers, remain to be identified.

1.2.5. The Cytopathic Effect (CPE).

Following an adenovirus infection, during the synthesis of viral components inside infected host cells, the infected cells undergo observable biochemical and morphological changes – swelling, rounded morphology, and formation of basophilic intra-nuclear inclusions. These cellular changes induced by adenovirus are termed cellular cytopathic effect [33].

1.3. The Adenovirus E4orf4 protein.

Adenovirus Early Region 4 Open Reading Frame 4 (E4orf4) protein is one of the seven proteins encoded in E4 transcription unit. It is a small multifunctional protein best known for its ability to induce p53 independent and tumour cell specific killing [34-36] .

In the context of viral infection, most of the functions associated with E4orf4 have been concluded through the use of an adenovirus that lacks the expression of E4orf4 (E4orf4$^-$ virus). Though not absolutely required for viral growth, E4orf4 is known to regulate adenoviral gene expression by enhancing viral transcription and splicing activities [4, 14, 26, 37]; however, its role in viral replication remain controversial [37, 38].

1.3.1. The structure of E4orf4 and Arginine Rich Motif (ARM).

E4orf4 is conserved among all six subtypes and fifty-one serotypes of human adenoviruses. The sequences of E4orf4 show considerable homology, and they differ only in the carboxy-terminus [35]. Among all six subtypes of adenoviruses, the best studied homologue of E4orf4 is from the Subgroup C [35]. In Ad2 and Ad5, E4orf4 is a 114 amino acids protein with no homology to eukaryotic proteins. Despite its small size, its structure remains unsolved; due to its high solubility, multiple attempts have failed in obtaining a structure by using both crystallization and NMR (personal communication with Drs. Jose Teodoro and Phil Branton). Deletion of regions on E4orf4 often render the mutants unstable and unfunctional, which suggests that E4orf4 may have very well defined tertiary and quaternary confirmations that are crucial for its functions [35]. Meanwhile, through extensive mutagenesis study, Dr. Branton's lab has generated a series of point-mutants along the full length of E4orf4 and identified many regions on E4orf4 that are required for function [35].

At the N terminus of E4orf4, there is a motif of 11 amino acids that is rich in proline, resembling the consensus sequence of SH3-binding site. However, the exact function of this motif remains to be characterized.

From residues 66 to 75, E4orf4 contains a characteristics motif that is rich in arginine, termed Arginine Rich Motif (E4orf4-ARM) [39]. This motif has been previously identified to be required for the nuclear and nucleolar localization, Src-kinase

binding and tumour cell killing functions of E4orf4 [39, 40]. The ARM is common among nuclear localized viral proteins, and its function often includes RNA binding and nuclear targeting of the viral protein. Examples of these viral proteins include Chicken Anemia Virus Apoptin (CAV-Ap) [41, 42], Human Immunodeficiency Virus (HIV) Tat [43] and Rev [44, 45]; each of these viral proteins contains an ARM and normally localizes to the nucleus. Differing from the conventional Nuclear Localization Signal (NLS), ARM contains preferentially arginine over lysine. Illustrated in Figure I-2.4. in the Results section, it compares the ARMs in Apoptin, Tat and Rev to the conventional NLS found in SV40-Large T antigen. Despite the ubiquitous nature of ARMs among these viral proteins, little is known regarding the molecular mechanisms mediating the nuclear import of ARM-containing proteins or why viruses have evolved to exploit ARMs over other nuclear localization signals.

1.3.2. The function of E4orf4.

Most of the studies of E4orf4 focus on its ability in causing p53-independent tumour cells specific destruction [36, 46, 47]; such studies were often conducted in the absence of other viral products, and hence outside of a viral context. In a viral context, relatively little is known about the function of E4orf4, and most of which was obtained through early studies; most notably, E4orf4 is involved in the regulation of transcription, splicing, and signal transduction (reviewed in [48, 49]).

When expressed alone, directed by the E4orf4-ARM, E4orf4 localizes predominately into the nucleus; however, significant amount of E4orf4 can also be detected in the cytoplasm later following expression [39, 50], and this is believed to be achieved through passive diffusion [39]. The localization of E4orf4 is believed to be important for the function of E4orf4 during a lytic infection and the E4orf4-induced cell killing [37, 39].

E4orf4 has no enzymatic activity, and almost all of its functions depend upon the activity of the cellular serine/threonine protein phosphatase 2A (PP2A) [26, 35, 37, 51-56]. Specifically, E4orf4 can bind to the regulatory subunit, Bα, of PP2A, while it recruits target phosphoproteins into complexes with PP2A resulting in dephosphorylation of these host factors [4, 26, 35, 51, 52, 55-57].

1.3.2.1. E4orf4 mediated cell killing and cell cycle arrest.

When expressed alone, E4orf4 is sufficient to induce p53-independent death in a wide range of cancer cells, and this killing is dependent upon the activity of PP2A [34-36, 56, 58]. In both mammalian cells and *S. cerevisiae*, E4orf4-expressing cells became arrested in G_2/M [54, 59], and a significant amount of them became tetraploid and polyploidy [54]. Although the precise mechanism of E4orf4-dependent killing remains to be identified, it is believed that E4orf4 exerts its toxicity by inducing mitotic catastrophe in infected cells [54]. Specifically, E4orf4 can interact with the cellular Anaphase Promoting Complex/Cyclosome (APC/C), an important protein complex responsible for the mitotic progression; it is believed that by recruiting PP2A into complex with APC/C, E4orf4 can induce the premature activation of the APC/C^{cdc20} form of the APC/C complex, and arrest cells at G_2/M stage [54, 59, 60].

1.3.2.2. E4orf4 and transcription.

One of the first biological functions of E4orf4 identified was that it can antagonize the transcription activity of cellular AP-1 transcription factor [57]. Adenovirus E1A and the cellular cyclic-adenosine monophosphate (cAMP) can together induce the transcription of JunB and c-Fos genes, which are the two components that form the AP-1 transcription factor [61]. Upon formation, AP-1 can then bind to the E1A-inducible viral promoters of early viral genes, and activate the transcription of these viral genes [61].

E4orf4 can both inhibit the transcription of c-Fos and JunB [26], and the translation of c-Fos, resulting in reduced AP-1 formation that has been stimulated by E1A and cAMP [57]. Meanwhile, the phosphorylation state of AP-1 complex can also affect its transcription activity [57]. By forming a complex with PP2A, E4orf4 can induce hypophosphorylation of both c-Fos and the 289R form of E1A, and hence it antagonizes the AP-1 activity [57]. Furthermore, since the phosphorylation of E1A by mitogen-activated protein kinase (MAPK) can specifically activate E4 promoter [25], by dephosphorylating E1A via PP2A, E4orf4 can down-regulate the E4 promoter activity, and hence negatively feedback regulate its own expression [57]. Finally, a later study demonstrated that E4orf4 can also down-regulate the transcription of the cellular c-Myc transcription factor, and this down-regulation is PP2A-dependent [55].

Similarly, E4orf4 has been demonstrated to down-regulate the E2 transcription by inhibiting the E1A transactivation of the E2 promoter as well as the E2F-1/DP-1 mediated activation of the E2 promoter [62]. The viral E2 promoter contains a binding site for E2F, which can be activated by heterodimers of E2F-1/DP-1. By inhibiting the E2F-1/DP-1 mediated transactivation of E2 promoter, E4orf4 inhibits the expression of E2 genes [62]. Similar to other E4orf4 related functions, this inhibition is dependent upon the activity of PP2A; the inhibitory effect can be effectively abolished through the addition of Okadaic Acid, a potent PP2A inhibitor [62]. E2 transcription unit encodes viral genes that are involved in viral DNA replication, including DNA Binding Protein (DBP), AdPol and pTP; the expression of E4orf4 results in reduced cytoplasmic mRNA of both DBP and pTP, and a decrease in protein levels of DBP, AdPol, and pTP [63].

Finally, an early study has also demonstrated that E4orf4 can inhibit viral DNA synthesis. It was observed that virus lacking the expression of E4orf4 can effectively replicate its DNA, whereas a mutant virus expressing E4orf4 as the only E4 product was defective in viral DNA synthesis [64]. Such defect in DNA synthesis can potentially be

explained by the reduced expression of E2 genes that are required for viral DNA replication [63].

Taken together, E4orf4 plays a negative role in viral and cellular gene expression, and such negative feedback effects are believed to contribute to efficient virus infection [55].

1.3.2.3. E4orf4 and splicing.

In addition to transcriptional regulation, the E4orf4-PP2A complex can also regulate post-transcriptional processes [18, 65, 66]. In particular, E4orf4 can enhance the alternative splicing and the production of late viral mRNA L1-IIIa, hence temporally shifting the viral gene expression from early to late phase [18]. During early phase of an adenovirus infection, the alternative splicing of the L1-IIIa pre-mRNA is repressed by the cellular SR (serine/arginine) splicing factors, which bind to the 3RE intronic repressor element at the IIIa 3' splicing site; as a result, L1-52,55K is the only form of L1 messenger produced at early phase. The IIIa form of L1 messenger is unique to the late phase, and it is only produced upon removal of the SR factors from the 3RE. E4orf4 can specifically interact with the hyperphosphorylated forms of two subsets of SR proteins, SF2/ASF and SRp30c [4]. By targeting hyperphosphorylated SR proteins into complex with PP2A, E4orf4 causes the hypophosphorylation of SF2/ASF and SRp30c, and hence reduces their repressing effect by releasing them from the binding with 3RE element [4]. As a consequence, the E4orf4-PP2A complex allows the splicing of the IIIa-pre-mRNA, entering the late phase of viral gene expression [4, 66].

Taken together, E4orf4 can function as a viral signal in controlling the temporal switch from early to late viral gene expression [18, 65, 66].

1.3.3. E4orf4 interacting partners.

Viral proteins often carry out their function via interacting with multiple host factors. Given the wide range of functions associated with E4orf4, it is believed that E4orf4 can also interact with a wide range of host factors. As reviewed above, one of the first discovered host factors is the Bα subunit of PP2A, and most of the known functions of E4orf4, including cell killing, seem to be dependent upon both the interaction with and the phosphatase activity of PP2A [4, 26, 35, 51, 52, 55-57]. Another major interacting partner of E4orf4 is c-Src, a proto-oncogene tyrosine kinase, and this interaction is believed to be required for the cytoplasmic killing pathway activated by E4orf4 [67]. Other studies have also identified AP-1 and ASF/SF2 splicing factors [4, 14, 26], as discussed above in 1.3.2.2. and 1.3.2.3.; moreover, a recent study has identified the ACF chromatin-remodeling factor as another interacting partner of E4orf4 [51]. However, the full complement of host factors that interact with E4orf4, together with the molecular pathways that E4orf4 utilizes during adenovirus replication and gene expression remain to be elucidated.

2. Protein Phosphatase 2A (PP2A).

The Protein Phosphatase 2A (PP2A) is a major cellular serine/threonine phosphatase. PP2A has broad substrate specificity and diverse cellular functions [68-70]. In mammalian cells, the PP2A holoenzyme consists of a heterodimeric core enzyme; it consists of the A scaffolding subunit and the C catalytic subunit, and a variable regulatory subunit, B. There are four classes of regulatory subunits, B (B55, PR55), B' (B56 or PR61), B" (PR72), and B"' (PR93/PR110/SG2NA/Striatin) [71, 72]. These four classes can be further divided into 16 members, and the B class of regulatory subunit has four different members, Bα, Bβ, Bγ, and Bδ, and all of which have the size of 55 KDa [73]. Specifically, Bα isoform is required for the interaction with E4orf4 [34]. The variety of

regulatory B subunits enables the substrate specificity as well as the spatial and temporal functions of PP2A [71, 72].

Okadaic Acid (OA) is a potent natural inhibitor of PP2A. Although the exact mechanism remain unclear, Okadaic Acid is shown to specifically inhibit the Protein Phosphatase 1 (PP1) and PP2A [74]. In nearly all identified functions of E4orf4, the addition of OA will abolish the effects, indicating such functions are dependent upon PP2A [4, 26, 35, 51, 52, 55-57].

2.1. E4orf4 and PP2A.

The link between E4orf4 and PP2A was first discovered in a study to identify interacting partners of E4orf4. The Bα subunit of the PP2A holoenzyme complex was shown to co-immunoprecipitate with E4orf4. Interestingly, via Bα, E4orf4 brings down the functional PP2A holoenzyme complex that exhibits the phosphatase activity; besides Bα, this immunoprecipitated complex is found to also includes the A and C subunits [26].

To date, nearly all identified functions of E4orf4, including cell killing, seem to be dependent upon both the interaction with and the phosphatase activity of PP2A. One of the most common mechanisms identified is that E4orf4 can recruit target phosphoproteins into complex with PP2A; this results in the hypophosphorylation of the target protein, which are often host regulatory factors whose activities depend largely upon their phosphorylation states [4, 26, 35, 51, 52, 55-57]. This mechanism is summarized in Figure I-4. Despite the availability of the crystal structure of PP2A, the exact mechanism and regions that are required for the interaction between E4orf4 and PP2A remain unclear.

Through extensive mutational analysis, the correlation between E4orf4 functionality and the PP2A-Bα binding has been studied in the context of the E4orf4-induced cell death [35]. By generating point mutants along the full length of E4orf4, Marcellus *et al*

categorized different E4orf4 mutants into two classes. Class I mutants have reduced ability in interacting with PP2A-Bα, and they are also highly defective in inducing cell killings. Meanwhile, Class II mutants can bind to PP2A-Bα as wild type E4orf4, but their killing abilities are greatly defective [35]. Therefore, it is believed that PP2A alone may not be sufficient in causing the E4orf4-induced cytotoxicity. The series of point mutants generated in this study are used in our study to identify regions on E4orf4 that are required for interaction with other partners. Figure I-3 summarizes the mutants generated in this study [35]. Mutants highlighted in red are later used in our study.

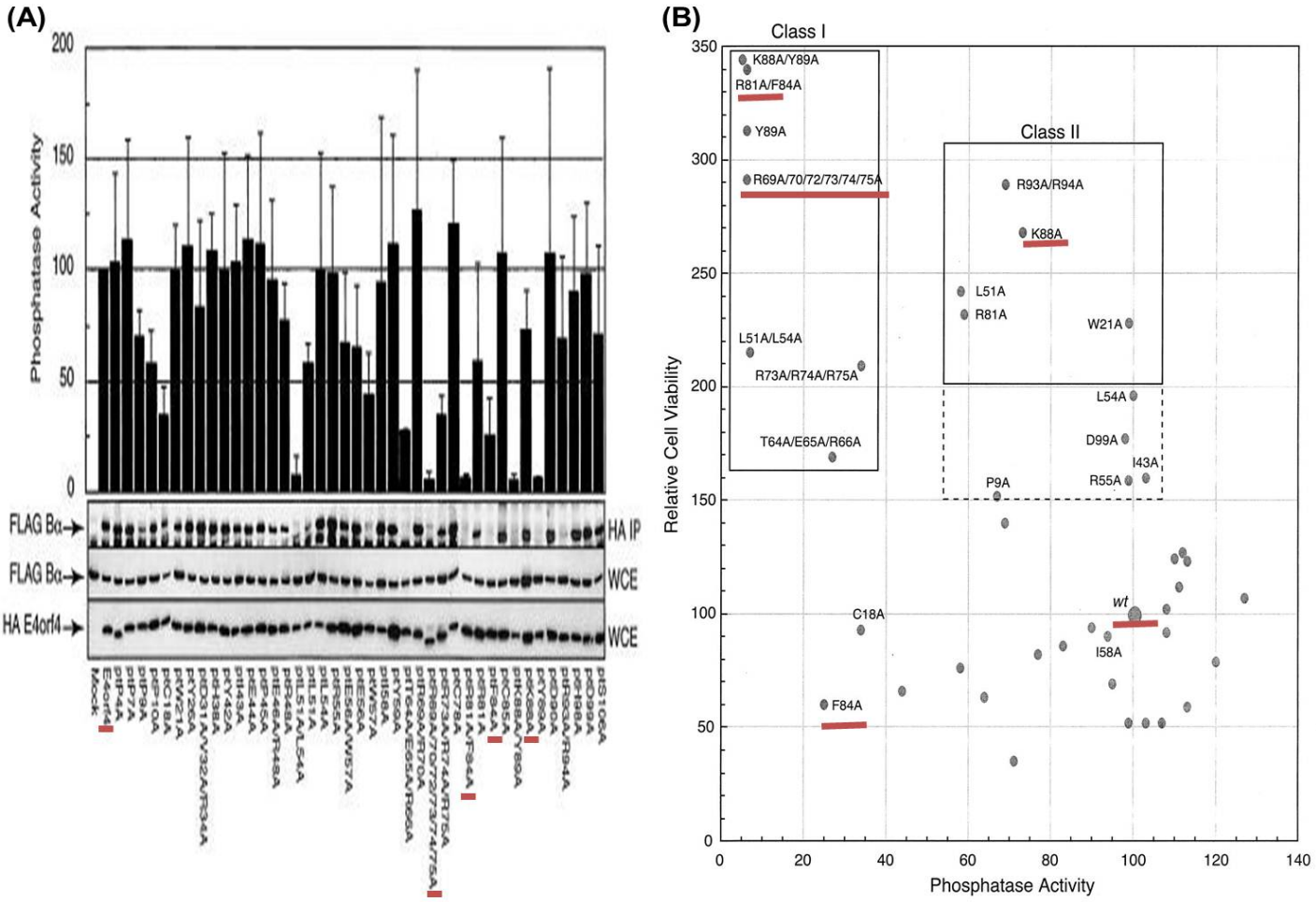

Figure I-3. Correlations among E4orf4-PP2A binding, E4orf4-PP2A Phosphatase Activity and E4orf4 killing.

(A) Analysis of Bα-subunit binding and associated phosphatase activity of E4orf4 mutants. The interactions between PP2A and the mutant forms of E4orf4 were examined using co-immunoprecipitations by co-transfecting Flag-tagged PP2A-Bα and HA-tagged E4orf4s. Red-underlined E4orf4 mutants correspond to the ones in. (B) Analysis of cell killing versus associated phosphatase activity for E4orf4 mutants. Red-underlined mutants were chosen to test their binding to Nup 205 because of their distinct phenotypes shown in this three-way correlation study. Both (A) and (B) panels were modified from published figures in [35] with the publisher's permission (Appendix II).

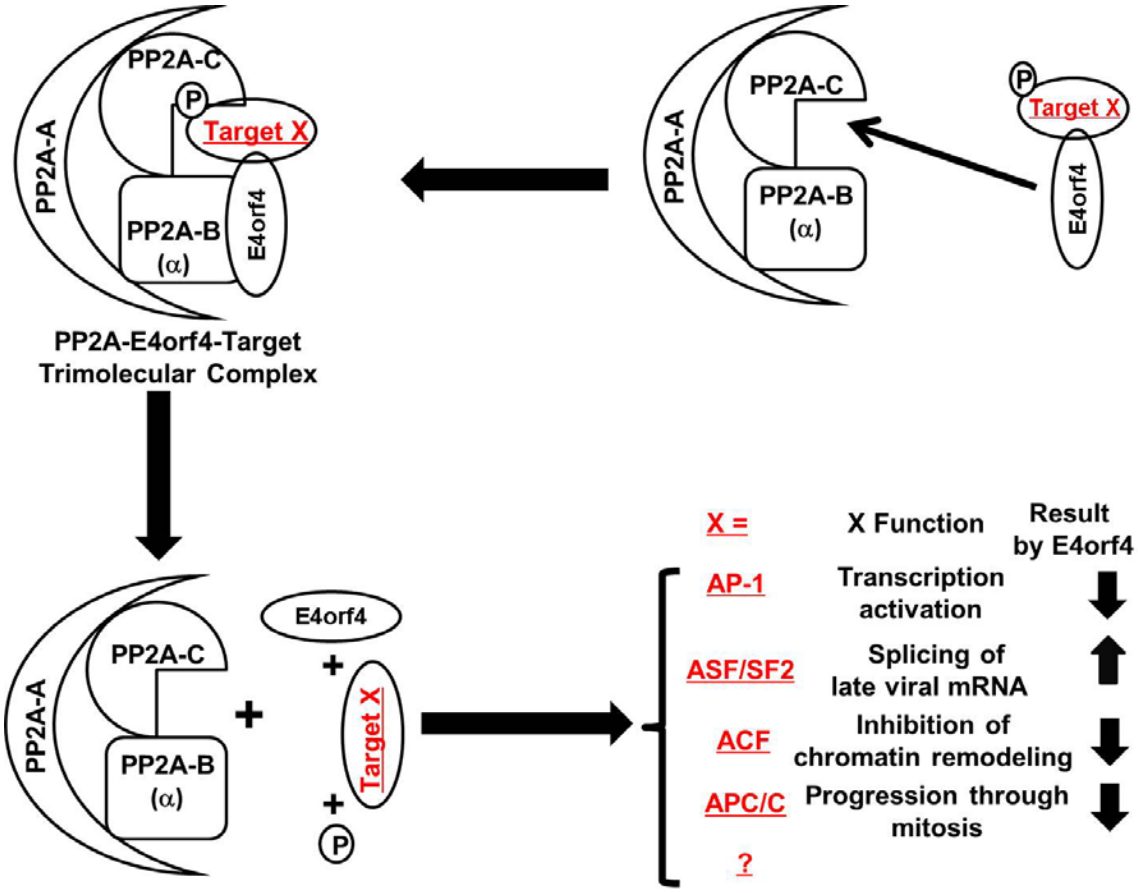

Figure I-4. The mechanism of E4orf4-PP2A complex.

Nearly all of the identified activities of E4orf4 are believed to be mediated through the Protein Phosphatase 2A (PP2A). E4orf4 can interact with the Bα regulatory subunit of PP2A; meanwhile, it also recruits target (shown as Target X) phosphoproteins into complexes with PP2A, forming PP2A-E4orf4-Target trimolecular complex. This results in dephosphorylation of the host factors, such as SR splicing factors and the AP-1 transcription factor.

2.2. PP2A and cell cycle regulation.

The cell cycle is tightly regulated by a series of concerted events. Protein kinases and phosphatases play important roles in cell cycle regulation. Specifically, the entry into one phase of the cell cycle is often triggered by the phosphorylation of regulatory proteins, such as cyclins, and this has to be reversed to facilitate cells to enter the next phase of cell cycle [75].

Given its broad substrate specificity, PP2A is therefore believed to be involved in a wide range of regulations of the cell cycle. One of them is that PP2A can negatively regulate the entry into mitosis. Specifically, PP2A can maintain the hypophosphorylated and thus inactivated precursor form of the Mitosis Promoting Factor (MPF), a Cdk1-Cyclin B protein kinase complex required for the G_2 to M transition (reviewed in [76]).

Besides regulating cyclins, phosphorylation is also involved in other cellular events that are essential for proper cell cycle progression. For example, the disassembly of the nuclear envelope is a crucial step for the entry into mitosis, and this process is largely regulated by phosphorylation. Meanwhile, to exit mitosis, phosphatases are required to dephosphorylate the nuclear pore complex, facilitating the reassembly process of the nuclear envelope (reviewed in [77]). Although certain kinases have been identified [78], very little is known about the specific phosphatases that are required for these processes.

3. The nuclear pore complex (NPC).

Every eukaryotic cell has two distinct but connected cellular compartments, the nucleus and cytoplasm. This compartmentalization allows both spatial and temporal separations of transcriptional and translational activities, resulting in complex and fine-tuned regulations which cannot be achieved in prokaryotic cells. The physical barrier

that separates these two compartments is termed the Nuclear Envelope (NE), a membrane system consisting of two lipid bi-layer membranes, the Outer Nuclear Membrane (ONM) and the Inner Nuclear Membrane (INM). Spanning the nucleus nearly in parallel, these two membranes encircle the nucleus (reviewed in [79]).

Along the nuclear envelop, there are numerous places where the ONM and INM fuse together, forming the ~100 nm diameter porous structures, termed the Nuclear Pores (NPs). Along the Nuclear Envelope, there are millions Nuclear Pores, and these are the sole gateways for all transportation of molecules, including proteins, mRNAs, viral DNA genome and metabolites, between the nucleus and cytoplasm. The macromolecular complexes that occupy the Nuclear Pores are termed the Nuclear Pore Complexes (NPCs). Nuclear Pore Complexes have an estimated mass of 60 million Daltons, and they are the largest protein complexes in an eukaryotic cell (reviewed in [79]).

The individual protein constituents that make up of the macromolecular Nuclear Pore Complex are termed Nucleoporins (Nups). In vertebrate, there have been about thirty Nucleoporins identified to date [80]. Locally, multiple Nucleoporins form sub-complexes, which can maintain a well-defined structure and carry out functions. The Nuclear Pore Complex poses an eightfold symmetrical spoke-like structure (reviewed in [79]). Two-thirds of the thirty Nucloporins are highly conserved through evolution. Most of the thirty Nucleoporin have been mapped within the Nuclear Pore Complexes, yet the detailed function of each Nucleoporin remains unclear [81, 82]. Despite the fact that each Nucleoporin has unique functions and location in the Nuclear Pore Complexes, Nucleoporins within the same sub-complexes function coordinately to maintain the integrity of the Nuclear Pore Complexes and to mediate the trafficking into and out of the nucleus (reviewed in [79]).

Considerable effort has been directed toward identifying the function of sub-complexes and individual Nucleoporins. One of the most extensively studied

sub-complexes, the Nup107-160 sub-complexes, consisting of Nups 107, 133 and 160, have been shown to function early in post-mitotic NPC formation, and to maintain the structure of the NPC [83]. Other sub-complexes, such as the Nup 205-93-188 sub-complex, consisting of Nups 35, 93, 188 and 205 [84-86], has been proposed to be responsible for the nuclear import of cellular proteins such as Smad4 and c-myc [87, 88].

Given the location of NPC, two major functions have been associated with individual Nups, facilitating the transportation of macromolecules, and maintaining the NPC integrity (reviewed in [79]). Recently, the function of nucleoporins has further been associated with gene expression and chromatin organizations (reviewed in [89]), and the overexpression of certain Nups (Nup 88) is considered as a marker for cancer [90].

Figure I-5 illustrated the Nups present in plants, yeast and veterbrates [91].

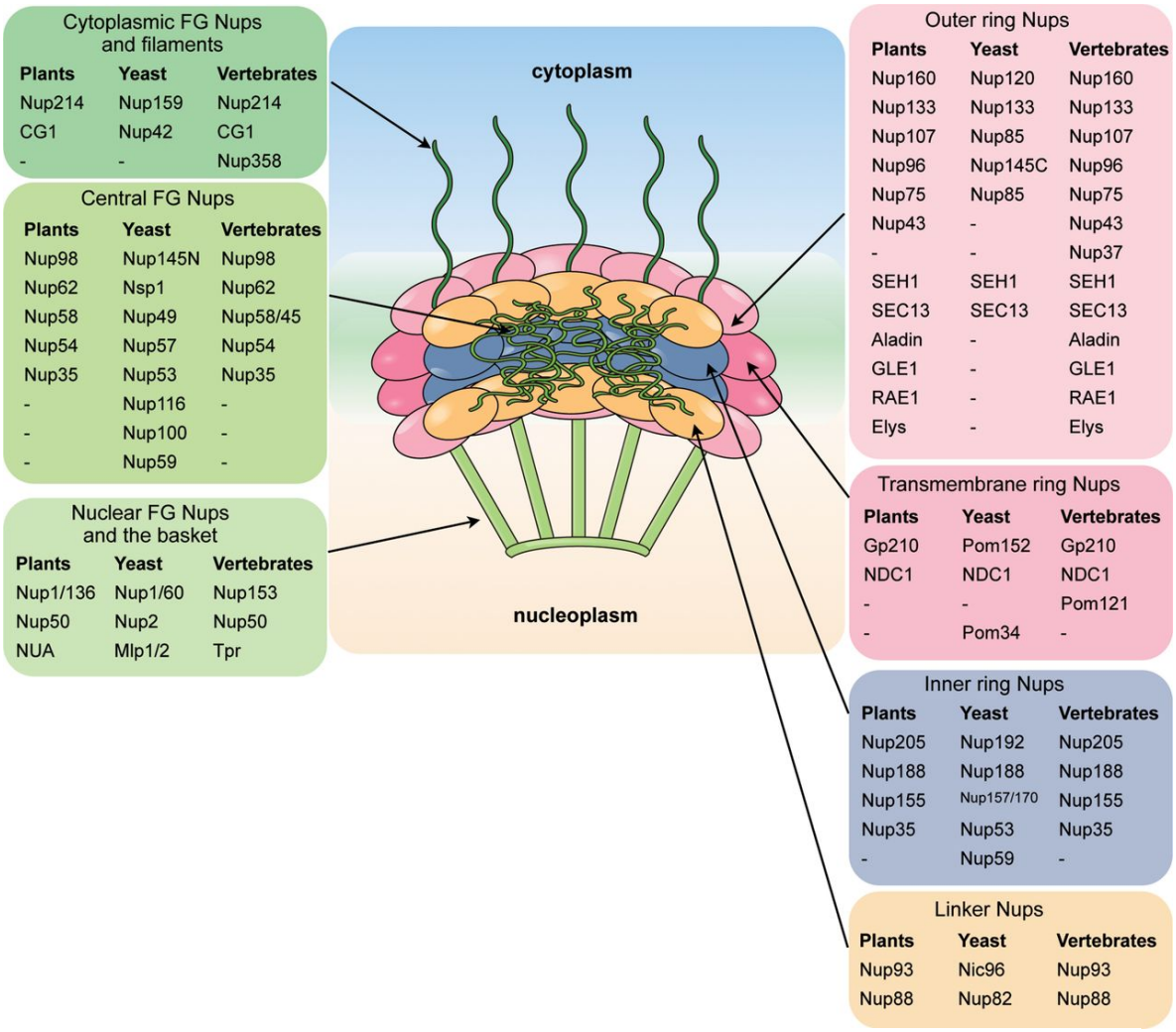

Figure I-5. The Nuclear Pore Complex Structure.

The nucleoporins are divided into seven groups according to their location inside the NPC. Nup 205 locates at the inner ring of the central channel within the NPC, and it is part of the Nup 205-93-188 sub-complexes, which also includes Nup 93, Nup 188 and Nup 35. Nup 205 is highly conserved through evolution. Adapted from [91].

3.1. Nup 205 and its function.

Nup 205 is a member of the Nup 205-93-188 sub-complexes [84-86]. It is a linker protein with a size of 228 KDa (reviewed in [79]). Its position is mapped as in the central channel of the Nuclear Pore Complexes (reviewed in [79]). Nup 205, or Nup 192 in yeast and npp-3 in *C. elegans*, is highly conserved from yeasts to human. The giant size of Nup 205 renders difficulty in determining its structure, and there is no known motif or domain identified. Within the Nup 205-93-188 sub-complexes, Nup 93 can form two distinct and mutually exclusive types of complexes with Nup 205 and Nup 188; however, Nup 205 does not interact with Nup 188 [92].

Proteomic studies using mass-spectrometry have discovered multiple sites along Nup 205 that are subject to phosphorylation and ubiquitination modification [93-95]. Among them, there are 13 serine and threonine phosphorylation sites identified to date [95], and all of them fall into the consensus of mitotic kinases Aurora, Cdk1, NIMA-Like Kinase, and Polo Like Kinase [96].

The exact function of Nup 205 remains unknown. Recent studies have attributed a series of scattered functions to Nup 205. In *Caenorhabditis elegans,* Nup 205 is required for defining the NPC exclusion size [97], and the phosphorylation-dependent removal of Nup 205 from the centrosomes is required for the timely mitosis onset in *C. elegans* embryos [98]; in *Drosophila melanogaster*, it is required for the nuclear import of the transcription factor Smad1 [88]; and a recent study in mammalian cells has implied that a trans-membrane protein, TMEM 209, that interact with Nup 205, is required for the nuclear import of transcription factor c-myc [87]. Depletion of Nup 205 has significant impacts on the host cells: deletion of Nup 205 from *C. elegans* embryo results in impaired nuclear assembly [99]; and knock-out of Nup 205 in yeast is lethal (personal communication, Dr. Richard Wozniak). A recent genome-wide association study also demonstrated that Nup 205, along with Nup 98, is among the many proteins whose

depletion using siRNA reduces the replication ability of Influenza A virus; Nup 205 and Nup 98 are the only two nucleoporins that show effect on the replication [100].

In summary, these initial observations have indicated Nup 205 plays important roles in a wide range of cellular activities, including selective nuclear-cytoplasmic transport of transcription factors, nuclear pore structural integrity, cell cycle regulation, and early embryo development. However, it remains unclear how Nup 205 is regulated to execute these functions.

3.2. NPC and nuclear-cytoplasmic trafficking.

The NPC allows passive diffusion of small and hydrophobic molecules between the nucleus and the cytoplasm. However, highly charged molecules and those that are of 60 KDa or more in size, require carrier proteins, termed Karyopherins, to facilitate targeted delivery of cargos (reviewed in [101]). Nuclear Pore Complexes interact with these soluble transport factors to control the active transportation of macromolecules through their central channels.

In order to be actively transported into the nucleus, macromolecules often harbour specific signals, termed Nuclear Localization Signals (NLSs), which function to direct them for nuclear import through soluble cellular transport receptors, termed Importins. Importin is a heterodimer complex composed of an Importinα and an Importinβ subunits. The NLS on a macromolecule is first recognized by Importinα, which then forms a complex with Importinβ [102]. With energy provided in the form of GTP, the Importinβ–Importinα–cargo complex then translocates the Nuclear Pore through sequential interactions between multiple Nucleoporins [103]. Once the translocated complex reaches the nucleus, RanGTP binds to Importinβ and dissociate it from the cargo, and the cargo is released to the nucleus. Meanwhile, the Importins are recycled back to the cytoplasm to transport other nuclear bound molecules. Certain cargos, however, can

directly interact with Importinβ without first binding to the Importinα. HIV-Rev and Tat are well characterized examples of such cargos [104]. This receptor mediated mechanism enables efficient and cargo specific import of macromolecules into the cell nucleus [105].

The nuclear export activities also occur through the same channel – NPC. Most exported proteins possess the Nuclear Export Signal (NES), which can be recognized by the export factor, Exportins (reviewed in [106, 107]). Similar to the import process, the exporting pathway also depend upon RanGTP. Upon formation of the RanGTP-exportin-cargo complex, the cargo can then be translocated out of the nucleus [107].

NPC can also facilitate the export of RNAs. The majority of mRNAs uses the Nxf1 pathway to export into the nucleus, whereas certain endogenous and viral mRNA also use the Karyopherin Crm1 for cytoplasmic delivery (reviewed in [107]). In particular, unspliced or partially spliced HIV mRNA can be exported through the Crm1 pathway by binding to the HIV-Rev protein [108].

3.3. Mitotic phosphorylation of NPC.

In interphase, the NE is the physical barrier that separates the nucleus and the cytoplasm. The NPC on NE maintains a well-defined structure that allows the selective transport of macromolecules in and out of the nucleus. During mitosis, most eukaryotic cells undergo nuclear envelope breakdown (NEBD). One major and decisive step of the NEBD is the disassembly of the NPCs [109]. This transient event starts early in the prometaphase and ends before anaphase, when NPCs are then promptly reassembled to reform the selection barrier [110].

The NPC disassembly involves the sequential departures of Nups from the NPC, and it is observed both in human cells and starfish oocytes [110, 111]. In mammalian cells, upon entry into mitosis, at prometaphase, Nup 98 is the first nucleoporin to dissociate

from the NPC [112]. Shortly after, the Nup 205-188-93 sub-complexes dissociate from the NPC; this is followed by the departures of the Nup 107-60 and Nup 214 sub-complexes, and finally the POM 121 [109]. Given the transient nature of the NEBD, it is believed that the Nups are not degraded; rather, they are re-distributed to the endoplasmic reticulum (ER) [113, 114].

Although the mechanism governing the disassembly of NPC remains unknown, it is believed to be phosphorylation-dependent [110]. At the onset of mitosis, multiple kinases are active and are required for the entry into mitosis; these include Cdk1, NIMA-related kinase, Polo Like kinase and Aurora-A Kinase [75]. Among them, NIMA-Kinase and Cdk1 are also required for the Nup 98 disassembly from the NPC, as well as the mitotic permeablization of the the NE [78]. Meanwhile, a recent study in *C. elegans* demonstrated that Aurora-A Kinase is required for the removal of Nup 205 from the NPC in the vicinity of the centrosomes at the onset of mitosis [98]. Therefore, it is believed that the mitotic phosphorylation of individual Nups by mitotic kinases signals the departure of Nups from the NPC.

The NEBD is a transient event, and shortly after this presumably phosphorylation-dependent departure of individual Nups, the NPC is promptly reassembled before the anaphase [110]. To reverse the effect of mitotic kinases on individual Nups, the reassembly process requires phosphatase activity. However, to date, no phosphatase has been identified to dephosphorylate the hyperphosphorylated forms of Nups, which contribute to the reassembly of the NPC.

3.4. NPC and virus.

During a lytic infection cycle, adenovirus needs to deliver its DNA genome into the nucleus; meanwhile, the transcribed mRNAs also need to be effectively exported into the cytoplasm. For adenovirus, the NPC is not only a selection barrier that prevents the entry

of viral particles, but it is also a secure layer ensuring the spatial and temporal separation of genetic materials, which is essential for the expression of viral genes.

Earlier study has demonstrated that the NPC can facilitate the entry of adenovirus into the nucleus in multiple ways; it can not only serve as a docking site for uncoating the viral genome from the virus core, but also can it provide the gateway for incoming DNA genome into the nucleus [115]. The cytosolic Nup 214 and Nup 358 are largely involved in this process (reviewed in [116, 117]). However, the involvement of other Nups in the viral DNA import, especially those positioned in the central and nucleoplasmic faces, remains unknown.

Effective nuclear export of mRNAs is essential for the proliferation of viruses replicating in the nucleus [118]. As discussed in Section 1.2.4., the Host Shut-off process depends heavily upon an efficient and intact NPC to export the viral messengers [18-22]. Therefore, to ensure an optimal condition for viral gene expression, it is to the interest of a virus to maintain the NPC intact.

Conversely, certain viral proteins can also induce partial nuclear envelope break down and the transient disassembly of NPC. For example, the HIV-Vpr protein can cause “herniation” in the infected cells nuclear envelope [119]. This results in the mixing of nuclear and cytoplasmic contents, which allows the HIV to deliver its genome packed inside the pre-integration complex, which is otherwise too large to enter the NPC [119]. Nuclear envelope break down is a natural process that occurs early in the Mitosis, and it is believed that HIV-Vpr can induce partial nuclear envelope breakdown by driving the cells to enter Mitosis [119, 120].

Taken together, effective nuclear-cytoplasmic transport is essential during a virus infection. Adenovirus is believed to target these pathways to import its genome and transcription factors that are required for DNA replication; meanwhile, it can also hijack cellular machinery to preferentially and effectively export the viral mRNAs. Although the

exact mechanisms involved in these processes remain largely unknown, existing evidence suggests that NPC plays an important role for adenovirus to regulate the nuclear-cytoplasmic trafficking.

4. Objective and thesis proposal.

Despite the advances made in understanding E4orf4-induced cell killings, the molecular mechanisms that E4orf4 utilizes, especially in a viral context, remain poorly understood. The objective of this study is to identify the cellular factors that interact with E4orf4, and delineate the molecular mechanisms E4orf4 employed during replication to regulate gene expression.

We focused on the interaction between E4orf4 and one of its newly identified host interacting partners, nucleoporin Nup 205. Upon identifying regions on both partners that are required for this interaction, we further examined the impact of this interaction on both the virus and the host. Specifically, we studied the effect of Nup 205 on adenoviral gene expression during replication, and the effect of E4orf4 on the biology of the nucleopore complex, such as the phosphorylation states of Nup 205 and the regulation of its phosphorylation and association with other nucleopore complex proteins. Together with future experiments, this research will elucidate the molecular mechanisms and biological effects of the interaction between E4orf4 and Nup 205, and reveal pathways involved in regulating nuclear-cytoplasmic trafficking and adenoviral gene expression.

Results

1. E4orf4 Interaction Profile.

To identify the host interacting partners of E4orf4, we performed an immunoprecipitation of E4orf4 followed by Mass Spectrometry.

H1299 cells were infected with either adenoviral vector expressing FLAG-tagged E4orf4 (Ad-FLAG-E4orf4) or control β-galactosidase (Ad-LacZ). E4orf4 interacting proteins were immunoprecipitated from cell extracts using a monoclonal FLAG antibody. The results – interacting partners of E4orf4 – are listed in Table II-1.

Among the proteins we identified, the ASF/SF2 splicing factor had previously been shown to interact with E4orf4 [4, 66]. We also identified some novel interacting partners of E4orf4; KIAA 0225, also known as Nup 205, was one of them.

We then confirmed the interaction between Nup 205 and E4orf4 by Western blotting using Nup 205 specific antibody, shown in Figure II-1.

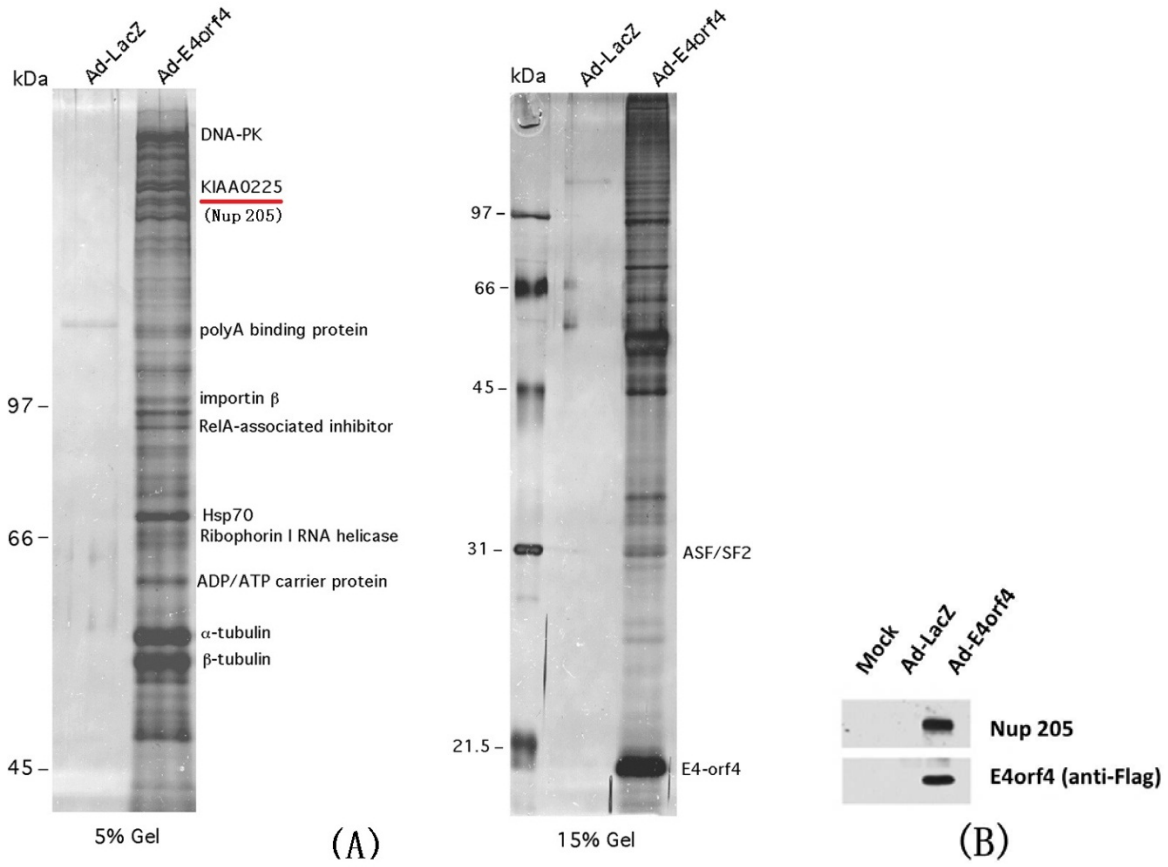

Figure II-1. Interaction profile of E4orf4 interacting proteins in H1299 cells.

(A) Silverstain of SDS-Page gels. H1299 cell extracts were immunoprecipitated with FLAG antibody. E4orf4-specific interacting proteins were subsequently eluted and resolved by 5% (for targets >50kDa) and 15% (for targets <50kDa) SDS-PAGE and stained with $AgNO_3$. The resulting E4orf4 interaction profile was specific and composed of bands of distinct size and intensity, representing putative proteins interacting with E4orf4. (B) Validation of the identity of Nup 205 as an E4orf4 interacting protein. The specific interaction between Nup 205 and E4orf4 was further confirmed by Western blotting using a Nup 205 specific antibody. The expression of Ad-FLAG-E4orf4 was also confirmed using FLAG antibody. This figure was generated by Dr. Jose Teodoro and used here with his permission.

List of Identified Proteins
DNA-PK
KIAA0225 (Nup 205)
PolyA Binding Protein
Importin β
RelA-Associated Inhibitor
Hsp70
Ribophorin I RNA Helicase
ADP/ATP Carrier Protein
α-tubulin
β-tubulin
ASF/SF2

Table II-1. Characterized E4orf4 interacting partners in H1299 cells.

2. The characterization of the interaction between Nup 205 and E4orf4.

2.1. The Arginine Rich Motif is required by E4orf4 for the interaction with Nup 205.

Having discovered Nup 205 as a novel interacting partner of E4orf4, we then studied in detail how these two proteins interact. First, we examined which region on each protein is required for this interaction.

Although the structure of neither protein is known, relative to the 2012 amino acid (aa) size of Nup 205, the 114 aa E4orf4 is much smaller and easier to manipulate. Furthermore, earlier work from the laboratory of Dr. Phil Branton has generated a series of point-mutants along the full length of E4orf4 (alanine walking) as previously described in [35] and shown on Figure I-3 (in introduction); therefore, we first examined which region on E4orf4 is required for interaction with Nup 205.

2.1.1. E4orf4 mutants.

Modified from the original figures published in [35], Figure I-3.A. correlates the affinity of the interaction between PP2A and each E4orf4 mutant, with the enzymatic activity of E4orf4-PP2A complex formed with each E4orf4 mutant. Figure II-3.B. further correlates the phosphatase activity with the cell killing ability, a characteristic of E4orf4 protein. Although there was no known correlation between the affinities of PP2A-E4orf4 binding and Nup 205-E4orf4 binding, we began our search by choosing five E4orf4 mutants, underlined in red in Figure II-3. Specifically, Class I mutants R81A/F84A and R69-75A had severely disrupted interactions with PP2A, and much reduced phosphatase enzymatic activities and cell killing abilities; Class II mutant K88A had its affinity of interaction with PP2A and its phosphatase activity similar to Wild Type E4orf4, but its killing ability was much disrupted; and the outlier F84A had much reduced PP2A binding and phosphatase activity, but had rather increased killing ability.

2.1.2. The ARM is necessary for E4orf4 to interact with Nup 205.

Previous studies have shown that HA epitope tags did not interfere with the biological activities of E4orf4 [35, 121]; in particular, this set of HA-tagged E4orf4 mutants in 2.1.1. have been used to successfully test the interaction between E4orf4 and PP2A-Bα [35]. Therefore, we utilized these HA-tagged E4orf4 point mutants -- Wild Type, R69-75A (ARM mutant), R81A/F84A, F84A, and K88A -- to test their interactions with Nup 205 by co-immunoprecipitation. HA-E4orf4 and p3XFLAG-Nup 205 were co-transfected into H1299 cells, and FLAG-Nup 205 was immunoprecipitated with FLAG-agarose beads from the whole cell lysates. Shown in Figure II-2.1., the expression of Nup 205 and E4orf4 mutants were confirmed in the whole-cell-lysates, but the amount of E4orf4 co-precipitated with Nup 205 was severely reduced for the R69-75A mutant,

suggesting an attenuated binding between this mutant and Nup 205. The R69-75A mutant, also called ARM mutant, was a mutant having all the arginines between residues 69 and 75 mutated to alanines. ARM appears to be an essential region of E4orf4 necessary for interaction with Nup 205 (Figure II-2.1.).

It is noticed that there were also small decreases observed in the interactions between Nup 205 and the other three E4orf4 mutants. Since these mutants were all around the same region on E4orf4 that was ~10 aa away from the ARM region, it is speculated that such mutations might have indirectly affected the interaction with Nup 205 by altering the local folding of E4orf4.

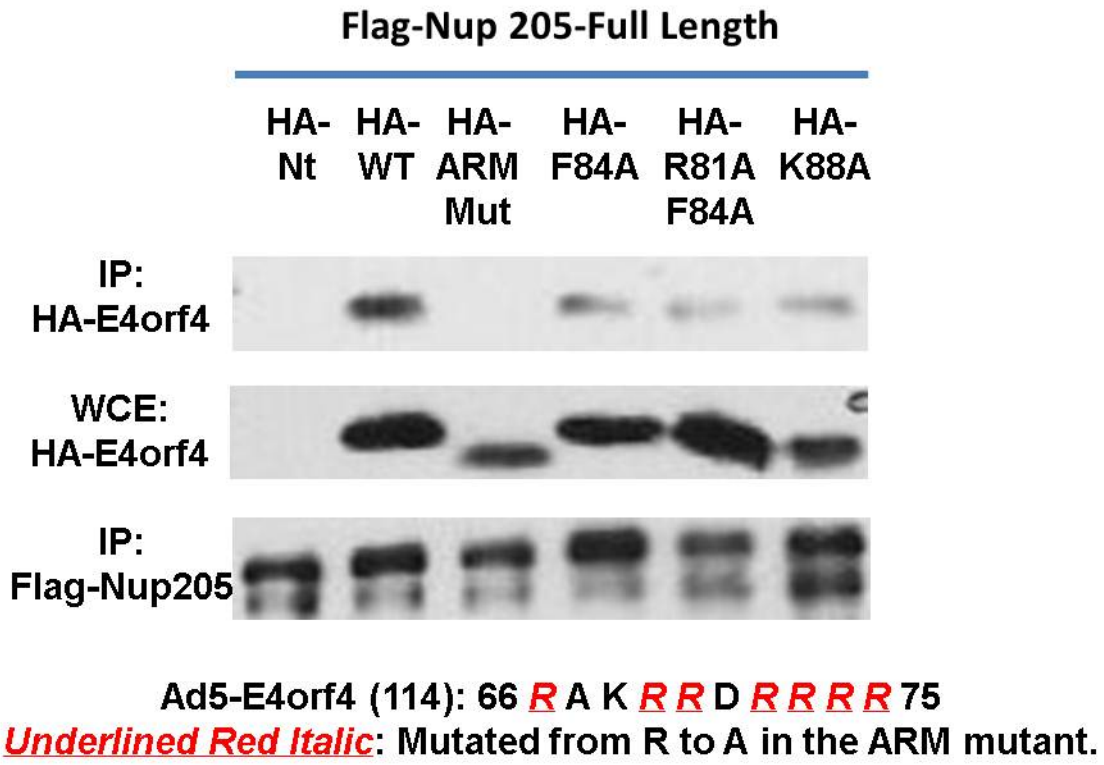

Figure II-2. 1. Analysis of the interactions between Nup 205 and E4orf4 mutants.

H1299 cells were co-transfected with the HA-E4orf4 mutants, together with FLAG-tagged Nup 205. Cell extracts were prepared 42 hours post-lipofection, and anti-FLAG immunoprecipitations were performed. The IP products from each mutant were separated by SDS-PAGE, and the amounts of HA-tagged E4orf4s that came down with Nup 205 were compared by immuno-blotting with an anti-HA antibody. Empty HA vector was used as a negative control to demonstrate the specificity of interaction between E4orf4 and Nup 205. The sequence on E4orf4 that was mutated in its ARM mutant is also listed below, and the mutated residues are red and underlined.

2.1.3. The ARM is sufficient for E4orf4 to interact with Nup 205.

Having identified the ARM motif of E4orf4 as being necessary for E4orf4 to bind Nup 205, we then tested whether this ARM region was sufficient for the binding with Nup 205. To test this, we again utilized constructs made in earlier studies [39, 122] – myc-PK-ARM, the ARM sequence of E4orf4 fused to a myc-tagged Pyruvate Kinase construct, and myc-PK, myc-tagged Pyruvate Kinase without the ARM fusion, which is used as a negative control. This set of myc-PK and myc-PK-E4ORF4-ARM constructs were previously shown to be functional [39, 122]. These two myc-constructs were first co-transfected with p3XFLAG-Nup 205 into H1299 cells, and the FLAG-Nup 205 was immunoprecipitated with FLAG-agarose beads from the whole cell lysates. The expressions of Nup 205 and both myc-PK-ARM and myc-PK was confirmed by immunobloting (Figure II-2.2.). We observed that the ARM fusion alone was enough to co-immunoprecipitated myc-PK with FLAG-tagged Nup 205.

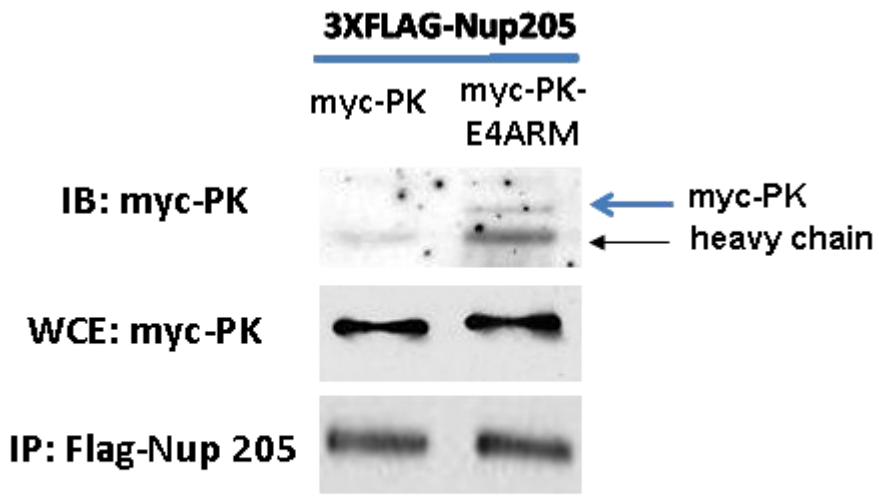

Ad5-E4orf4(114): 66 *R* A K *R R* D *R R R R* 75
***Underlined Red Italic*: the ARM sequence that is fused to myc-PK.**

Figure II-2. 2. Analysis of the interactions between Nup 205 and E4orf4 mutants.

H1299 cells were co-transfected with the myc-tagged Pyruvate Kinase (myc-PK) constructs with or without E4ORF4-ARM fusion, together with FLAG-tagged Nup 205. Cell extracts were prepared 42 hours post-lipofection, and anti-FLAG immunoprecipitations were performed. myc-PK, without the ARM fusion, was used as a negative control to demonstrate the sufficiency of E4ORF4-ARM to bind to Nup 205. The exact sequence of E4ORF4-ARM on E4orf4 is listed below. Note that among the multiple bands in the IB-myc blot, the one identified by the arrow-head is PK [122].

2.2. The Arginine Rich Motif is required for viral protein nuclear localization.

The above result where ARM is necessary and sufficient for E4orf4 to interact with Nup 205 was intriguing because E4orf4 has also been shown to use this same ARM as its Nuclear Localization Sequence (NLS) to localize into the nucleus [39]. The same study also demonstrated that E4orf4-ARM alone was sufficient to function as an NLS to target cargos to localize into the nucleus [39].

Many nuclear-localized viral proteins also contain an ARM. For example, Apoptin (CAV-Ap) from Chicken Anemia Virus, and Tat and Rev from Human Immunodeficiency Virus (HIV) all are nuclear localized viral proteins that contain ARMs.

We then tested if the ARMs in CAV-Ap, Tat and Rev are also required for their nuclear localization. We transfected HeLa cells with each of the GFP-fusion constructs of these viral proteins, and as shown in Figure II-2.3., they all can localize, predominately, into the nucleus. However, upon mutating the arginines to alanines in their ARM regions, their nuclear localization patterns were all severely disrupted, showing significantly increased cytoplasmic staining and reduced nuclear staining. Unlike E4orf4, the ARM mutants of Apoptin, Tat and Rev all had predominant cytoplasmic staining, where the E4orf4-ARM mutant showed equal distribution between the cytoplasm and the nucleus. This observation may be due to the fact that these other three proteins, but not E4orf4, all encode a Nuclear Export Sequence (NES).

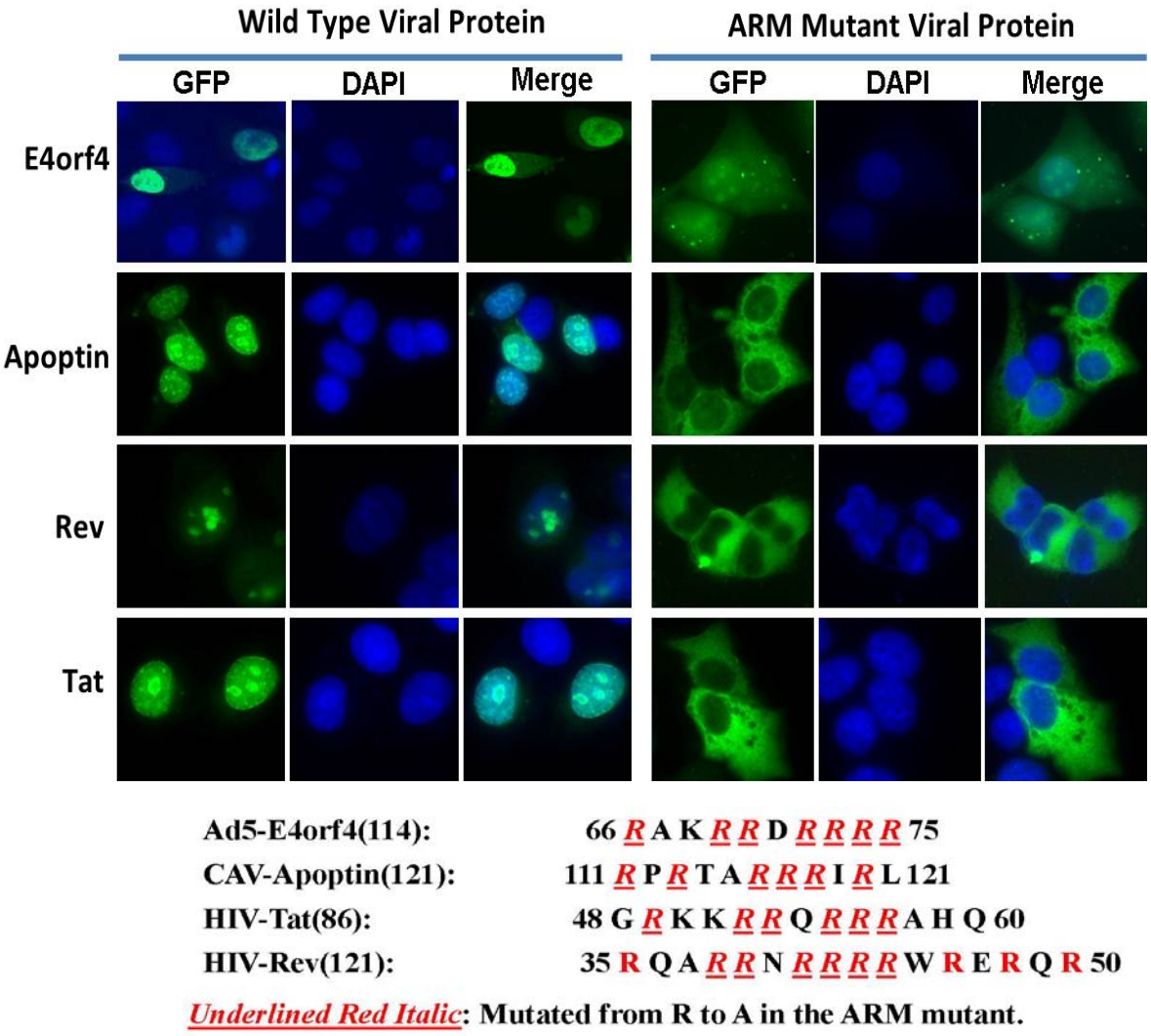

Figure II-2. 3. The requirement of the ARM sequence for the nuclear localization of E4orf4, Apoptin, Tat and Rev.

GFP-fusion constructs of E4orf4, Apoptin, Rev and Tat were generated, together with their ARM region mutants (mutated residues are shown in red, italic and underlined). HeLa cells grown on coverslips were then transfected with each of these GFP-fusion constructs, and fixed and permeablized at 14 hours post-lipofection. They were then stained with DAPI to mark the nucleus, mounted on glass slides and observed using a fluorescence microscope at ×400 magnification.

2.3. The Arginine Rich Motif is also required by Apoptin and Rev for interaction with Nup 205.

Having discovered that the ARM is required for nuclear localization among E4orf4 and other viral proteins we have examined, we further tested whether the interaction with Nup 205 was specific to E4orf4, or if it was also common to these ARM containing proteins.

To test this, we first fused an HA tag to these viral proteins and created mutants by converting the arginines to alanines in the ARM region; the same series of mutants were also fused to EGFP. To determine if Nup 205 interaction was specific to any nuclear localized viral protein or only one that contained an ARM sequence, we also included SV40-Large T antigen, a nuclear localized viral protein that only encodes a conventional/canonical NLS instead of the ARM.

HA-tagged E4orf4, Apoptin and Rev, their ARM mutants and HA-tagged SV40-LT were transfected into H1299 cells, and HA-tagged viral proteins were immunoprecipitated with the HA antibody from whole cell lysates. The interaction between these viral proteins and Nup 205 was evaluated by the amount of endogenous Nup 205 that co-immunoprecipitated with them. As shown in Figure II-2.4., by Western blotting, E4orf4, Apoptin and Rev all brought down Nup 205; however, only the Wild Type form of these viral proteins, but not their ARM-mutants could pull down Nup 205. Furthermore, HA-SV40-LT, which also localized into the nucleus, could not bring down Nup 205.

Note that the main product of SV40-LT was the band at 95kDa, and the other bands detected were Super T, Small T and degradation products. The ARM mutant form of Apoptin was more abundant than its Wild Type version.

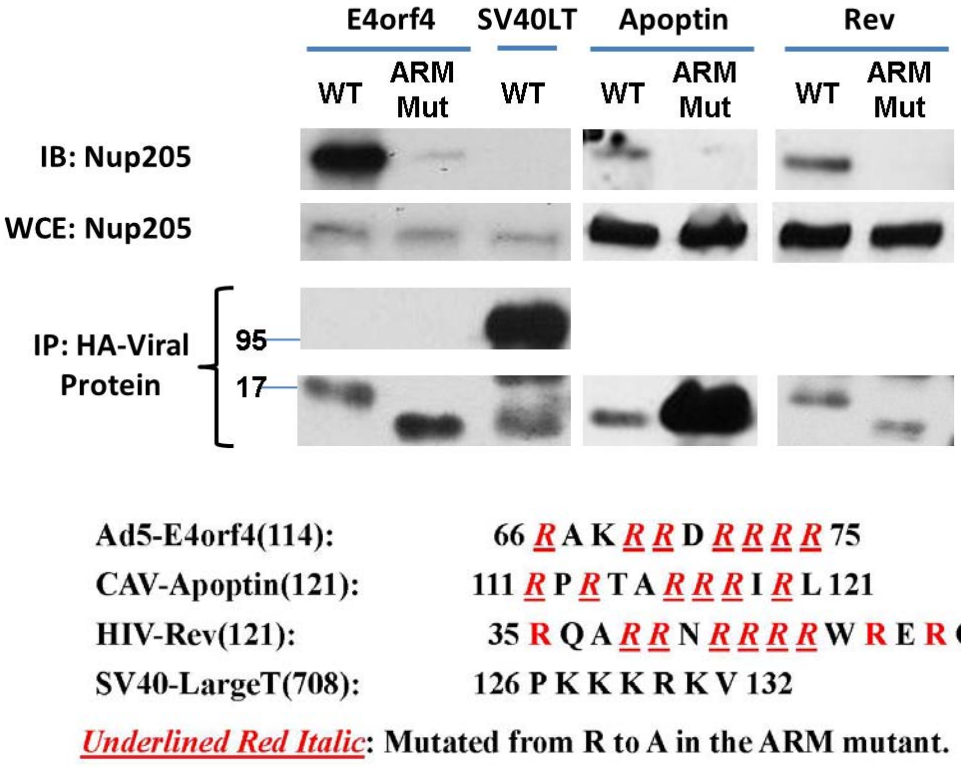

Figure II-2. 4. Analysis of the interactions between Nup 205 and ARM containing viral proteins.

H1299 cells were transfected with HA-tagged E4orf4, Apoptin and Rev, their ARM mutants, and SV40-LT. Cell extracts were prepared 42 hours post-lipofection, and anti-HA immunoprecipitations (IPs) were performed. The IP product from each viral protein was separated by SDS-PAGE with its ARM mutant, and SV40-LT was run beside E4orf4 and its ARM mutant. The level of endogenous Nup 205 that came down with these viral proteins was evaluated by immune-blotting with an anti-Nup 205 antibody. The ARM sequence and its mutant form of each of the viral proteins are also listed below the immuno-blots, and the mutated residues are red, italic and underlined. The NLS on SV40-LT is also listed as a comparison to the ARMs on the other viral proteins.

2.4. The region on Nup 205 required for its interaction with E4orf4.

Having identified a region on E4orf4 that is required for the interaction with Nup 205, we then tested the region on Nup 205 that is required for this interaction. The three-dimensional structure of E4orf4 and Nup 205 have not been determined; furthermore, no obvious domains or motifs have been identified on Nup 205. Therefore, we started by breaking down Nup 205 into two pieces and testing which retained interaction with E4orf4.

FLAG-tagged constructs were generated for each of the Nup 205 truncations, and their interactions with E4orf4 were tested by co-immunoprecipitation. HA-E4orf4 (Wild Type) and p3XFLAG-tagged Nup 205 truncations were co-transfected into H1299 cells, HA-tagged E4orf4 proteins were immunoprecipitated with the HA antibody from whole cell lysates. The IP products were run on SDS-PAGE, and the amount of Nup 205 brought down by HA-E4orf4 was evaluated by immuno-blotting with an anti-FLAG antibody. The piece that retained the interaction with HA-E4orf4 was further broken down into two mutually exclusive pieces, and this above procedure repeated.

Figure II-2.5. shows a schematic of the truncations that we have created and tested for their interactions with Nup 205. B1/4 truncation, the piece located near the N-terminus, and is one-quarter of the original size of Nup 205, is the smallest one we have identified to still bound to E4orf4. Beyond this, we have further broken B1/4 into C1/8 and D1/8, and neither of the two was able to interact with E4orf4 (data not shown). The immuno-blot of Figure II-2.5. is shown in the left panel of Figure II-2.6.

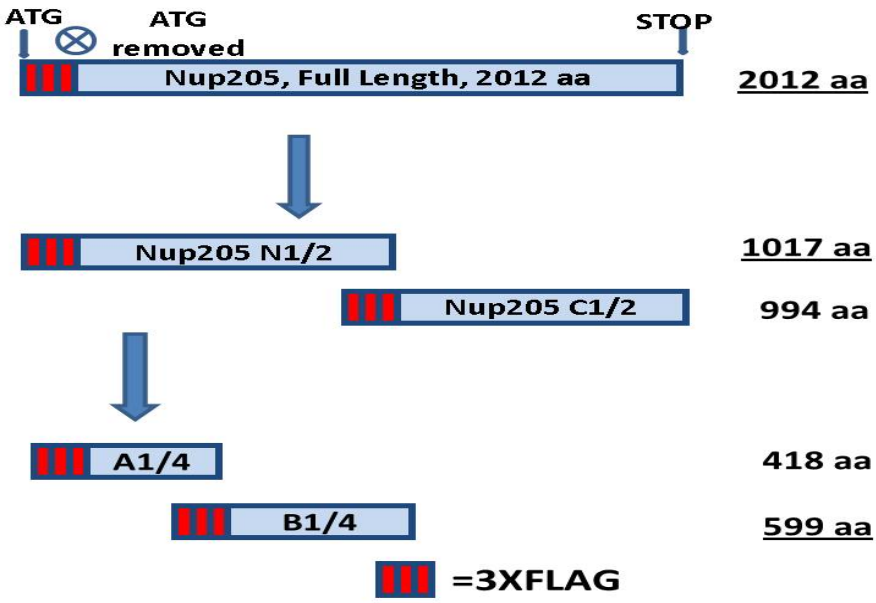

Figure II-2.5. A schematic representation of the analysis of interaction between E4orf4 and different Nup 205 truncations.

Nup 205 and its truncations were each fused with an N-terminal FLAG-tag (3XFLAG) as shown in this schematic drawing. H1299 cells were then co-transfected with FLAG-tagged Nup 205 and its various mutants, together with HA-E4orf4. While maintaining an equal amount of transfected HA-E4orf4, the amount of transfected Nup 205 was adjusted to account for the lower expression level of larger sized Nup 205s (i.e. the amount used in Full Length = 3 Quarter, Half = 1.5 Quarter), but the same amount was used for each of the two pieces that were being compared (i.e. N1/2 = C1/2, A1/4 = B1/4, and Full Length = Empty FLAG). Cell extracts were prepared 42 hours post-lipofection, and anti-HA immunoprecipitations were performed. The IP material from all truncations was separated by SDS-PAGE, and the amounts of FLAG-tagged truncations that came down with HA-E4orf4 were compared by immuno-blotting with an anti-FLAG antibody. Empty FLAG vector was used as a negative control to demonstrate the specificity of interaction between E4orf4 and Nup 205. The immuno-blot of this schematic is shown in the left panel of Figure II-2.6. The length of each fragment is listed, and the pieces that retained the interaction with E4orf4 were underlined.

2.5. The same general region on Nup 205 is required for the interaction with the three ARM-containing viral nuclear proteins.

Having identified the B1/4 region as the one on Nup 205 required for its interaction with E4orf4, we further tested if other viral proteins that interact with Nup 205 would also require this region for the interaction.

To test this, we repeated the previous procedure done for E4orf4 for Apoptin and Rev, and tested their interactions with Nup 205.

The IP products from these experiments were run on SDS-PAGE, and the amount of Nup 205 brought down by HA-E4orf4 was evaluated by immuno-blotting with an anti-FLAG antibody.

As shown on Figure II-2.6., using these FLAG-tagged deletion mutants of Nup 205, we observed that all of these three ARM-containing viral proteins, E4orf4, Apoptin and Rev, bound to the same general region on Nup 205 in the N-terminal region of the protein.

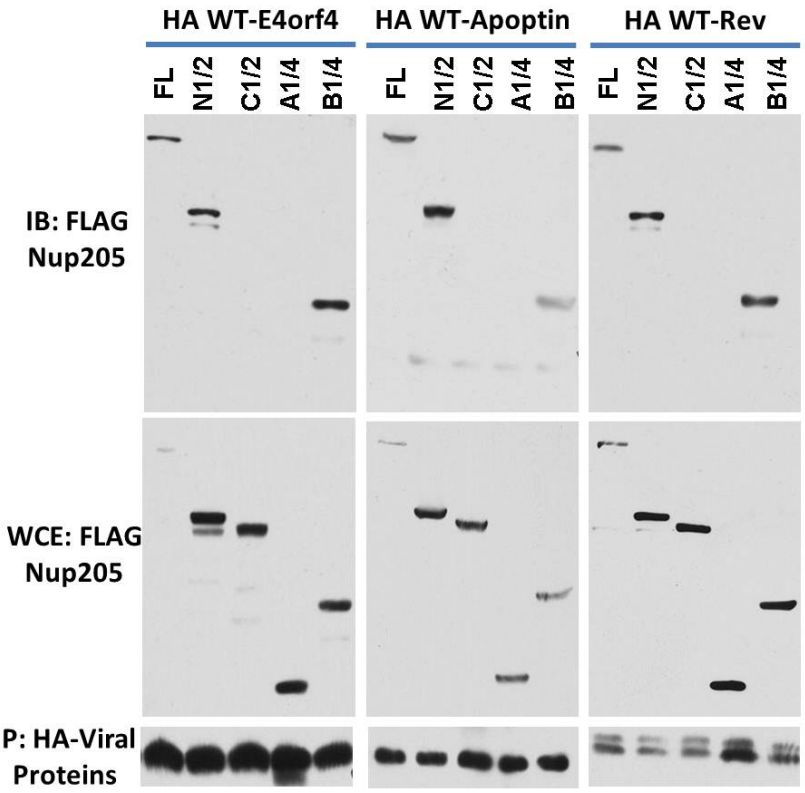

Figure II-2.6. Testing the region on Nup 205 required for its interaction with ARM-containing viral proteins.

H1299 cells were co-transfected with FLAG-tagged Nup 205 and its various mutants, together with one of the three HA-tagged viral proteins, E4orf4, Apoptin and Rev. The amount of transfected Nup 205 was adjusted to account for the lower expression level of larger sized Nup 205 constructs. Cell extracts were prepared 42 hours post-lipofection, and anti-HA immunoprecipitations were performed. The IP products from all truncations were separated by SDS-PAGE, and the amounts of FLAG-tagged truncations that came down with the HA-tagged viral proteins were compared by immuno-blotting with an anti-FLAG antibody. Empty FLAG vector was used as a negative control to demonstrate the specificity of interaction between each viral protein and Nup 205.

2.6. The requirement of Nup 205 for the nuclear localization of ARM-containing viral nuclear proteins.

Having identified that the ARM is required for E4orf4, Apoptin, and Rev to interact with Nup 205 and to localize into the nucleus, we then tested whether the ARM-dependent nuclear localization was dependent upon Nup 205.

To test the requirement of Nup 205, we utilized a commercially available small interfering RNA (siRNA) of Nup 205 to silence its expression. We then used the same set of GFP-fusion Wild Type viral proteins used in Section 2.2., and compared their localization in HeLa cells with or without Nup 205 knocked down. Furthermore, to test the specificity of the requirement of Nup 205 for ARM-related nuclear import, we also generated and included a GFP-fusion of the SV40-Large T protein, which is a nuclear localized protein that uses a canonical NLS.

HeLa cells were transfected with Nup 205 siRNA and Non-Silencing control siRNA; following this, each of the four Wild Type GFP-fusion viral proteins were transfected into the siRNA treated cells. An additional set of knock-down cells were collected to confirm the efficiency of knock-down by immuno-blotting using an anti-Nup 205 antibody (Figure II-2.7.A.).

In Figure II-2.7.B, we observed that, following the Nup 205 depletion, the nuclear localization was significantly affected only for HIV-Rev, where Rev was predominately in the nucleus as punctate shaped clusters under the Non-Silencing siRNA treatment, and significant cytoplasmic staining with reduced nuclear staining were observed upon Nup 205 knockdown. Apoptin and E4orf4 only had marginal to no change observed; and SV40-LT had no change at all. The above qualitative observations were further converted to quantitative data by analyzing the ratio of distribution of the viral protein in the

nucleus over the cytoplasm, i.e. Nuc/Cyto. (Data not shown for SV40-LT, Apoptin and E4orf4).

These observations were not conclusive in terms of whether or not Nup 205 was required for ARM-mediated nuclear localizations, and we did not further pursue the requirement of Nup 205 for the nuclear localization of E4orf4 and Apoptin.

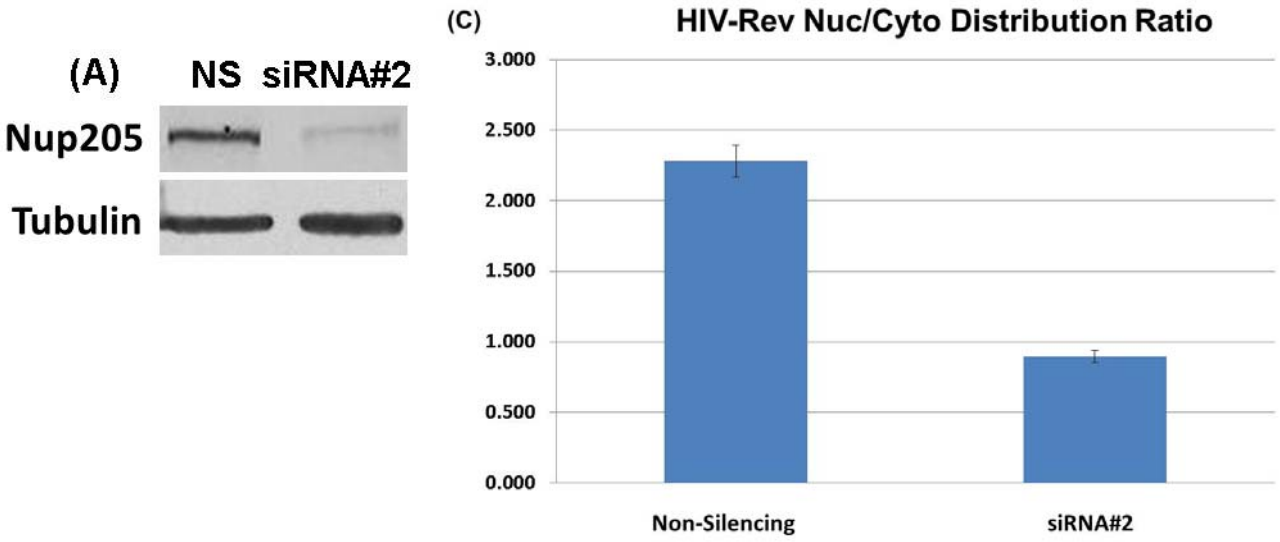

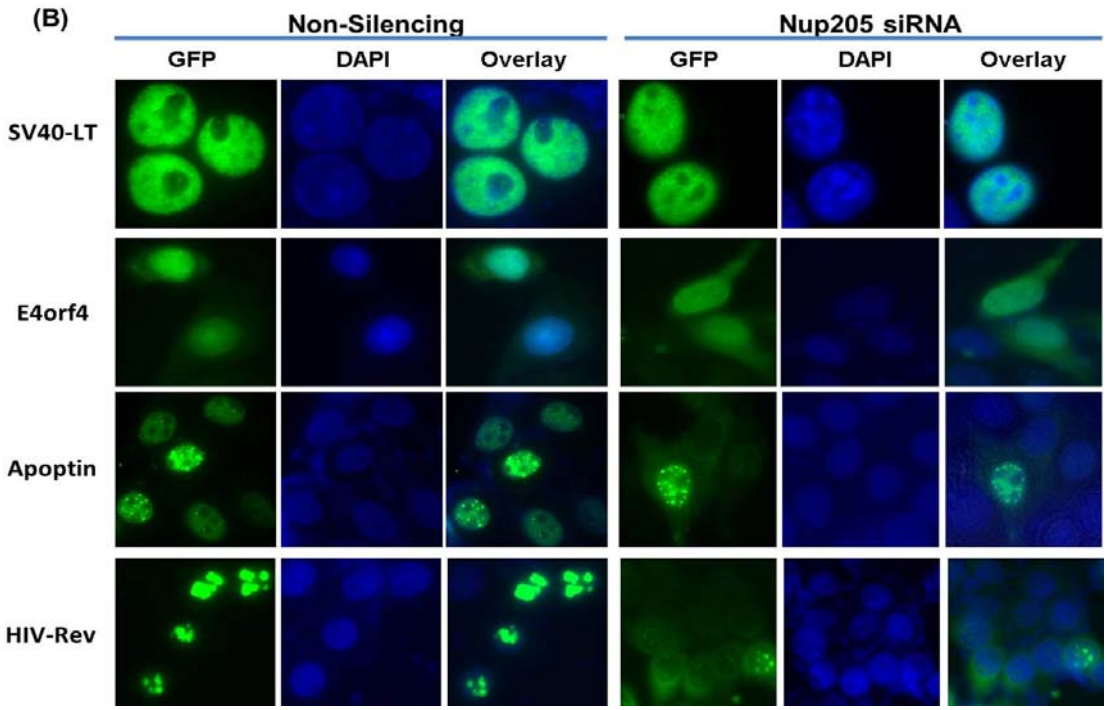

Figure II-2.7. The requirement of Nup 205 for the nuclear localization of ARM-containing viral nuclear proteins.

HeLa cells were first treated with siRNAs by transfecting with either the Non-Silencing siRNA or Nup 205 siRNA#2 for 40 hours. (A) At 40 hours after knockdown, NS-siRNA and Nup 205 siRNA#2 treated HeLa cells were harvested, lysed and quantified following standard procedure described above. Equal amount of total proteins from NS-siRNA and Nup 205-siRNA#2 were loaded on SDS-PAGE . They were then immuno-blotted with an anti-Nup 205 antibody to confirm the Nup 205 knockdown; tubulin was used as a loading control. (B) After 40 hours of knockdown, HeLa cells were immediately transfected with each of the four Wild Type GFP-fusion viral proteins, GFP-E4orf4, GFP-Apoptin, GFP-Rev and GFP-SV40-LT, for another 14 hours. Cells were then fixed, stained with DAPI to mark the nucleus, and mounted on glass slides. They were then observed using a fluorescence microscope at ×400 magnification. (C) The qualitative observations were further converted to quantitative ratio, where the ratio of the distributions of HIV-Rev in nucleus and cytoplasm was calculated. Result was reported from more than 60 cells from 15 fields in three independent experiments. Error bar represents the standard deviation of the mean.

3. The effect of E4orf4 on Nup 205.

We then examined the biological functions achieved through interaction between E4orf4 and Nup 205.

3.1. E4orf4 forms a trimolecular complex with PP2A-Bα and Nup 205.

Although E4orf4 itself has no enzymatic activity, most of its functions have been shown to be carried out through interaction with the Protein Phosphatase PP2A. E4orf4 recruits target phosphoproteins into complexes with PP2A resulting in changes of phosphorylation states of the host factors, such as the hypo-phosphorylation of SR splicing factors and the AP1 transcription factor. [4, 61] Therefore, since most of the functions of E4orf4 require PP2A, we determined if PP2A was recruited into a complex with Nup 205 and E4orf4.

In order to test this, we generated a V5-tagged PP2A-Bα construct. A schematic illustration of the experiment is presented in Figure II-3.1.

As shown in Figure II-3.1.A., PP2A-Bα can bring down endogenous Nup 205, but only in the present of WT E4orf4. Conversely, in Figure II-3.1.B., Nup 205 could also bring down PP2A-Bα, but again, only in the presence of E4orf4. Interestingly, all three forms of Nup 205, Full Length, Half and Quarter, which have been previously shown to interact with E4orf4, could bring down PP2A-Bα with E4orf4.

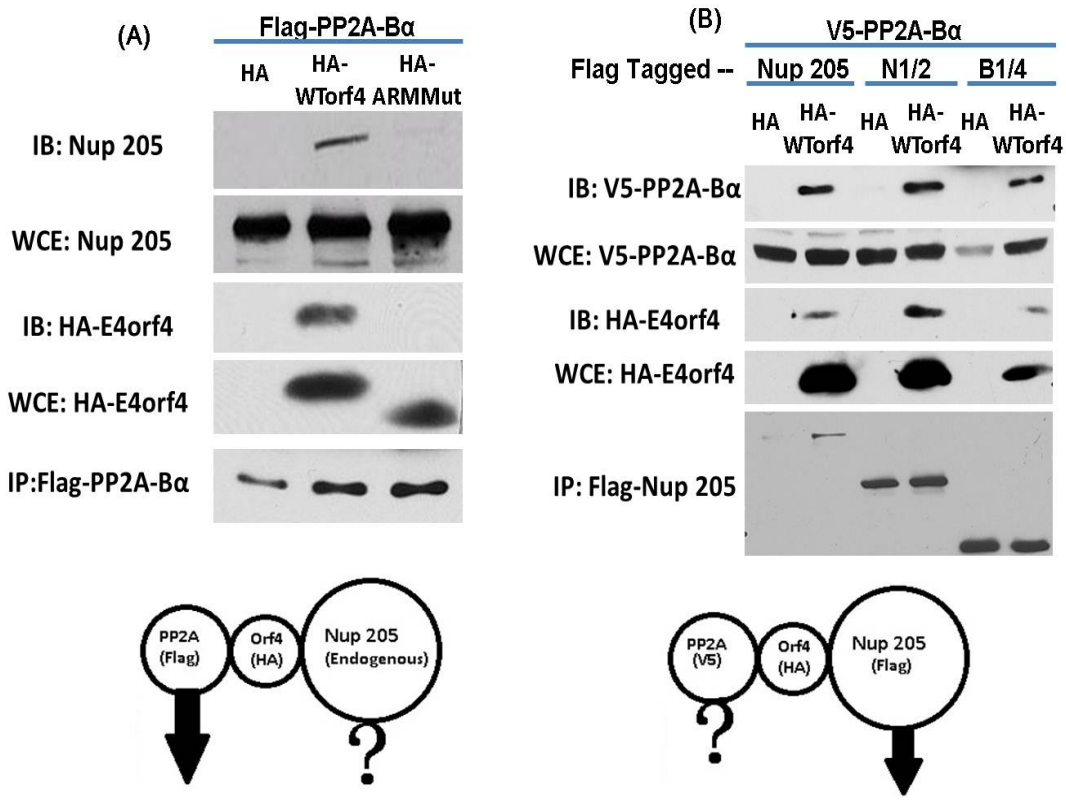

Figure II-3.1. E4orf4 brings PP2A-Bα to Nup 205 to form a tri-molecular complex. (A) Forward IP. H1299 cells were co-transfected with FLAG-tagged PP2A-Bα, together with one of the following, Empty HA-vector, HA-E4orf4 or HA-E4orf4-ARM-mutant. After 42 hours, the cells were harvested, lysed, and PP2A-Bα was immunoprecipitated from the whole cell lysates with an anti-FLAG antibody. The IP products were then run on SDS-PAGE, and the amount of endogenous Nup 205 brought down was examined by immuno-blotting with an anti-Nup 205 antibody. (B) Similar to the Forward IP, we co-transfected H1299 cells with V5-tagged PP2A-Bα, FLAG-tagged Nup 205 or the other two truncations, together with either Empty HA-vector or HA-E4orf4. After 42 hours, the cells were harvested, lysed, and the Nup 205 was immunoprecipitated from whole cell lysates with an anti-FLAG antibody. The IP products were then run on SDS-PAGE, and the amount of V5-tagged PP2A-Bα brought down was examined by immuno-blotting with an anti-V5 antibody.

3.2. E4orf4 modulates the phosphorylation state of Nup 205.

The above results show that E4orf4 may function by bringing the phosphatase PP2A to Nup 205. This pattern is similar to the way that E4orf4 modulates the host splicing factor ASF/SF2, where by bringing in PP2A to dephosphorylate this SR splicing factor, E4orf4 regulates the viral splicing activity [66]. We therefore determined whether E4orf4 could also modulate the phosphorylation state of Nup 205.

3.2.1. Multiple potential phosphorylation sites are present on Nup 205.

We first confirmed there are PP2A targeted phosphorylation sites present on Nup 205. We utilized a bioinformatics tool, PhosphoSitePlus® and *NetPhos 2.0*, to predict the potential serine, threonine and tyrosine phosphorylation sites on Nup 205 [93-95]. Since PP2A is a serine/threonine phosphatase, we focused only on the serine and threonine phosphorylation sites. There are 48 Serine phosphorylation sties, and 16 Threonine phosphorylation sites. Conversely, the specific kinases associated with these sites were also predicted using *NetPhosK 1.0*. [96] The result from this bioinformatics study is tabulated in the Appendix I.

3.2.2. E4orf4 causes changes in the isoelectric points of Nup 205.

We then track the changes in the Nup 205's state of phosphorylation is by measuring the Isoelectric Point (pI) of a protein using Two Dimensional Gel Electrophoresis (2-D gel). The changes of pI of Nup 205 in the presence and absence of E4orf4, and also in the presence of the E4orf4-ARM mutant using 2-D gels. To concentrate the samples, Nup 205 was first enriched by immunoprecipitation with anti-FLAG affinity agarose beads (Sigma, M2). Samples were then run on 2-D gels, and Nup 205 was detected by immuno-blotting using an anti-FLAG antibody. Predicted by the bioinformatics tool *Compute pI/Mw*, which calculates the pI of a phosphor-protein, Nup 205 has a theoretical

pI of 5.81 when none of its site is phosphorylated, and it has a theoretical pI of 4.81 when all of its 64 Ser and Thr sites are phosphorylated. [123-125]

Shown in Figure II-3.2., the first dimension of the gel separated the proteins based on pI, from 3 to 11, from left to the right. We observed that in the presence of Wild Type HA-tagged E4orf4, the position of Nup 205 in the first dimension was shifted to the positive end (higher pH), compared to the ones with HA and HA-tagged E4orf4-ARM-mutant. Meanwhile, the presence of HA-tagged E4orf4-ARM-mutant, which is defective in binding to both Nup 205 and PP2A, caused little or no change in the position of Nup 205 in the first dimension, relative to empty vector. Since a more phosphorylated protein generally has a lower pI value due to the negatively charged phosphate groups, a decreased pI value usually indicates the protein is being hyper-phosphorylated compared to the other state. Therefore, the increased pI value of Nup 205 in the presence of E4orf4 suggested a potential dephosphorylation of Nup 205. This suggests that E4orf4 is causing dephosphorylation of Nup 205.

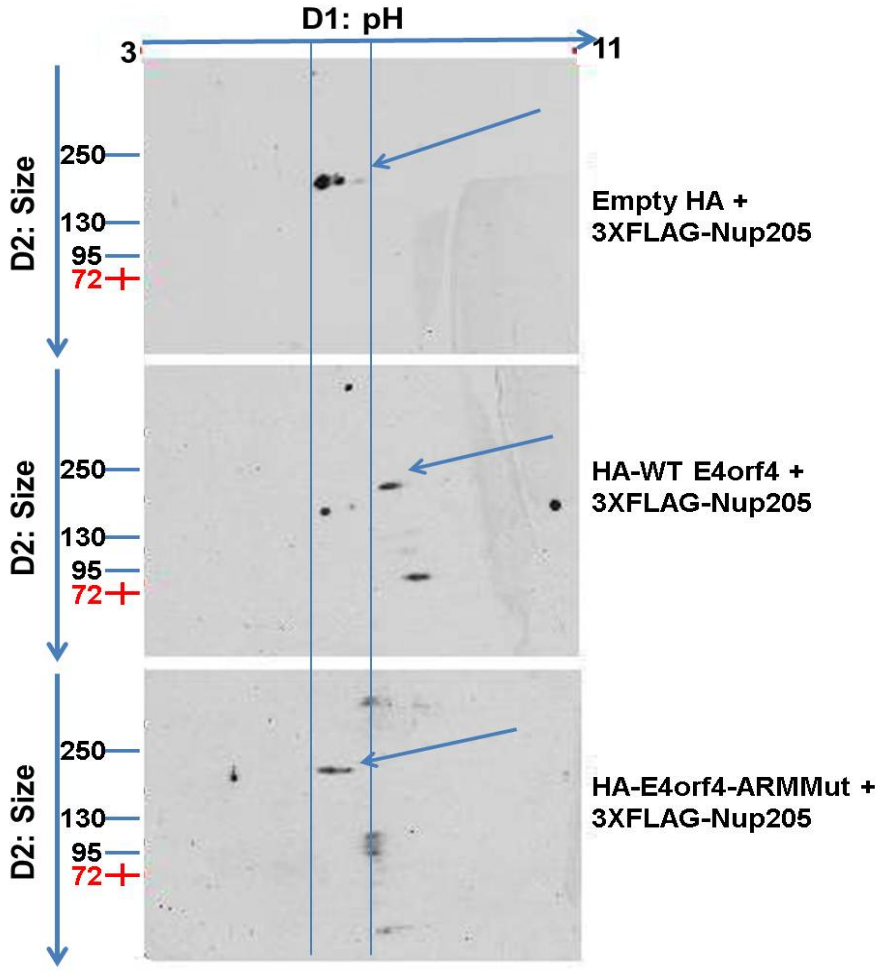

Figure II-3.2. E4orf4 increases the isoelectric point of Nup 205.

H1299 cells were co-transfected with 3XFLAG-tagged Nup 205, together with either of Empty-HA vector, HA-E4orf4-WT, or HA-E4orf4-ARM-mutant, for 42 hours. The cells from each of the three conditions was harvested and lysed, and the whole cell lysate was concentrated by immunoprecipitating FLAG-Nup 205 with anti-FLAG affinity agarose beads (Sigma, M2). The products were eluted, and samples were then loaded onto the first dimension gel which separated proteins based on pI from 3 to 11. Upon completing the second dimension on standard SDS-PAGE, the position of Nup 205 was revealed by immuno-blotting with an anti-FLAG antibody. Nup 205 has a molecular weight of 227 kDa, and the arrow-heads point at the bands that correspond to Nup 205; the other bands are thought to be degradation products.

4. The effect of Nup 205 on E4orf4 and Adenovirus.

In Section 3, in the context of Nup 205, we examined the biological functions achieved through the interaction between Nup 205 and E4orf4. We examined the effect of E4orf4 on Nup 205, in particular, the formation of a tri-molecular complex involving Nup 205, E4orf4 and PP2A-Bα, and the changes in the phosphorylation state of Nup 205.

In the following section, we studied these biological functions in a viral context. Since viruses are known to hijack and utilize host machinery and pathways to promote viral entry, gene expression, replication and reproduction of virions, in this study, we specifically tested the effects of Nup 205 on adenoviral gene expression, cytopathic effect and replication.

4.1. E4orf4 and Nup 205 regulate viral gene expression.

We first tested the effect of E4orf4 and Nup 205 on adenoviral gene expression. To test this, we infected H1299 cells with either WT-Ad5 or E4orf4$^-$ virus, and compared the gene expression at both protein and mRNA levels. We tested three adenoviral proteins – E1A, whose gene is the first to be transcribed after infection and regulates the expression of almost all other adenoviral genes; E4orf6, another early protein who shares the same transcript as E4orf4 and has its expression regulated by E1A; and Capsid Protein, a late protein.

The expression of viral proteins starts just 6 hours after the infection, and the onset of expression of late proteins could happens after 20 hours; therefore, a time course spanning the first 48 hours after infection was used.

4.1.1. The effect of E4orf4 on viral gene expression.

We started by testing the effect of E4orf4. To test this, we infected H1299 cells with either WT-Ad5 or E4orf4$^-$ virus, and compared the protein expressions of E1A, E4orf6

and Capsid at 0, 24, 48 and 72 hours after the infection. This initial experiment was conducted by Dr. Paola Blanchette, and the result was repeated in later experiment in this research. Showing the effect of E4orf4 on Ad5 gene expression, Figure II-4.1. was presented with her permission.

As shown in Figure II-4.1., compared to WT-Ad5, adenovirus lacking E4orf4 (E4orf4$^-$ virus) had defects in gene expression. Compared to the Wild Type virus, the E4orf4$^-$ adenovirus resulted in elevated level of early protein E1A; E1A is the first adenoviral gene to be transcribed after infection, and E1A protein regulates the expression of all other adenoviral genes. Further, E4orf6, another early protein could also be seen to be up-regulated at the absence of E4orf4. Finally, the absence of E4orf4 also caused reduced level of late proteins.

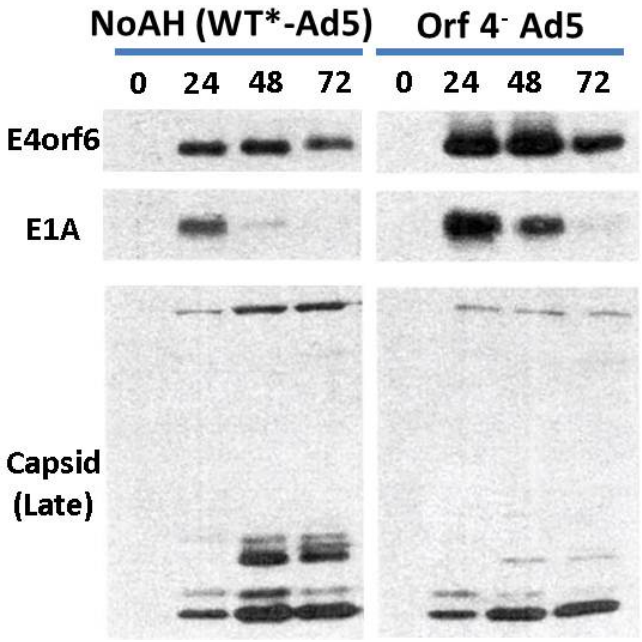

Figure II-4.1. The effect of E4orf4 on adenoviral gene expression.

H1299 cells were infected with either WT-Ad5 or E4orf4$^-$ virus at 5 M.O.I. Cells were harvested at different time points over a time course of 0, 24, 48 and 72 hours. 0 hour cells were not infected with either virus. Cells were then lysed and quantified, and equal amount of proteins were loaded onto SDS-PAGE. The protein levels of E1A, E4orf6 and Capsid was monitored by immuno-blotting with their specific antibodies. This figure was presented with the permission from Dr. Paola Blanchette.

4.1.2. The effect of Nup 205 on viral gene expression.

Having tested the effect of E4orf4 on viral gene expression, we then examined the effect of Nup 205 on viral gene expression. To test whether Nup 205 is essential, we silenced the expression of Nup 205 in H1299 cells with Nup 205 siRNA#2, which was the same one used in Section 2.6. Following the knockdown for 40 hours, H1299 cells treated with either Non-Silencing siRNA or Nup 205 siRNA were infected with WT-Ad5.

4.1.2.1. The effect of Nup 205 on viral proteins production.

Similar to the previous study on the effect of E4orf4 on viral gene expression, we compared the protein expressions of E1A, E4orf6 and Capsid in infected H1299 cells after siRNA treatments. Both E1A and E4orf6 are early adenoviral proteins which start to be transcribed and translated shortly after infection. Based on the result of 4.1.1., we placed more focus on the changes occurred during the first 24 hours after infection, which is the time required for one cycle of Ad5 replication, by adding two more time points, 14 and 21 hours after infection; these two additional points enabled us to observe the changes in expression in more detail.

Shown in Figure II-4.2.A., the knockdown effect of Nup 205 was confirmed by immuno-blotting. Following siRNA treatment, cells were then infected with Ad5 at 35 M.O.I., and collected and processed at designated time points. Equal amount of total protein were loaded, and the protein levels of E1A, E4orf6 and Capsid were measured (Figure II-4.2.B.). Interestingly, by knocking down Nup 205 in H1299 cells, we observed elevated levels of both E1A and E4orf6 proteins, and reduced amount of late protein production. This was very similar to the effects on gene expression caused by virus without E4orf4 (E4orf4$^-$ virus).

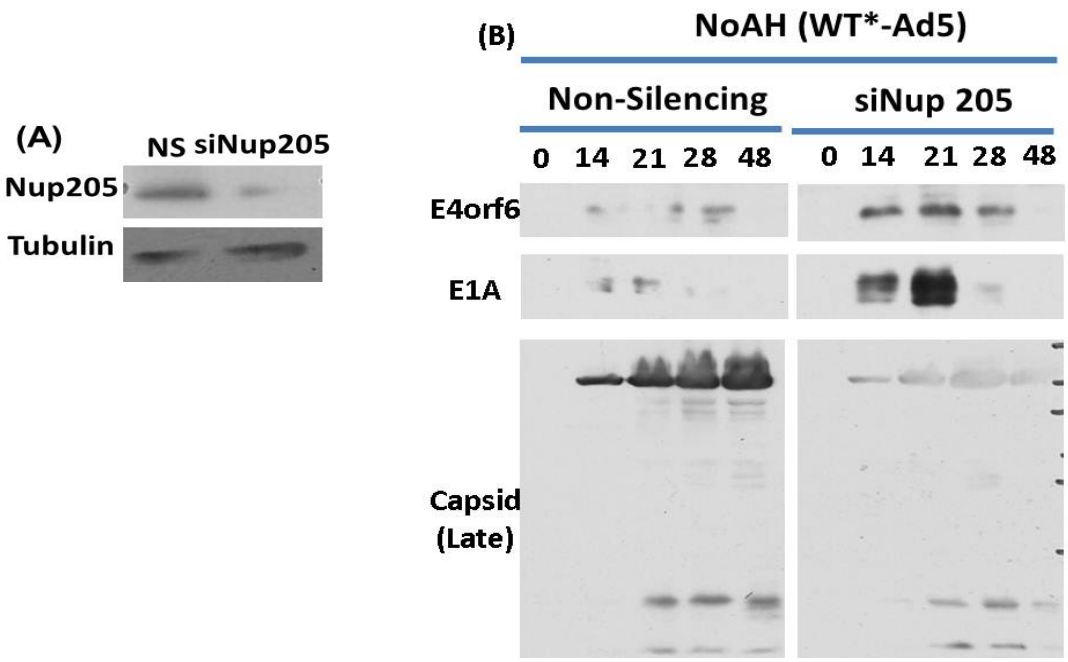

Figure II-4.2. The effect of Nup 205 on viral gene expression.

H1299 cells were first transfected with Non-Silencing siRNA or Nup 205 siRNA#2 for 40 hours before they were infected with WT-Ad5 at 35 M.O.I. Cells were harvested over a time course of 0, 14, 21, 28 and 48 hours. 0 hours cells were uninfected. Equal amounts of protein were loaded onto SDS-PAGE. (A) The Nup 205 knockdown was confirmed by comparing the amount of Nup 205 present in H1299 cells that had been treated with Non-Silencing siRNA and Nup 205 siRNA#2 for 40 hours; they were the same samples as infection Time Point 0. Both samples were loaded onto SDS-PAGE, and the Nup 205 amount was determined by immuno-blotting with an endogenous Nup 205 antibody. (B) The effect of Nup 205 on E1A, E4orf6 and Capsid was determined by comparing the protein expression of these three proteins in Non-Silencing and Nup 205-#2 siRNA treated cells following WT-Ad5 infection. Samples from all time points were loaded onto one SDS-PAGE for comparison. The protein levels of E1A, E4orf6 and Capsid were monitored by immuno-blotting with their specific antibodies.

4.1.2.2. The effect of Nup 205 on viral mRNA level.

Having observed the changes in protein levels of E1A, E4orf6 and Capsid caused by Nup 205 depletion, we further examined if these changes in gene expression occurred at the transcriptional level. Specifically, we measured the mRNA levels of E1A and Late genes using Quantitative RT PCR. This experiment was carried out concurrently with the one for protein level, as described in 4.1.2.1. Since compared to translation, the transcription of viral genes takes places at an even earlier stage following an adenoviral infection, we observed the mRNA level at more time points in the first 24 hours post-infection, which is the usual time to complete an adenovirus replication cycle. Therefore, a time course of 0, 7.5, 14 and 23 hours was set to monitor the changes in mRNA levels of E1A and late products. Since all of the adenoviral late products are transcribed using the same promoter, the Major Late Promoter, and the mRNA of all late viral products contain the same Tripartite Leader Sequence (TPL), the mRNA level of late products was monitored by amplifying the TPL. [27, 126-128]

Shown in Figure II-4.3., following the same siRNA treatment as in 4.1.2.1., H1299 cells were infected with Ad5 at 5 M.O.I., and collected and processed at designated time points. This was followed by Quantitative RT-PCR using primers specific to E1A, TPL and 18S. The levels of viral mRNA were normalized to cellular 18S rRNA. The result was tabulated in Table II-4.1. and plotted in Figure II-4.3. Shown in Figure II-4.3.A., comparing the E1A mRNA levels in both Non-Silencing and Nup 205-#2 siRNAs treated cells, we observed a near two-fold increase when Nup 205 was depleted, along all three time points. Conversely, in Figure II-4.3.A., we observed a near three-fold reduction in late products mRNA when Nup 205 was depleted. These changes had similar trends as the ones measuring protein levels. Since this experiment was only performed in duplicate, no statistical test was conducted.

Treatment/ h.p.i.	NS	siNup205#2	Ratio siNup205 / NS	NS	siNup205#2	Ratio siNup205 / NS
0	**1.44E-06**	**5.63E-07**	**-**	***3.87E-06***	***2.28E-06***	**-**
7.5	**0.04**	**0.13**	**3.14**	***0.00***	***0.00***	**-**
14	**0.13**	**0.27**	**2.01**	***0.70***	***0.15***	***0.22***
23	**0.20**	**0.30**	**1.51**	***5.82***	***1.89***	***0.33***
Target	**Ad5-E1A**			***Ad5-TPL (Late Product)***		

Table II-4.1. Quantification of E1A and Late Product mRNAs relative to the amount of 18S rRNA.

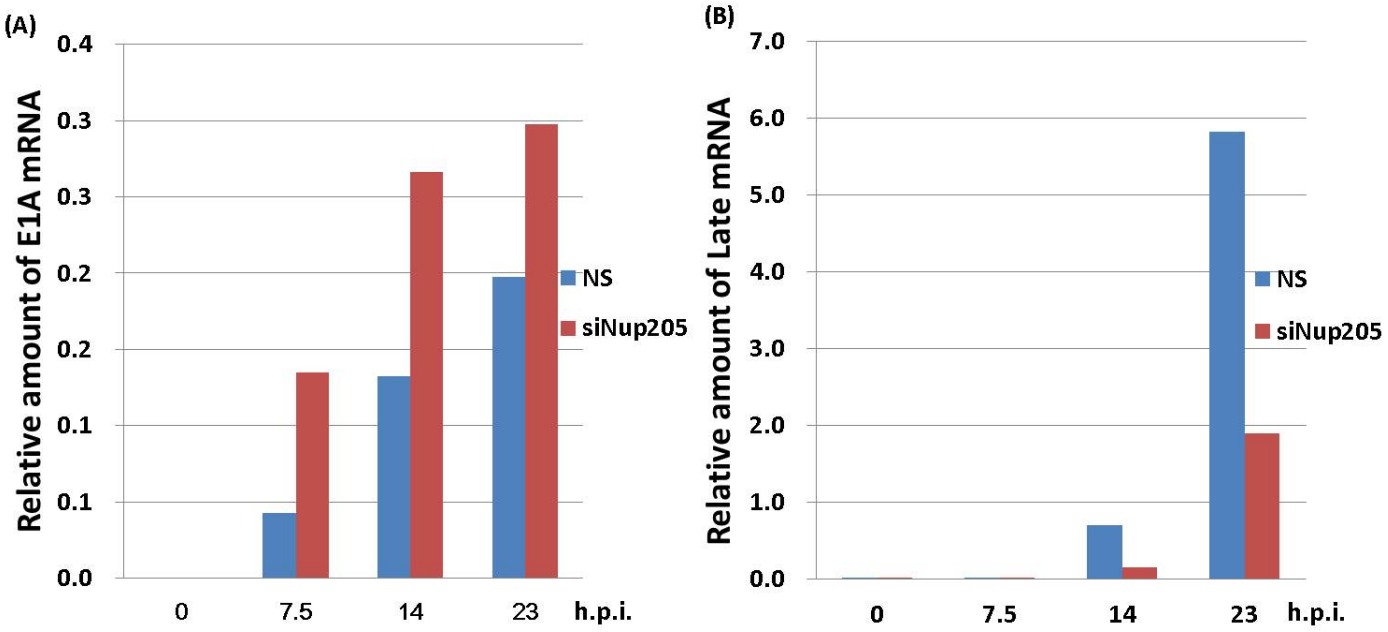

Figure II-4.3. The effect of Nup 205 on viral mRNA levels.

H1299 cells were first transfected with Non-Silencing siRNA or Nup 205 siRNA#2 for 40 hours before they were infected with WT-Ad5 at 5 M.O.I. Cells were harvested at 4 different time points over a time course of 0, 7.5, 14 and 23 hours. 0 hours cells were uninfected. Cells were then processed for mRNA extraction. They were quantified by Quantitative RT-PCRs using primers specific for E1A and TPL, and the viral mRNA levels were normalized to 18S rRNA levels. (A) The E1A mRNA levels at different time points after WT-Ad5 infection. (B) The late product mRNA levels at different time points after WT-Ad5 infection. The late mRNA was measured by detecting the TPL.

4.2. Nup 205 is required for efficient viral cytopathic effect and replication.

Having tested the effect of Nup 205 on viral gene expression, we then looked at other effects that Nup 205 may have during the adenovirus replication cycle. We specifically focused on two parameters of adenoviral infection by most viruses, the Cytopathic Effect (CPE) and viral replication.

4.2.1. Nup 205 enhances viral cytopathic effect.

In Figure II-4.1., following infections with WT-Ad5, we always observed differences in morphology of the H1299 cells with and without Nup 205 depletion. Like many other viruses, following infection, Adenovirus is known to result in rounded and swollen cells with basophilic intranuclear inclusions [129-131], and this is known as the Cytopathic Effect (CPE). Therefore, we went back and compared the CPE of WT-Ad5 on both Non-Silencing and Nup 205-#2 siRNAs treated H1299 cells by qualitatively observing the morphological differences following WT-Ad5 infections.

We first depleted Nup 205 from H1299 cells by treating them with either Non-Silencing or two Nup 205 siRNAs, siRNA#1 and siRNA#2, for 40 hours. The cells were then infected with WT-Ad5 at 5 M.O.I., and the morphology was observed 30 hours post-infection.

Shown in Figure II-4.4.B., 30 hours after infection, most of the H1299 cells treated with Non-Silencing siRNA were rounded and swollen; meanwhile, in both H1299 cells treated with the two Nup 205 siRNAs, only half of them had such morphology, and the rest remained attached and maintained the same appearance as uninfected cells. Both Nup 205 siRNAs used in this set of experiment achieved effective knockdown effects, and as shown Figure II-4.4.A, these effects were confirmed by immuno-blotting.

Following microscopy observation, the samples were returned to incubation for another 10 hours, until they were collected for virus yield measurement at 42 hours post-infection.

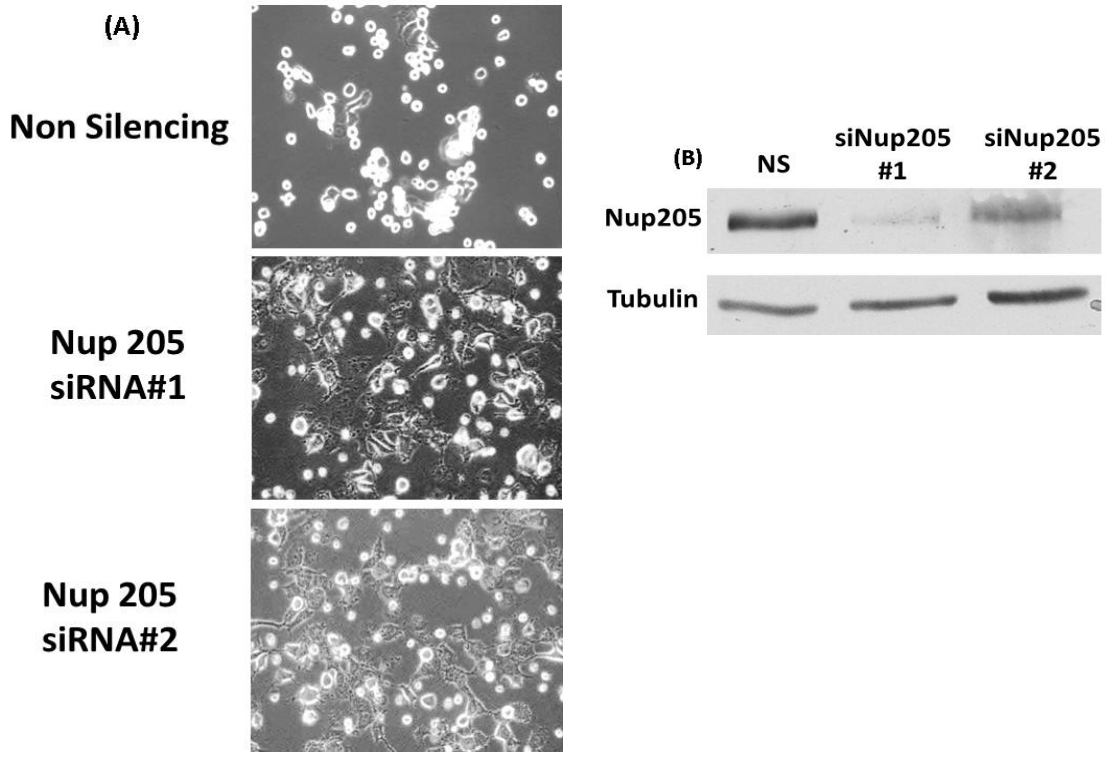

Figure II-4.4. The effect of Nup 205 on the Cytopathic Effect of WT-Ad5.

H1299 cells were first transfected with Non-Silencing siRNA or either of the two Nup 205 siRNAs for 40 hours before they were infected with WT-Ad5 at 5 M.O.I. (A) 30 hours post-infection, the morphology of the cells was observed using a Zeiss Axiovert 25 microscope. The cell morphology was qualitatively evaluated based on their appearance of rounded and swollen shape and their attachment to the tissue culture plates. (B) The knockdown effects of the two Nup 205 siRNAs were confirmed by immuno-blotting with a Nup 205 specific antibody. The same membrane was cut into two parts, and the top part was blotted for Nup 205, and the bottom part was blotted for tubulin as a loading control.

4.2.2. Nup 205 is required for efficient adenovirus replication.

Having observed that the depletion of Nup 205 could cause defects in CPE in H1299 cells, we then tested if Nup 205 was ultimately required for the replication of adenovirus. To test this, we compared the abilities of WT-Ad5 to replicate in H1299 cells both with and without Nup 205 depletion. In order to evaluate the replication ability, we measured the total virus yield from H1299 cells following an infection with WT-Ad5. The virus yield was quantitatively determined by FFU assay utilizing adenoviral E2A immunofluorescence staining. [132, 133]

This experiment carried on the same infected samples as the ones used in testing the CPE. Following the knockdown of Nup 205 in H1299 cells and the infection with WT-Ad5, the infected cells were first observed for the CPE at 30 hours post-infection; they were then all promptly returned to incubation for another 10 hours, until they were harvested by scraping at 42 hours post-infection for the virus yield experiment. The collected cells were lysed by freeze-thawing, and viruses produced were released into the lysate. The amount of these viruses, which was the virus yield, was subsequently determined by a second infection in H1299 cells and quantification by adenovirus E2A protein immunofluorescence staining. Specifically, the presence of Adenovirus E2A DNA Binding Protein (DBP), a protein unique to Adenovirus that was detectable by immunofluorescence with an anti-DBP (E2A) antibody, indicated a cell had been infected with WT-Ad5; therefore, by counting the number of E2A positive cells from a sample, the virus yield could then be determined.

In this experiment, the average number of cells that were positive for E2A-staining was calculated from 24 fields, 8 fields from each of three independent replicates; the average count for viruses collected from H1299 cells treated with Non-Silencing control siRNA was arbitrarily set as 100%, and the counts from the other two Nup 205 siRNA

treated cells were expressed in respect to the Non-Silencing control count. Since this experiment was a continuation of the CPE experiment, the knockdown effect of Nup 205 siRNAs had been previously confirmed via immuno-blotting shown in Figure II-4.4.

Shown in Figure II-4.5., upon depletion of Nup 205 from H1299 cells using one of the two Nup 205 siRNAs, the virus yields of WT-Ad5 in these H1299 cells were reduced by more than 4 folds, to 12.38% after treatment of Nup 205 siRNA#1 and to 17.07% after Nup 205 siRNA#2. This result was in agreement with the observations made on the defect in CPE with reduced level of Nup 205.

It is noticed that the virus yield should also depend upon the amount of cells present for the production of the viruses. Therefore, before conducting this experiment, the growth of H1299 cells after siRNA treatment had been monitored, and the result from one of these experiments was presented in Section 5.1. on Figure II-5.1.A. Overall, within the first 96 hours after the siRNA lipofection, Nup 205 depletion slowed down the H1299 cell growth by no more than 50%, which was relatively small compared to the 5 to 6 folds reduction in viral production. Furthermore, the infection was carried out at 5 M.O.I., and through immuno-staining with an antibody against DBP, it was shown that only a portion of the cells were infected at the time of the collection of viruses produced in this experiment (data not shown); therefore, it was unlikely that the capacity of H1299 cells to be infected had been saturated.

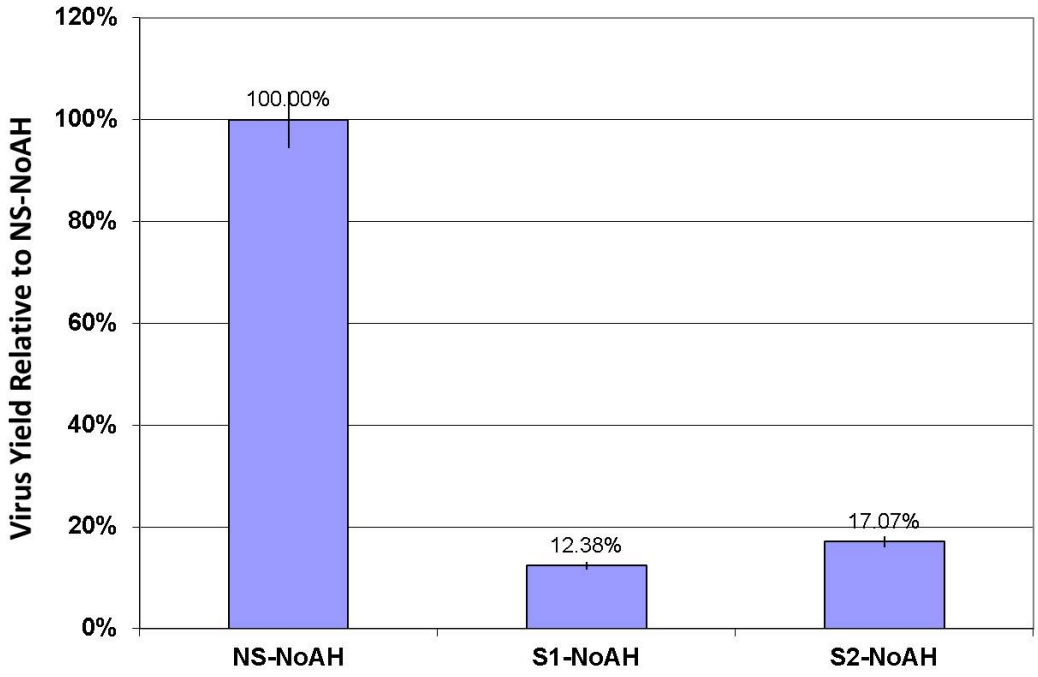

Figure II-4. 5. The effect of Nup 205 on the replication ability of WT-Ad5 (NOAH).

Following the Cytopathic Effect experiment, 42 hours post-infection, the samples were collected to measure the replication ability of WT-Ad5 in H1299 cells with or without reduced level of Nup 205. They were harvested by scraping, lysed by three cycles of freeze-thawing, and the cell lysates were serially diluted in Infection Medium for infection of H1299 cells. The replication ability was measured by the virus yield, which was determined by quantitative E2A immunofluorescence staining (FFU assay) [132, 133]. The virus yields were represented by the averages of cells having positive E2A-staining after all three types of treatments, Non-Silencing control, Nup 205 #1 and Nup 205 #2 siRNAs, and they were plotted for comparison. The averages were calculated from 24 different fields, 8 fields from each of three independent replicates; the average count for viruses collected from H1299 cells treated with Non-Silencing control siRNA was the highest and was arbitrarily set as 100%, and the counts from the other two Nup 205 siRNA treated cells were expressed in percentages relative to the Non-Silencing control count. The error bar represented the standard deviation.

5. The effect of Nup 205 on other cellular processes.

In the previous section, we have examined the effects of Nup 205 on the biology of Adenovirus and its E4orf4 protein, in particular, the gene expression, CPE and replication ability of the adenovirus. We then tested the effects of the interaction between Nup 205 and E4orf4 on the host system.

5.1. Nup 205 depletion slows down cell growth.

Nucleoporins are the basic constituents of the NPC, the gatekeeper of the nucleus, which plays an essential role in mediating the trafficking of macromolecules between the nucleus and the cytoplasm. The amount of each nucleoporin is tightly regulated, and alterations by depletion, and sometimes even overexpression, of nucleoporins often result in changes and disruptions in the cellular processes, such as the disruption of the cell growth, embryonic development and nuclear cytoplasmic trafficking of transcription factors; altogether, the combination of such alterations may ultimately lead to severe consequences, such as growth arrest and apoptosis. [90, 134-136]

Therefore, we began with testing whether Nup 205 was essential for the cells by measuring the growth rate of H1299 cells after silencing Nup 205 by siRNA. By comparing the number of living cells in culture after H1299 cells were treated with either Non-Silencing Control or Nup 205 siRNA, a lower number in the count of cells could be a result of either a slower growth or an increased cell death, and it could also be due to the combination of these two; therefore, in addition to the growth curve measuring the living cells, we also monitored the accumulation of dead cells by Trypan Blue staining.

The counting of cells started following transfection of H1299 cells with Non-Silencing Control and Nup 205-#2 siRNAs. Given the fast growth nature of H1299 cells and the short period which the effect of siRNA could sustain, only the first four days following siRNA lipofection were monitored. As shown in Figure II-5.1.A., over a

four-day time course, the NS-siRNA treated H1299 cells followed an exponential growth curve, doubling in number every 24 hours, reaching 1.41×10^6 4 days after the knockdown. Meanwhile, the growth rate of H1299 cells treated with Nup 205-siRNA#2 had a much lower count; while both started with the same amount of 9×10^3 cells, by the fourth day following lipofection, those H1299 cells with reduced level of Nup 205 grew to only 8.20×10^5 cells in culture, which accounted for only 58% of the amount of 1.41×10^6 in cells treated with NS-siRNA. To test whether this difference was due to an increased cell death rate or a slower growth, we also monitored the number of dead cells over the time. As shown in Figure II-5.1.B., by the fourth day after knockdown, the dead cell count in the culture of H1299 cells with Nup 205 depletion was more than doubled compared to the control group; however, the amount of dead cells accounted for no more than 1/80 of the number of total cells. Therefore, the low count in the cell number seemed more likely due to the slow growth of H1299 cells after Nup 205 depletion, rather than an increased death rate, or at least it was a combination of the two.

The cell counts over the 4 days following the depletion of Nup 205 were also tabulated in Table II-5.1., and the reduction in cell counts were presented as the difference in cell counts between NS and Nup 205 siRNAs treated groups, in respect to the cell counts from the Non-Silencing Control group. It could be observed that the difference increased over the time, starting from a 6.3% reduction on Day 1 and ending with a 41.7% reduction on Day 4. In all previous experiments involving siRNA treatments, our default procedure required a 40 hours of incubation after the siRNA lipofection before any further treatments. At 40 hours post-lipofection, which was around Day 2, the reduction in cell counts was measured to be 16.7%; therefore, all downstream experiment following Nup 205 siRNA treatment was assumed to have started with only ~85% of the amount of cells in Non-Silencing Control group.

Day	0	1	2	3	4
Treatment	Number of Cells (10^4)				
NS	9.0	18.8	37.5	73.9	140.6
siNup205#2	9.0	17.6	31.3	52.3	82.0
Growth Reduction After Depletion of Nup 205	0.0%	6.3%	16.7%	29.2%	41.7%

Table II-5. 1. The reduction of H1299 cell growth following the depletion of Nup 205. Over the first 96 hours after H1299 cells were lipofected with siRNAs, their growth was monitored, and the differences in growth between the Non-Silencing Control and Nup 205-#2 siRNAs treated H1299 cells were calculated in respect to the growth in Non-Silencing Control treated cells.

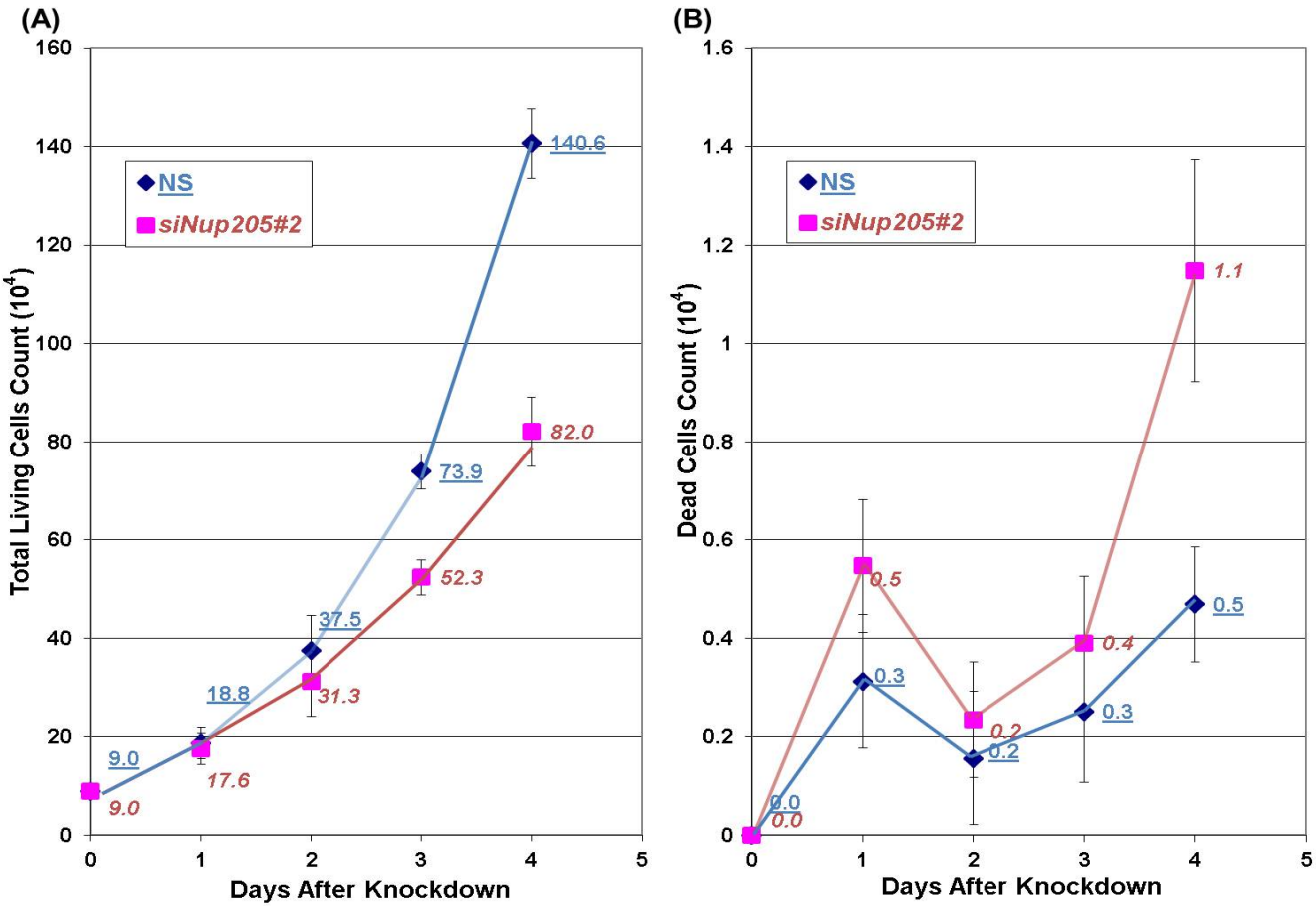

Figure II-5. 1. The growth curve of Non-Silencing Control and Nup 205 siRNAs treated H1299 cells.

4×10^3 H1299 cells were seeded on each well of a 12-well plate, and 24 hours later, were transfected with either Non-Silencing Control or Nup 205-#2 siRNA at Day 0. (A) The growth of H1299 cells treated with either type of siRNA in the first 4 days after lipofection was plotted as growth curves. (B) The amount of dead cells after each treatment was also plotted along these first four days. Dead cells were counted by Trypan Blue staining. The number of cells in each well was extrapolated by considering the dilution factors as explained above. The count for each time point and treatment was labelled on the curve, and it was an average of 24 different counts, 8 from each of three independent replicates. The error bars represents the standard deviations.

5.2. The effects of Nup 205 and E4orf4 on the nuclear size of H1299 cells.

Immuno-depletion of the Nup 205-93-188 sub-complexes has been shown to enlarge the nuclear size of *Xenopus laevis* [92], we therefore tested if knockdown of Nup 205 can also cause this effect in mammalian cells.

5.2.1. Nup 205 depletion resulted in an enlarged H1299 cell nuclear size.

To test this, we first depleted Nup 205 from H1299 cells by treating them with either Non-Silencing or two Nup 205 siRNAs, siRNA#1 and siRNA#2, for 40 hours, similar to previous experiments. The cells were then fixed with Methanol and stained with DAPI (4',6-diamidino-2-phenylindole) to mark the area of the nucleus. They were then observed under a Zeiss Axiovision 3.1 fluorescence microscope, and images were recorded using Axiocam HR (Zeiss, Thornwood, NY) digital camera. The images were then processed, and the size of the nucleus was measured from the pictures using Volocity 3D Image Analysis Software (PerkinElmer).

As shown in Figure II-5.2.A., upon depletions of Nup 205 from H1299 cells using either of the two Nup 205 siRNAs, the average nuclear size of H1299 cells was increased from 512 μm^2 to more than 650 μm^2, and these increases were statistically significant with p value smaller than 0.01. This result was in agreement with observations made in *Xenopus laevis* extracts, where immuno-depleting Nup 205 from the *in vitro* assembled nucleus resulted in enlarged nucleus, although such difference was only marginal ([92] and personal communication, Dr. Wolfram Antonin).

5.2.2. The presence of E4orf4 also enlarged the nucleus of H1299 cells.

Following adenovirus infection, an enlarged nucleus filled with basophilic intranuclear inclusion bodies and other viral particles could be observed in every infected cell, and multiple viral proteins and processes were involved in causing this enlargement

of the nucleus. Having observed that Nup 205 was required for controlling the nuclear size of H1299 cells, we then tested whether E4orf4 is essential in causing enlarged nucleus following an adenoviral infection.

To test this, we used the WT-Ad5 virus and the E4orf4$^-$ virus, and compared the sizes of H1299 cells infected with adenoviruses with or without functional E4orf4. Further, to test whether the presence of E4orf4 alone was sufficient in causing the enlargement, we also compared the resulting nuclear sizes following infections with adenoviral vectors Ad-LacZ and Ad-FLAG-E4orf4, which overexpressed E4orf4. H1299 cells were infected with each of the four viruses at 35 M.O.I. for 15 hours before they were fixed by Methanol and stained with DAPI for observation. Although at 35 M.O.I., almost all cells had been infected, to ensure only the nuclei of infected cells were included in counting, we further labeled infected by an antibody against the adenovirus DBP protein. Finally, a similar procedure as used in Section 5.1.1. was followed to measure the nuclear size of these infected cells, and the result was plotted on Figure II-5.2.B. The 15 hours infection time was chosen because it was optimal to measure the effect of E4orf4 without interference of other factors. It was long enough for E4orf4 and LacZ to express, but it was not enough for WT-Ad5 and E4orf4$^-$ to complete one round of replication. Furthermore, this time was also before the cells started to shrink and swell due to the toxicity induced by E4orf4, and before they started to get rounded and detached from the plate due to CPE.

As shown in Figure II-5.2.B., the average nuclei sizes were plotted and labeled on the corresponding columns. The nuclear size of H1299 cells without any viral infection was used as the baseline, which averaged at around 612 μm^2. First, comparing the average nuclear size of 650 μm^2 of H1299 cells infected with Ad-LacZ, and 822 μm^2 of ones infected with Ad-E4orf4, the overexpression of E4orf4 alone resulted in ~25% increase in nuclear size in infected H1299 cells. Compared to the H1299 cells infected

with adenovirus vectors, the sizes of nuclei significantly increased, by another ~40%, after the Wild Type adenovirus WT-Ad5 and the one defected only in E4orf4 infected the cells. Meanwhile, comparing the sizes of nuclei of WT-Ad5 and E4orf4$^-$ infected H1299 cells, with the absence of E4orf4, the resulting nuclear size reduced from 1175 μm^2 in WT-Ad5 infected cells to 1055 μm^2 in E4orf4$^-$ infected H1299 cells; this reduction was more than 10%.

Taken together, we have confirmed the requirement of Nup 205 for cell growth and the control of the size of the nucleus. Further, we have also confirmed that E4orf4 could cause the enlargement of H1299 nuclei. Following this result, our future work will test the mechanism involved in these two functions, and how E4orf4 interaction with Nup 205 can induce these effects in the host.

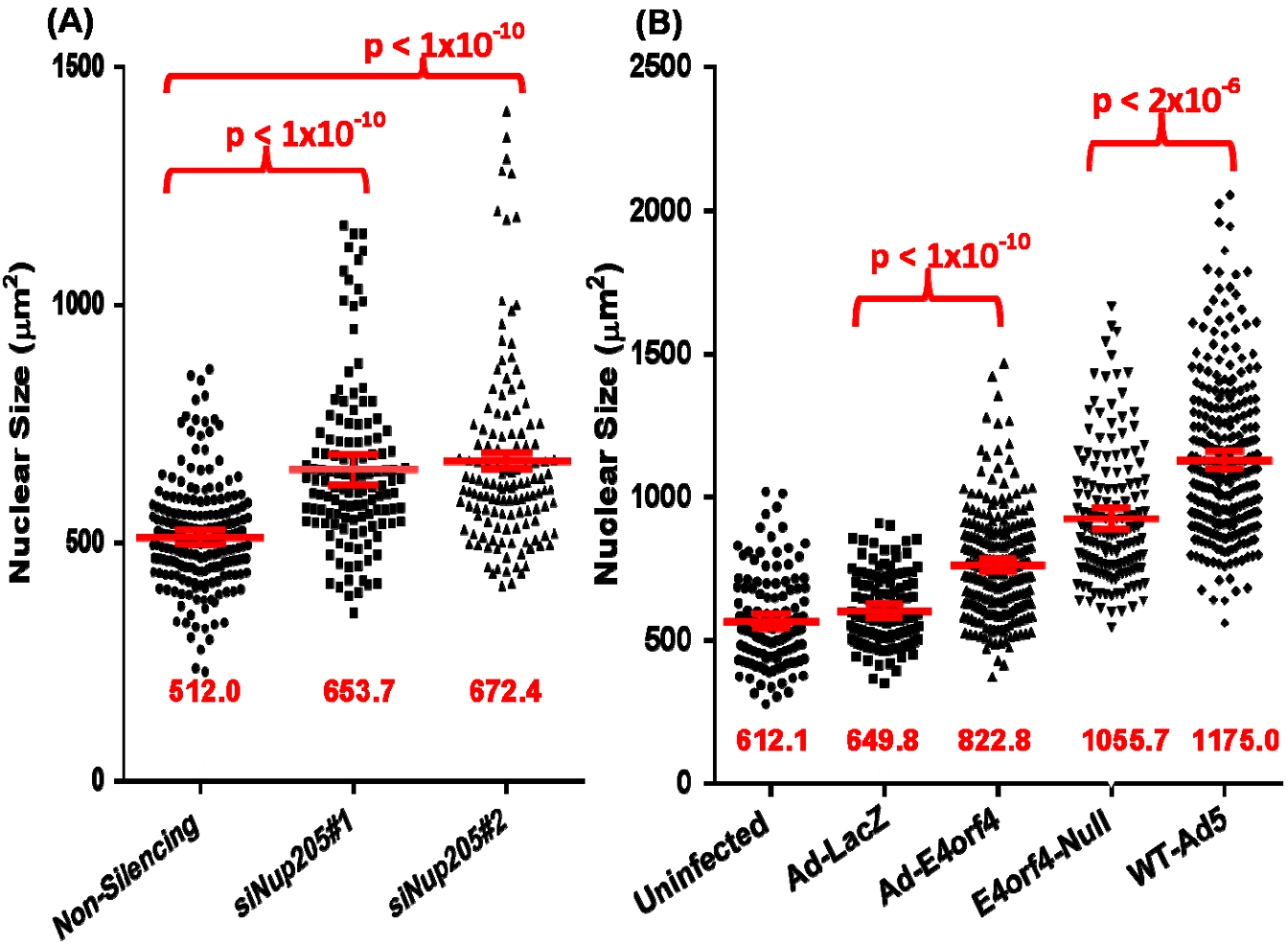

Figure II-5. 2. The effect of Nup 205 and E4orf4 on the nuclear size of H1299 cells.

H1299 cells were cultured on glass coverslips in 6-well plates and achieved ~50% confluence before siRNA lipofection and ~80% confluence before viral infections. (A) H1299 cells were lipofected with either Non-Silencing Control or the two Nup 205 siRNAs and cultured for 40 hours before they were fixed for observation. (B) H1299 cells were infected with one of the four viruses, Ad-LacZ, Ad-FLAG-E4orf4, WT-Ad5 and Ad5-E4orf4^{-}, at 35 M.O.I. for 15 hours before they were fixed for observation. The average nuclear size of a control group of H1299 cells that were not infected with any viruses was used as the baseline. Since only infected cells should be measured, each infected samples were further immuno-blotted for adenoviral DBP protein with an antibody against DBP to mark the cells that had been infected. The cells were fixed with Methanol, stained with DAPI to mark the area of the nucleus and mounted on

glass slides for observation and images capturing using a fluorescence microscope at ×400 magnification. The images were recorded using Axiocam HR (Zeiss, Thornwood, NY) digital camera and processed, and the size of the nucleus was measured from the pictures using Volocity 3D Image Analysis Software (PerkinElmer). The nuclear size of H1299 cells after each treatment was expressed as the average of more than 200 cells, taken from at least 3 fields from each of the 3 different replicates. The error bar represented the 95% confident interval for the mean. P values smaller than 0.01 were considered to be statistically significant, and values less than 10^{-10} were expressed as $p<10^{-10}$.

Discussion

Viruses are known to efficiently exploit host cell machinery for their own benefit; therefore, the study of protein interaction between host and viral protein provides fundamental insights into pathways and molecular mechanisms in virology and cell biology. In this study, we identified the nuclear pore complex component Nup 205 as a novel host binding partner of the multifunctional Adenovirus Early Region 4 Open Reading Frame 4 (E4orf4) protein. We also further characterized the mechanism of this interaction. Examining the effect of this interaction in the context of both the virus and the host, we found that E4orf4 utilizes Nup 205 to regulate adenovirus gene expression and to localize into the cell nucleus as well. We also examined the effect of E4orf4 on the biology of Nup 205, such as the regulation of its phosphorylation, stability, and association with other proteins of the nucleopore complex.

1. Nup 205 is a novel host interacting partner of E4orf4.

Adenovirus Early Region 4 Open Reading Frame 4 (E4orf4) protein has been extensively studied in the past. Much of its activity requires the binding of Protein Phosphatase 2A (PP2A). However, the full complement of cellular factors that interact with E4orf4, and the molecular mechanisms utilized by E4orf4 during viral replication to regulate gene expression remain poorly understood [4, 26, 35, 58, 59, 121]. Using Immunoprecipitation followed by Mass Spectrometry, we identified Nup 205 as a novel host factor that interacts with E4orf4 (Figure II-1).

Although Mass Spectrometry is an extremely sensitive method in detecting and identifying interacting proteins, the interaction between E4orf4 and Nup 205 needed to be validated to determine whether the binding was specific and direct. An indirect interaction between Nup 205 and E4orf4, such as one achieved through an adaptor

protein or other cellular intermediates could have led to the detection of Nup 205 in mass spectrometry of E4orf4 immunoprecipitates. To partly address this issue, we have used a stringent lysis buffer of high salt concentration (250 mM NaCl), which would disrupt most ionic and RNA-bridging based non-specific interactions. Furthermore, through co-immunoprecipitation experiments, we further characterized the interaction between E4orf4 and Nup 205 by identifying regions on both proteins involved in this interaction. To further demonstrate that this is a direct interaction, future experiments will be needed to test whether these two proteins alone directly interact, using recombinant proteins in *in vitro* binding assay [85].

Besides Nup 205, we also identified Importinβ, a karyopherin that we believe is responsible for the targeted nuclear localization of E4orf4, as discussed below in Section 4 [39]. We also identified some other targets that have been previously reported to interact with E4orf4. One of them is ASF/SF2, as further discussed in 2.1., is an important host splicing factor that E4orf4 utilizes to regulate the virus late messenger splicing activity [4].

We believe that we have missed identifying some proteins due to the strong expression of Tubulin and Hsp 70 which both masked some potential targets such as PP2A, a known interacting protein of E4orf4. We believe that PP2A was masked by tubulin when separating on SDS-PAGE. Furthermore, among all 30 vertebrate nucleoporins, Nup 205 was the only one identified to interact with E4orf4 from our Mass Spectrometry, and it is likely that E4orf4 can interact with other proteins that make up the nuclear pore complex, since Nup 205 is localized mostly in the inner and central part of the nuclear pore complex. However, within the Nup 93-188-205 sub-complex to which Nup 205 belongs, we tested the potential interaction between E4orf4 and Nup 93, a pivotal member of this sub-complex, and unlike endogenous Nup 205, we did not observe Nup 93 co-immuno-precipitating with E4orf4, suggesting the specificity of this

interaction between Nup 205 and E4orf4 (author, unpublished data). Furthermore, by targeted silencing of Nup 205 using siRNA, the functions reported in this research as a result of the E4orf4-Nup 205 interaction should be specific to Nup 205. Finally, it is also our long term goal to delineate the pathway that could potentially involve multiple nucleoporins sequentially interacting with E4orf4 along its translocation from the cytoplasm to the nucleus.

2. The Nup 205-E4orf4 interaction in the context of Adenovirus infection.

Much of the existing knowledge of E4orf4 was obtained in the absence of other viral products and outside of a viral context. E4orf4 is best known for its ability in inducing p53-independent and apparently tumour specific cell killing, and most studies have focused on the pathways it explores from an anti-cancer perspective. However, the amount of E4orf4 required to induce toxicity within target cells, a level achieved by transient plasmid transfections or Ad-E4orf4 adenoviral expression vectors, is much higher than the usual level of E4orf4 expressed in cells following a wild-type adenovirus infection. In the context of viral replication, E4orf4 is known to regulate viral gene expression by regulating transcription and splicing of viral genes; nonetheless, most of this research was conducted in early studies, and the molecular mechanisms that E4orf4 utilizes to regulate gene expression and to enhance replication remain poorly understood. Therefore, in this study, we examined the interaction between E4orf4 and Nup 205 in a viral context to explore how this interaction is advantageous to the viral infection cycle.

2.1. E4orf4 interacts with Nup 205 to regulate adenovirus gene expression.

Effective gene regulation is essential for all viruses because it ensures the expression of specific products at a precise time when needed during the infectious cycle; such regulation is often achieved by exploiting the cellular pathways by viral proteins. Despite

the fact that the nucleopore complex is the sole gateway for macromolecules, including mRNAs and transcription factors, to traverse between the nucleus and cytoplasm, little is known about Nup 205 and its role in regulating viral gene expression. In this study, we reveal that both the viral E4orf4 protein and host nucleoporin Nup 205 are involved in this regulation. We concluded that E4orf4 is required for regulating adenovirus gene expression. Specifically, we found that infection of adenovirus lacking E4orf4 (E4orf4$^-$ virus) resulted in elevated protein expression levels of early proteins E1A and E4orf6, and reduced level of late Capsid proteins as compared to wild type virus. (Figure II-4.1.) Moreover, we identified the requirement of Nup 205, a nucleopore protein that interacts with E4orf4, to be a host factor required for the regulation of adenovirus gene expression. In particular, when replicating in cells lacking Nup 205, wild type adenovirus phenotypically copied the defects in viral gene expression of the E4orf4$^-$ adenovirus. (Figure II-4.2.) The similar effects obtained through the loss of either of the two interacting partners, E4orf4 and Nup 205, suggested that E4orf4 may exploit a cellular pathway involving Nup 205 to regulate adenovirus gene expression.

This result is consistent with the current knowledge of the function of these target viral proteins, E1A, E4orf6 and Capsids proteins. E1A is the first viral gene to be transcribed following an infection, and the resulting E1A protein is required for the transcriptional activation of all other adenovirus early genes, including all products coded by the E4 transcription unit, such as E4orf6 and E4orf4 itself [5, 15-17]; therefore, strict regulation of E1A expression and E1A induced transcription activation is required. Earlier study has revealed several feedback mechanisms involving E1A and E4orf4; E4orf4 formed a complex with PP2A to inhibit E1A mRNA production, and the same complex could also negatively regulate E1A induced transcriptional activation by down-regulating JunB transcription and AP-1 activity. [14, 26] Therefore, the excess expression of E1A resulting from E4orf4 depletion (Figure II-4.2.) could be partially or

fully explained by these previous studies where E1A mRNA level was down-regulated by E4orf4. [14, 26] The level of E1A protein served as a pivotal indicator of the adenovirus gene expression under the regulation of E4orf4, and the cascades of defects in the expression level of other adenovirus genes, such as elevated E4orf6 level, were also in agreement with the existing knowledge where E1A regulates the expression of all early viral genes. In addition, E4orf6 shares the same E4 transcription unit as E4orf4; besides being activated by E1A, the mRNA expression of the E4 transcription unit is also negatively regulated by E4orf4. Therefore, the elevated E4orf6 level could also be a result of the absence of E4orf4-initiated down-regulation. The third adenovirus product we tested were the Capsid proteins, representing the late adenovirus product, which are essential for the structure and packaging of the progeny viruses. Earlier studies have demonstrated that E4orf4 could enhance the production of late mRNAs, and it could also activate the splicing of late mRNA, the IIIa pre-mRNA form of L1 mRNA, by bringing in PP2A to dephosphorylate the repressive SF2/ASF protein and release it from the repressive element binding site (3RE) of IIIa pre-mRNA. [4, 66] The observed reduced expression of Capsid proteins following an infection with E4orf4$^-$ virus could be explained by the model proposed in these studies, where E4orf4 enhances the production and splicing of the late mRNA. Since the expression of late proteins depends on the production of early proteins, this reduction in expression could also be attributed to the result of a cascade of defects in expressing early proteins, and in fact, also the deregulation in many other steps ranging from mRNA production to translation, as discussed in detail below. Meanwhile, notably, for all three targets, these defects in gene expression resulting from the absence of E4orf4 regulation were phenotypically similar to the expression of wild type adenoviruses in cells with depleted Nup 205. Therefore, we hypothesize that these regulations involving E4orf4 were dependent upon Nup 205,

where E4orf4 exploits a cellular pathway involving Nup 205 to control the expression of viral genes.

Since these above defects in gene expression were observed at the level of protein production, questions remain whether this regulation involving Nup 205 and E4orf4 was at the transcriptional level (including Transcriptional Control, RNA processing, RNA transport and RNA stability), the translational level, or a combination of them, and why E4orf4 chose the pathway involving Nup 205 and what was the function of Nup 205?

E4orf4 is known to regulate adenoviral gene expression at the transcriptional level [4, 66]. Adenoviral genes are arranged in a set of early transcription units and one single late transcription unit, and the expression of adenovirus genes is also known to be controlled at the level of transcription [137]. In particular, by forming a functional complex with PP2A, E4orf4 has been shown to inhibit both the E1A mRNA production, and E1A induced transcriptional activation by down-regulating JunB transcription and AP-1 activity [14, 26]. Moreover, the same complex could also repress the expression of Adenovirus E2 transcript by destabilizing the interaction between the E2F transcription factor and viral DNA [62]. In section 4.1.2.2., we confirmed that Nup 205 was also required for Adenovirus gene regulation. The depletion of Nup 205 by siRNA resulted in elevated expression of E1A by nearly 2 folds in all time points in 7.5, 14 and 23 hours following infection; meanwhile, the reduction of late transcripts mRNAs was by more than 3 folds. The elevation in E1A mRNA and reduction in late transcript were phenotypically similar to the defects resulted from an infection of adenovirus lacking the expression E4orf4. Interestingly, not only were the total mRNA levels altered upon knocking down Nup 205, but also an increase in nuclear to cytoplasmic ratio of the distribution of these viral genes was observed, suggesting a role of Nup 205 in the export of mRNAs from the nucleus to the cytoplasm.

In fact, adenovirus is known to have adapted mechanisms to allow preferential expression of viral genes over cellular product by blocking the nucleus to cytoplasm transport of cellular mRNAs, which results in shut-off of the expression of many host genes [29-32]. Moreover, recent research has attributed Nup 205 to the proper nuclear import of two important host transcription factors, Smad1 and c-myc, where loss of Nup 205 by siRNA silencing resulted in reduced nuclear localization of Smad1 in *Drosophila* and c-myc in certain human lung carcinoma cell lines [88, 138]. Preliminary results in the human H1299 and HeLa cell lines suggest that Nup 205 plays a role in controlling the expression of both the viral and cellular products, at the transcriptional level (author, unpublished results). We are currently investigating the role of Nup 205 in the selective export of viral and cellular mRNAs.

The targeted silencing of Nup 205 expression using siRNA ensured the specificity of the requirement of Nup 205 by these pathways utilized by E4orf4. To ensure the specificity of this targeted knockdown of Nup 205, our future experiment would include rescue experiments, where we would test whether the effects induced by E4orf4 would still be affected after restoring Nup 205 levels by overexpression following silencing by siRNA.

2.2. Nup 205 enhances viral multiplication.

Viruses are known to hijack and manipulate the host machinery to effectively replicate and produce progeny viruses. Our research reveals that when replicating in cells with reduced levels of Nup 205, the multiplicity of the wild type adenovirus decreased by more than 6-fold, suggesting that Nup 205 is required for viral replication. Moreover, we also observed that Nup 205 is also required for efficient CPE following an adenoviral infection.

Replication ability is a measure of a complete viral life cycle, which involves multiple processes, including attachment, penetration, uncoating, transcription and translation of viral products, and assembly and release of progeny viruses. The precise mechanism by which Nup 205 exerts its effect on adenoviral replication remains to be investigated. Earlier studies have revealed that the cytosolic faced nucleoporins Nup 214 and Nup 358 are required for the docking of adenoviral capsids and the uncoating processes [116, 139]. Given the localization of Nup 205, which is in the inner and central region of the NPC, our future work will specifically examine its role in gene expression in viral replication.

It is also unclear whether the adenoviral replication is dependent upon E4orf4 or the interaction between E4orf4 and Nup 205. Conflicting results from published work were obtained as to whether or not E4orf4 is essential for adenoviral replication [37, 38]. We observed that the mutant adenovirus that does not express E4orf4 (E4orf4$^-$ virus) has the same replicative ability as the wild type virus, and this data is consistent with recent published work [37, 38]. Miron et al., have also suggested that the defect in replication exhibited by an E4orf4-mutant adenovirus, *dl359*, may have been due to interactions between E4orf4 mutant with structures in the nucleus, which interfered with the viral replication [37, 38]. Based on these studies, we believe E4orf4, though not essentially required, may still enhance the viral replication, possibly through stabilizing another factor that is required for viral replication, such as its host interacting partner Nup 205. We are currently investigating whether E4orf4 could enhance viral replication and gene expression by stabilizing Nup 205 and the NPC.

3. E4orf4 causes hypo-phosphorylation of Nup 205 by bringing PP2A-Bα to Nup 205 to form a tri-molecular complex.

Although E4orf4 itself has no enzymatic activity, it often exerts its function through the binding of Protein Phosphatase 2A (PP2A). Our research reveals that E4orf4 can form a tri-molecular complex with two of its host interacting partners, Nup 205 and PP2A-Bα. In addition to the full length Nup 205, we further observed that such tri-molecular complex can also be formed with all smaller truncations of Nup 205 that can still bind to E4orf4, suggesting this is likely an E4orf4-mediated complex formation (Figure II-3.1.). Finally, we further demonstrated that Nup 205 is hypo-phosphorylated in the presence of E4orf4, which may very likely be due to the formation of this tri-molecular complex.

In fact, this tri-molecular complex may represent a common mechanism by which E4orf4 carries out its function -- E4orf4 recruits target phosphoproteins into complexes with PP2A, resulting in changes of phosphorylation states of these host factors, such as the hypo-phosphorylation of SR splicing factors and the AP1 transcription factor [4, 61]. We believe that by bringing PP2A to Nup 205, PP2A causes hypo-phosphorylation of Nup 205.

The phosphorylation sites on Nup 205, and the natural phosphatases that dephosphorylate Nup 205, are currently not known. Although there is very limited information on Nup 205, using a Bioinformatics tools (PhosphoSitePlus® and *NetPhos 2.0)*, we observed that there are at least 13 very well conserved potential serine, threonine and tyrosine phosphorylation sites on Nup 205. Eleven of these sites are serine and threonine sites that are potential targets of some well-known mitotic kinases, such as CDK1, NIMA-like Kinase and Polo Like Kinase [93-95]. PP2A is one of the most important Serine/Threonine Phosphatases in the cell, having a wide range of targets, including many that are substrates of kinases such as CDK1, NIMA, and Polo-Like Kinase [140]. However, since we only observe the association between Nup 205 and

PP2A in the presence of E4orf4, we believe that PP2A may not be a natural phosphatase employed by Nup 205. It is our long term goal to map out and characterize these phosphorylation sites on Nup 205. Finally, our future experiments will use Okadaic Acid, an inhibitor of PP2A, to confirm the observed hypo-phosphorylation of Nup 205 in the presence of E4orf4 is indeed due to PP2A (Figure II-3.2.).

One important question remaining is why E4orf4 needs to regulate the phosphorylation states of Nup 205? The role of phosphorylation sites on Nup 205 has never been studied. However, recent studies have linked the phosphorylation of Nup 98, another inner and centrally localized nucleoporin, with the disassembly of Nuclear Pore Complex [78, 112]. During mitosis, many nucleoporins are phosphorylated and then sequentially dissociated from the NPC as part of the nuclear membrane disassembly process, which is an important step for cells to enter mitosis. In particular, during early mitosis, upon phosphorylation, Nup 98 is the first nucleoporin to dissociate from the Nuclear Pore Complex [112], and it is followed by the rapid departure of members of the Nup 188-93-205 sub-complex from the pore, although the mechanism of how this later sub-complex dissociates remains unclear [78, 85, 97-99]. In late mitosis, hyper-phosphorylated Nups are then rapidly dephosphorylated and the Nuclear Pore Complex reassembled. Finally, earlier studies have suggested that PP2A-B55α is required for cells to exit mitosis [140]. By bringing PP2A to Nup 205, E4orf4 can cause the hypo-phosphorylation of Nup 205 (Figure II-3.2.). Therefore, we speculate that the dissociation of Nup 205 is also a phosphorylation-dependent process, and by maintaining the dephosphorylated state through an interaction with PP2A and other phosphatases, it delays the disassembly of the nuclear pore complex.

Taken together, we believe that by maintaining Nup 205 in its dephosphorylated form, E4orf4 prevents the disassembly of the Nup 188-93-205 sub-complex from the Nuclear Pore Complex, which secures a nuclear-cytoplasmic trafficking pathway to

import viral DNA and export viral mRNAs. Considering the effect of Nup 205 on viral gene expression, as discussed in Section 2, we also speculate that Nup 205 is targeted by adenovirus to control the passages of cellular and viral mRNAs, and this mechanism may depend upon alternating the phosphorylation states of Nup 205, which likely falls into the regulation by E4orf4-PP2A-Nup 205 tri-molecular complex. We are currently investigating whether Nup 205 is phosphorylated and dissociated from the Nuclear Pore Complex during mitosis, and whether the presence of E4orf4 can delay and even prevent this process.

4. The Arginine Rich Motif is required for viral protein nuclear localization and interaction with Nup 205.

The Arginine Rich Motifs (ARMs) are present in many proteins and have been shown to bind RNA and mediate protein localization to the nucleus and nucleolus. Nuclear localized viral proteins, including E4orf4, commonly contain ARMs [39]. Our research reveals that the ARM of E4orf4 is required both for interaction with Nup 205 and for nuclear localization of E4orf4. Moreover, we show that Nup 205 can also interact with three other ARM containing viral proteins from two other different viruses, Chicken Anemia Virus Apoptin (CAV-Ap), and Human Immunodeficiency Virus (HIV) Tat and Rev; however, it does not bind to the conventional lysine based NLS containing viral protein, SV40-LT antigen. The result that HIV-Tat can interact with Nup 205 is consistent with an earlier study examining *in vitro* nuclear interactome of the HIV-1 Tat protein using GST-fusion HIV-Tat [141]. In fact, each viral ARM protein is also bound to the same region on Nup 205 that is on the N-terminal of the protein (Figure II-2.4b.). Point mutations of the ARM sequence on each of the three viral proteins resulted in loss of interaction with Nup 205 and loss of nuclear localization of the viral protein. Therefore,

we believe that Nup 205 may represent a common cellular target for viruses encoding ARM-containing proteins.

Questions remain on whether Nup 205 is essential for the nuclear localization of ARM- and conventional NLS-containing proteins. For cellular proteins, recent studies have demonstrated that the loss of Nup 205 by siRNA resulted in reduced nuclear localization of Smad1 in *Drosophila* and c-myc in certain human lung carcinoma cell lines [88, 138]. Interestingly, although both proteins have defect in nuclear localization in cells with reduced Nup 205, neither of them uses an ARM as their NLS; Smad1 has a conventional NLS which contains no arginine (LVKKLKKKKGAMEELE) [142], and the NLS in c-myc is not specific to arginine over lysine (M1: PAAKRVKLD and M2: RQRRNELKRSF; M1 being the major NLS) [143]. Meanwhile, for viral proteins, upon silencing Nup 205 by siRNAs, we only observed significant reduction of nuclear distribution for HIV-Rev, where neither the other three ARM-containing viral proteins, nor SV40-LT, the conventional NLS containing protein, showed any significant defect in nuclear cytoplasmic distribution (Figure II-2.6B). All of the above suggest that the requirement of Nup 205 for nuclear localization may not be dependent upon the cargo and its type of NLS. Another possibility is that the requirement of Nup 205 may be specific to the type of importins used to import the cargo. Both HIV-Rev and Tat have been shown to directly bind importin β without importin α; however, SV40-LT requires the binding of importin α [104, 144, 145]. Meanwhile, Smad1 uses importin 7/8 for its nuclear import [88]. Based on our Mass Spectrometry results, E4orf4 interacts with importin β, and together with an earlier study which shows that HIV-Rev and Tat compete with E4orf4-ARM for nuclear import [39], we believe that E4orf4 also requires only importin β for its nuclear import. Therefore, besides its potential role in the export of mRNAs, as discussed in Section 3, we believe that Nup 205 may also be required for the

import of selected nuclear proteins. We are in the process of identifying if there are common characteristics among these cargos.

Effective nuclear targeting is essential for the function of many viral proteins, and defects in these viral proteins may often negatively impact the downstream viral gene expression and virion production. For example, among the four viral ARM-containing proteins that interact with Nup 205, the nuclear localization is significantly reduced as a result of the loss of Nup 205. HIV-Rev is a shuttling protein that binds to unspliced and singly spliced viral mRNAs in the nucleus; Rev brings them to the cytoplasm, ensuring the export of HIV-genome and the efficient production of HIV structural proteins. Reduction in Rev nuclear localization can disrupt the timely export of viral mRNAs, causing defects in viral production and infectivity. [146-148]. Since many viruses, like HIV-Rev, extensively utilize ARM sequences, we believe targeting this pathway may represent a novel anti-viral strategy. Our future experiments will also examine the requirement of Nup 205 for HIV replication. This can be studied through the creation of stable cell lines expressing shRNAs targeting Nup 205 and assessing the ability of these cells to support HIV replication.

5. Conclusion.

Taken together, our research reveals novel molecular mechanisms involving the cellular nucleopore complex protein Nup 205 and the virus E4orf4 protein. E4orf4 utilizes Nup 205 to regulate the adenovirus gene expression and replication, and to localize into the cell nucleus (Figure III-1). Its involvement in the viral life cycle also makes Nup 205 an attractive target for future anti-viral therapy.

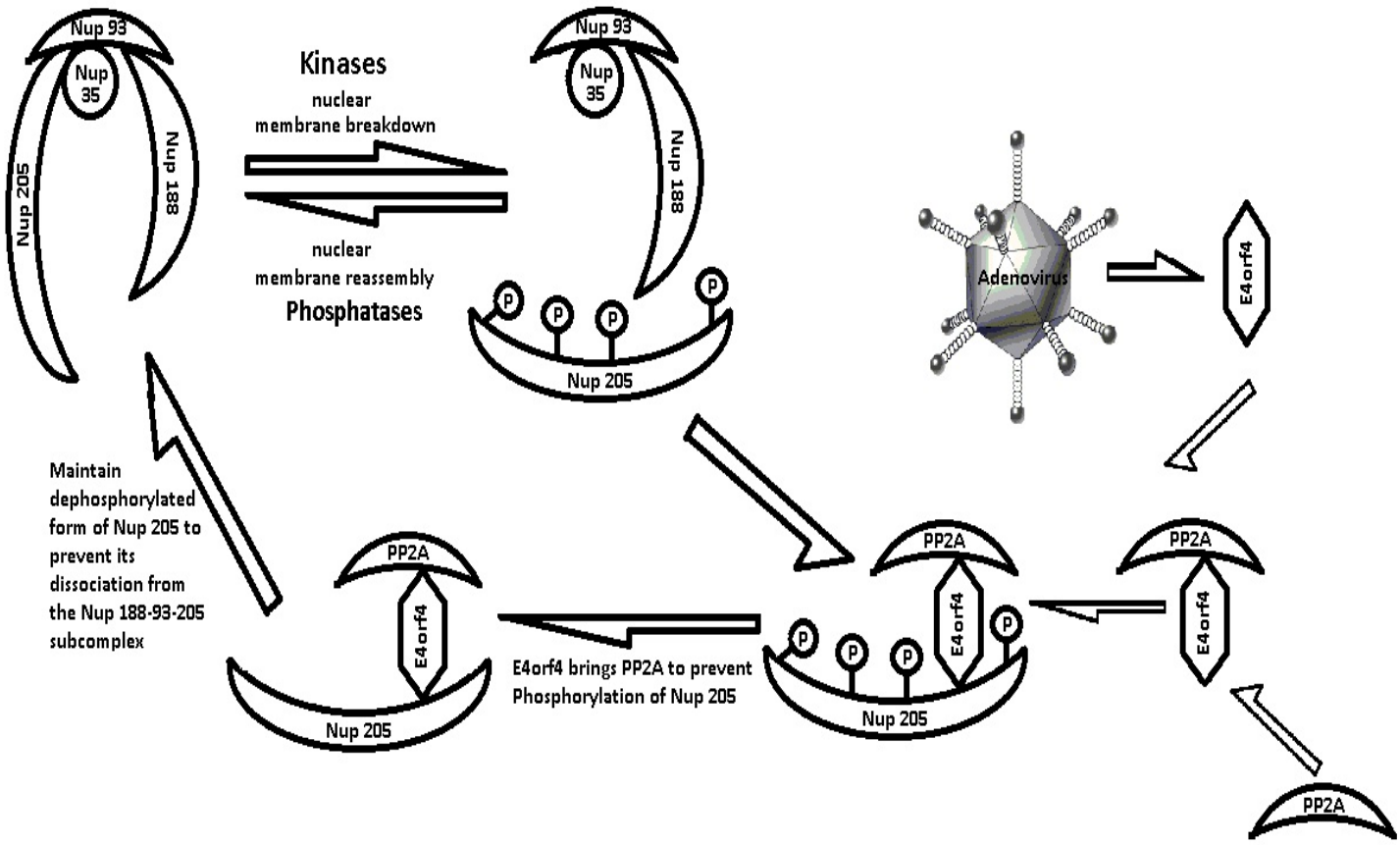

Figure III-1. Proposed mechanism of E4orf4 hypo-phosphorylating Nup 205 to prevent it from dissociating from the Nup 188-93-205 sub-complex.

Nup 205 forms a sub-complex with Nup 93 and Nup 188. During mitosis nuclear membrane breakdown, multiple kinases may phosphorylate Nup 205 to rapidly dissociate it from the Nup 188-93-205 sub-complex; during late mitosis, when the nuclear membrane reassembles, the hyper-phosphorylated Nup 205 will be dephosphorylated and reassembled to the Nup 188-93-205 sub-complex. With the presence of E4orf4, it will recruit PP2A to form a tri-molecular complex with Nup 205, which then maintains the hypo-phophosphorylated state of Nup 205, preventing it from disassembling from the Nuclear Pore Complex, delaying the global nuclear membrane breakdown. By maintaining a stable nuclear pore complex, adenovirus ensures the effective expression of its gene products by securing the efficient export of viral mRNAs to the cytoplasm for translation.

Materials and Methods

Cell culture

Two types of immortalized human cell lines were used in this research, H1299 (ATCC CRL-5803) and HeLa (ATCC CCL-2). Both cell lines were maintained in Dulbecco's Modification Eagle's Medium (DMEM, Multicell, Catalogue Number 319-005-CL), supplemented with 10% v/v Fetal Bovine Serum (HyClone), 100 U/mL of penicillin and 100 mg/mL of streptomycin (Wisent Bioproducts) at 37 °C under 5% CO_2 (95% air).

Plasmid Transfection

Cells were grown in 35mm (for immunofluorescence experiment) or 100mm (for immunoprecipitation experiments) dishes to about 70% confluence and transfected with the liposome reagent Lipofectamine™ 2000 (Invitrogen), according to the manufacturer's instructions. While maintaining the manufacturer recommended DNA/Lipofectamine ratio, for transfections in H1299 cells, only 1/3 of the recommended DNA and Lipofectamine™ 2000 amount was used, and for HeLa cells, only 1/2 of the recommended amount was used.

Small Interfering RNA (siRNA) and Transfection

Cells were grown in 24-well, 12-well, 35mm or 100mm dishes to about 50% confluence and transfected with the liposome reagent Lipofectamine™ 2000 (Invitrogen) to deliver siRNAs, according to the manufacturer's instructions. Downstream experiments were conducted after 42 hours after siRNA transfection. The sequences of siRNAs are tabulated in Table I-1.

Target Gene	Target Sequence	Commercial Code
Non Silencing	5'-AATTCTCCGAACGTGTCACGT-3'	Qiagen: 1022076
Nup 205 siRNA#1	5'-CTGCGTCAGTTTAAATTTCAA-3'	Qiagen: SI02665257
Nup 205 siRNA#2	5'-CTGACAGGAATTATAAGTAAA-3'	Qiagen: SI02665264

Table I-1. siRNA sequences.

Cell Lines

H1299 cells stably expressing the p3XFlag-myc-CMV-26-Nup 205 (p3XFlag-Nup 205 in short) construct were generated, and single clone was isolated. H1299 cells were transfected with p3XFlag-myc-CMV-26-Nup 205 construct, and it was selected under 1μg/μL of G418 for 14 days. Cultures were maintained at 0.4μg/μL of G418.

H1299 and HeLa cells with stable knock-down of Nup 205 were also generated using the MISSION® lentiviral (pLKO.1-puro) shRNA system (Sigma), following the manufacturer's instructions. Both Nup 205 knock-down and Non-Silencing control lines were generated at the same time. The cultures were kept under 0.2μg/μL of Puromycin selection. Due to the essential role of Nup 205, cells of more than 2 passages rarely maintained the Nup 205 knock-down effect. The detailed sequences are tabulated in Table I-2.

Target Gene	Target Sequence	Commercial Code
Non Silencing shRNA	5'-CCGGCAACAAGATGAAGAGCACCAACTCGAGTTGGTGCTCTTCATCTTGTTGTTTTT-3'	Sigma: SHC002
Nup 205 shRNA	5'-CCGGGCAACAATTCACTCTCGTCTTCTCCGAGAAGACGAGAGTGAATTGTTGCTTTTTG-3'	Sigma: NM_015135.2-953s21c1

Table I-2. shRNA sequences.

Viruses

Wild Type Ad5 (three notations, WT-Ad5, NOAH or H5pg4100), E4orf4-Minus (Orf4$^-$, E4orf4 null NOAH virus) and FLAG-tagged E4orf4 adenovirus (Ad-FLAG-E4orf4 or Ad-E4orf4) were developed by members of Drs. Thomas Dobner and Phil Brantons' laboratories, and their constructions have been previously described in [37, 132, 149]. LacZ adenovirus (Ad-LacZ) was previously described in [150]. The initial stocks of all four viruses were obtained from Dr. Phil Branton, and they were amplified in 293 cells, followed by purification by ultracentrifugation on a cesium chloride gradient, and titered using the $TCID_{50}$ method.

Infection

Cells had been cultured for at least 20 hours and at least with 70% confluence when they were infected with viruses. Old media was removed and cells were infected with viruses diluted in a minimum amount of (100µL for 24-well, 300µL for 12-well, 500µL for 35mm, and 3mL for 100mm plates) Infection Medium (0.2 mM $CaCl_2$, 0.2 mM $MgCl_2$, 1% heat inactivated serum in phosphate-buffered saline) for 90 minutes before its removal and addition of normal growth medium.

Viral Time Courses

For time course studies, cells were infected at a multiplicity of infection (MOI) of 5 or 35 FFU/cell depending on the experiment and harvested by scraping at different times post-infection (this included the initial 90 minutes for absorption). The cells were washed in phosphate-buffered saline and collected by centrifugation, and the pellets were immediately frozen until completion of the experiment. Pellets were then lysed in Buffer X (50 mM Tris [pH 8.5], 250 mM NaCl, 1mM EDTA, 1% NP40, Protease Inhibitor Mini

Tablet [Roche]) plus phosphatase inhibitors (4 mM NaF and 500 μM sodium vanadate) on ice for 30 minutes.

For Real-Time PCR experiment samples, the cells were not scraped at designated time points; rather, the media was removed, and the cells were washed twice with cold 1X PBS before 500μL (for 24-well) or 1mL (for 35mm) TRIzol reagent (Invitrogen) were added to the plates according to the manufacturer's protocol. Plates with TRIzol were immediately frozen until completion of the experiment.

Viral Replication and FFU Assay

To measure the replication ability of adenovirus in H1299 cells with or without reduced level of Nup 205, siRNA treated H1299 cells were infected with adenovirus at 5 MOI, and harvested at 42 hours post-infection (p.i.) by scraping. They were then lysed by three cycles of freeze-thawing, and the cell lysates were serially diluted in Infection Medium for infection of H1299 cells. The replication ability was measured by the virus yield, which was determined by quantitative E2A immunofluorescence staining (FFU assay) at 40 hours after infection. [132, 133]

To quantify the replication ability, the cells were fixed and permeabilized in ice-cold methanol at −20°C for 15 minutes, and blocked and further permeabilized in Tris-buffered saline-bovine serum albumin-glycine (TBS-BG) buffer for 1 hour. The cells were then incubated for 1 hour with the DBP primary antibody diluted in PBS and washed three times in PBS-0.1% Tween 20, followed by incubation with Alexa 588-conjugated goat-anti-mouse secondary antibodies (Invitrogen). Cells with DBP staining had been infected with adenovirus and were then counted as positive; the average of positive counts from 24 fields, 8 fields from each of the three independent experiments, were reported and tabulated.

The counts in other conditions were reported as percentages relative to the count from WT-Ad5 in Non-Silencing siRNA treated H1299 cells, which was arbitrarily set as 100%.

Western Blotting

Whole cell lysates were prepared by lysing cells in Lysis Buffer X (50 mM Tris [pH 8.5], 250 mM NaCl, 1mM EDTA, 1% NP40, Protease Inhibitor Mini Tablet [Roche]). Protein concentrations of lysates were measured using the Bradford protein assay (BioRad). Samples were mixed with Laemmli buffer and boiled for 5 minutes before loading. Equal amounts of protein (lysate or immunoprecipitation samples) were separated by SDS-polyacrylamide gel electrophoresis (SDS-PAGE) and transferred to 0.45 μm nitrocellulose membranes (BioRad). Membranes were incubated with primary antibodies followed by appropriate horse radish peroxidase-coupled secondary antibodies (anti-rabbit or anti-mouse, Jackson ImmunoResearch; TrueBlot® anti-mouse, eBioscience). Western Lightning Plus enhanced chemiluminescence substrate (Perkin Elmer) was used to visualize proteins on autoradiography film.

Microscopy

For nuclear localizations; Fluorescence microscopy. HeLa cells were cultured on glass coverslips in 6-well plates and achieved ~60% confluence at the time of transfection of GFP-fusion plasmids. Constructs were expressed for no more than 14 hours and washed 3 times each with cold PBS before fixation by immersing the coverslips in ice-cold methanol for 15 minutes (except for HIV-Rev constructs). For GFP-Rev and its mutants, the fixation was done by cold 3.2% Formaldehyde for 5 minutes at room temperature followed by permeablization with PBS-Triton. The coverslips were then washed again, counterstained with DAPI (4',6-diamidino-2-phenylindole), and mounted

on slides using DABCO mounting medium (Sigma). The cells were then viewed using a Zeiss Axiovision 3.1 microscope equipped with Axiocam HR (Zeiss, Thornwood, NY) digital camera. The channel used was Texas Red, DAPI and FITC.

For Cytopathic effect of viruses; light microscopy. Cell morphology was observed using a Zeiss Axiovert 25 microscope equipped with an LD A-PLAN 20/0.3 Ph1 objective. Images were recorded using a Zeiss Axiovision 3.1 microscope equipped with Axiocam HR (Zeiss, Thornwood, NY) digital camera.

A total of 15 measurements were taken for each sample, in each cell compartment, across at least three different experiments, although only one picture is presented.

Quantitative Real-Time PCR

To study the viral mRNA transcripts, samples were collected by adding TRIzol reagent (Invitrogen) after different time points. RNA was isolated from cells using TRIzol reagent (Invitrogen) according to the manufacturer's protocol. DNase treatment and cDNA synthesis were performed with the QuantiTect reverse transcription kit (Qiagen) using 1μg of RNA as a template according to the manufacturer's protocol.

Quantitative Real-time PCR (qPCR) was performed using a Realplex-2 Mastercycler (Eppendorf) and QuantiFast SYBR green master mix (Qiagen) supplemented with 1 μg of cDNA and 0.5 μM final concentration of primers per reaction. The PCR programme was as follows: 10 minutes at 95°C, followed by 40 cycles of 10 seconds at 95°C and 30 seconds at 59°C (universal for all primer set), then followed by and 15 seconds at 95°C, 15 seconds at 60°C, and after a slow increase to a final 15 seconds at 95°C.18S served as the internal control. All primer sequences are listed in Table I-3. Fold changes of viral transcripts were calculated using the delta-delta Ct method relative to the housekeeping gene 18S rRNA.

Gene	Forward/Reverse	Sequence
E1A	Forward	5'-GTGCCCCATTAAACCAGTTG-3'
E1A	Reverse	5'-GGCGTTTACAGCTCAAGTCC-3'
E1B (55K)	Forward	5'-GAGGGTAACTCCAGGGTGCG-3'
E1B (55K)	Reverse	5'-TTTCACTAGCATGAAGCAACCACA-3'
E2A (DBP)	Forward	5'-GAAATTACGGTGATGAACCCG-3'
E2A (DBP)	Reverse	5'-CAGCCTCCATGCCCTTCTCC-3'
E4orf6	Forward	5'-GCTGGTTTAGGATGGTGGTG-3'
E4orf6	Reverse	5'-CCCTCATAAACACGCTGGAC-3'
Hexon	Forward	5'-CGCTGGACATGACTTTTGAG-3'
Hexon	Reverse	5'-GAACGGTGTGCGCAGGTA-3'
L4-100K	Forward	5'-AAACTAATGATGGCCGCAGTG-3'
L4-100K	Reverse	5'-CGTCTGCCAGGTGTAGCATAG-3'
Major Late Promoter Tripartite Leader (TPL)	Forward	5'-CGCTGTCTGCGAGGGCCAG-3'
Major Late Promoter Tripartite Leader (TPL)	Reverse	5'-GGCGGCGGAGTACCGTTCG-3'
18S	Forward	5'-CGGCTACCACATCCAAGGAA-3'
18S	Reverse	5'-GCTGGAATTACCGCGGCT-3'

Table I-3. RT-PCR Primers.

Plasmid Construction

Nup 205 and truncations. Nup 205 cDNA was a gift from Dr. Douglass Forbes (University of California, San Diego). To generate Fluorophore tagged Nup 205, the Nup 205 sequence was excised from the untagged cDNA cloning vector by using PCR with the additional introduction of flanking KpnI (5') and BamHI (3') sites. The resulting product was then ligated into DsRed-C1 expression vector (Clonetech). To generate FLAG-tagged Nup 205, its sequence was again excised from the untagged cDNA cloning vector by using PCR with the additional introduction of flanking NotI (5') and BamHI (3') sites. The resulting product was further ligated into p3XFlag-myc-CMV-26 (Sigma), producing p3XFlag-myc-CMV-26-Nup 205-Full Length. Similarly, Nup 205 truncation mutants were generated by PCR from the full length template. All final products were confirmed by DNA sequencing. The forward and reverse oligonucleotides are listed in Table I-4.1..

E4orf4 and mutants. pcDNA3-HA-E4orf4 and all E4orf4 mutants were gifts of Dr. Phil Branton as previously described in [35]. The GFP-fusions of these mutants were generated by excising the inserted E4orf4 proteins with BamHI and EcoRI, and subcloning them into the pEGFP-C3 expression vector (Clonetech). For convenience, each GFP- E4orf4 construct was named after its HA-version template followed by a G3 to indicate the GFP-fusion; for example, HA-tagged Wild Type E4orf4 was named #309, and its GFP-fusion construct was therefore named as #309G3.

myc-PK and myc-PK-E4ARM. Pyruvate Kinase gene was fused with a myc-tag to study the intracellular trafficking. myc-PK was a gift of Dr. Gideon Dreyfuss as previously described in [122], and myc-PK-E4ARM, a myc-PK construct fused with the ARM motif of E4orf4, was a gift of Dr. Phil Branton as previously described in [39].

PP2A-Bα. pcDNA3-FLAG-PP2A-B55α and pcDNA3-HA-PP2A-B55α were gifts of Dr. Phil Branton as previously described in [35] and [52], respectively.

pcDNA4/V5-HisA-PP2A-B55α was generated based on pcDNA3-FLAG-PP2A-B55α. In short, the PP2A-B55α sequence was excised from the pcDNA3-FLAG-PP2A-B55α by using PCR with the additional introduction of flanking KpnI (5') and EcoRI (3') sites. The forward and reverse oligonucleotides were listed in Table I-4.1.. The resulting product was further ligated into pcDNA4/V5-His A (Invitrogen), producing pcDNA4/V5-His A-PP2A-B55α. The final product was confirmed by DNA sequencing.

Target	Primer Name	Remark	Sequence
Nup 205 Full Length (Red)	205Red Forward		5’-GAAGGTACCGCGACGCCTTTGGCGGTAAAT-3’
	205Red Reverse	The same as FL-Rev	5'-CGG GAT CCT CAG TTC CTT GAT ATC CT-3'
Nup 205 Full Length (Flag)	205FL Forward	#1	5’-GAA GCG GCC GCG GCG ACG CCT TTG G-3’
	205FL Reverse		5'-CGG GAT CCT CAG TTC CTT GAT ATC CT-3'
Nup 205 N1/2	N1/2 Forward	The same as #1	5'-GAA GCG GCC GCG GCG ACG CCT TTG G-3'
	N1/2 Reverse	#2	5’-CG GGATCC TCA TGT AGT ACT GAC AGG-3’
Nup 205 C1/2	C1/2 Forward		5'-GAA GCGGCCGC G AAC CTA CAA GAT CCA G-3'
	C1/2 Reverse		5'-CGG GAT CCT CAG TTC CTT GAT ATC CT-3'
Nup 205 A1/4	A1/4 Forward	The same as #1	5'-GAA GCG GCC GCG GCG ACG CCT TTG G-3'
	A1/4 Reverse		5'-CG GGATCC TCA TCG AGC ATC TTC ATC-3'
Nup 205 B1/4	B1/4 Forward		5'-GAA GCGGCCGC G ATG ATT CAC ATG AG-3'
	B1/4 Reverse	The same as #2	5’-CG GGATCC TCA TGT AGT ACT GAC AGG-3’
Nup 205 C1/8	C1/8 Forward	The same as #1	5’-GAA GCG GCC GCG GCG ACG CCT TTG G-3’
	C1/8 Reverse		5'-CG GGATCC TCA CTC AAT ACC AAT AGC-3'
Nup 205 D1/8	D1/8 Forward		5'-GAA GCGGCCGC G GTT GAA CTA AAT G-3'
	D1/8 Reverse	The same as #2	5’-CG GGATCC TCA TGT AGT ACT GAC AGG-3’

Table I-4.1. Nup 205 and PP2A-Bα Cloning Primers.

CAV-Apoptin. Both GFP and p3XFlag-tagged Apoptins were generated by Dr. Jose Teodoro as previously described in [41]. The pcDNA3-HA-Apoptin was generated by excising the Apoptin sequence with EcoRI and XbaI and subcloning into pcDNA3-HA-Nt vector (generated in Dr. Phil Branton lab). There are natural variations of Apoptin, and for the 118th amino acid of Apoptin, both Cys and Arg forms exist, i.e. both RIRL and CIRL forms of Apoptin exist. In this research, all of HA, p3XFlag- and GFP-tagged Apoptins used were exclusively in the RIRL form. They were generated from CIRL backbones by site directed mutagenesis PCRs (Around the World PCRs, QuikChange®, Stratagene), following manufacturer's instructions. All final products were confirmed by DNA sequencing. The forward and reverse oligonucleotides were listed in Table I-4.2..

HIV-Rev. GFP-Rev was a gift from Dr. Maria Zapp (University of Massachusetts, Medical School, Worcester). pcDNA3-HA-Nt tagged HIV-Rev was generated by excising target genes by PCR with the additional introduction of flanking EcoRI (5') and XbaI (3') sites. The forward and reverse oligonucleotides were listed in Table I-4.3.. The resulting product was further ligated into pcDNA3-HA-Nt (Dr. Phil Branton), producing pcDNA3-HA-Rev. The final product was confirmed by DNA sequencing.

HIV-Tat. pcDNA3-Tat-HA was purchased from Addgene (P#29), which was generated by Dr. Matija Peterlin [151]. pEGFP-C1-tagged HIV-Tat was generated by excising HIV-Tat sequence by PCR with the additional introduction of flanking BamHI (5') and EcoRI (3') sites. The forward and reverse oligonucleotides were listed in Table I-4.3.. The resulting product was further ligated into pEGFP-C1 (Clonetech), producing pEGFP-C1-Tat. The final product was confirmed by DNA sequencing.

SV40-LargeT-antigen. pcDNA3-HA-SV40-LT was generated by Dr. Jose Teodoro and Thomas Kucharski. pEGFP-C1-tagged SV40-LT was generated by excising target genes by PCR with the additional introduction of flanking EcoRI (5') and BamHI (3')

sites. The forward and reverse oligonucleotides were listed in Table I-4.3.. The resulting product was further ligated into pEGFP-C1 (Clonetech), producing pEGFP-C1-SV40-LT. The final product was confirmed by DNA sequencing.

Target	Primer Name	Remark	Sequence
Generate Apoptin RIRL	ApRIRL Forward	HA, Flag and GFP all used this same set of primers.	5'-C TACTCCCAGC GCA CCC GCA A CC GCA GCA GC G GCT ATA GCACTGTAAT CTA G AG G-3'
	ApRIRL Reverse		5’-CCT CTA GAT TAC AGT GCT ATA GCC GCT GCT GCG GTT GCG GGT GCG CTG GGA GTA G-3’

Table I-4.2. Mutagenesis Primers for Apoptin.

Target	Primer Name	Remark	Sequence
HA-Rev	HA3Rev Forward	pCDNA3-HA-Nt	5’-GAA GAA TTC A GCA GGA AGA AGC GGA GAC-3’
	HA3Rev Reverse		5'-GCC TCT AGA CTA CTC TTT AGT TCC TGA CTC-3'
GFP-Tat	G1Tat Forward	pEGFP-C1	5’-GAC GGA TCC A GAG CCA GTA GAT CCT AGA C -3’
	G1Tat Reverse		5'-GA GAA TTC CTA TTC CTT CGG GCC TGT C-3'
SV40-LT	G1SV Forward	pEGFP-C1	5’-GCC GAATTC A GAT AAA G TT TTA AAC AG A GAGG-3’
	G1SV Reverse		5'-GAA GGATCC TTA TGT TTC AGG TTC AGG GGG-3'

Table I-4.3. Cloning Primers for Rev, Tat and SV40-LT.

Arginine Rich Motif (ARM) Mutants. The ARM sequences on Rev, Tat and Apoptin were mutated into Alanine by site directed mutagenesis using PCR (Around the World PCRs, QuikChange®, Stratagene), following manufacturer's instructions. Both pCDNA3-HA-Nt and GFP-tagged ARM mutants were generated. The forward and reverse oligonucleotides were listed in Table I-4.4.. The final products were confirmed by DNA sequencing. The ARM mutant of E4orf4, #345, was a gift from Dr. Phil Branton as previously described in [35], and the generation of the corresponding GFP-tagged construct was described in E4orf4 and mutants section below.

.

Target	Primer Name	Remark	Sequence
CAV-Apoptin	ApARMFwd	Arg to Ala mutations in the ARM regions.	5'-C TACTCCCAGC GCA CCC GCA A CC GCA GCA GC G GCT ATA GCA CTGTAA T CTA G AG G-3'
	ApARMRev		5'-CCT CTA GAT TAC AGT GCT ATA GCC GCT GCT GCG GTT GCG GGT GCG CTG GGA GTA G-3'
HIV-Rev	RevARMFwd		5'-CC GAG GGG ACG GCT CAG GCG GCC GCG AAT GCA GCG GCC GCG TGG AGA GAG AGA CAG AGA CAG ATC C-3'
	RevARMRev		5'-G GAT CTG TCT CTG TCT CTC TCT CCA CGC GGC CGC TGC ATT CGC GGC CGC CTG AGC CGT CCC CTC GG-3'
HIV-Tat	TatARMFwd		5'-C TCC TAT GGC GCG AAG AAG GCG GCA CAG GCA GCA GCA GCT CCT CAG G -3'
	TatARMRev		5'-C CTG AGG AGC TGC TGC TGC CTG TGC CGC CTT CTT CGC GCC ATA GGA G-3'

Table I-4. 4. Site Directed Mutagenesis Primers for the ARM regions of Apoptin, Rev and Tat.

NES-mCherry and cNLS-mCherry. The NES from HIV-Rev and the NLS (termed in this research as canonical NLS, cNLS, to distinguish from the ARM sequences) of SV40-Large T antigen were individually fused to mCherry-C1 vector. The oligos were dissolved in distilled and deionized water (ddH_2O), and boiled for 20 minutes. They were then let slowly cool down, and followed by the excising of the NES and NLS sequences by restriction enzymatic digestions with EcoRI and BamHI. The resulting products were cloned into pmCherry-C1 (Clonetech) vector. The final products were confirmed by sequencing. They were further validated by fluorescence microscopy observations. The oligos used are listed in Table I-4.5..

Target	Oligo Name	Remark	Sequence
SV40LT-NLS-mCherry	cNLS-Fwd	pmCherry-C1	5’-GAA GAA G AAT TC A CCT AAG AAG AAG AGG AAG GTT GGA TCC TTC TTC -3’
	cNLS-Rev		5'-GAA GAA GGA TCC AAC CTT CCT CTT CTT CTT AGG T GA ATT C TTC TTC -3'
Rev-NES-mCherry	NES-Fwd	pmCherry-C1	5’-GAA GAA G AAT TC A CTT CAG CTA CCA CCG CTT GAG AGA CTT ACA CTT GAT GGA TCC TTC TTC-3’
	NES-Rev		5'-GAA GAA GGA TCC ATC AAG TGT AAG TCT CTC AAG CGG TGG TAG CTG AAG T GA ATT C TTC TTC-3'

Table I-4. 5. Oligo nucleotides used to generate NES-mCherry and cNLS-mCherry constructs.

Antibodies

Common epitope tags. Commercially available antibodies were used to target the common epitopes in constructs, and these included Monoclonal mouse anti-HA antibody (Covance, HA.11, 16B12), Monoclonal mouse anti-Flag (Sigma, M2), Polyclonal rabbit anti-Flag (Sigma, F7425), and Monoclonal mouse anti-V5 (Sigma, V5-10).

Loading controls. Monoclonal mouse anti-Tubulin (Santa Cruz Biotechnology, B-7) targeting Tubulin was used as a loading control in all siRNA experiments.

Nup 205. Rabbit polyclonal Nup 205 antibody was a gift from Dr. Douglass Forbes (University of California, San Diego) previously described in [86]. To minimize the loss in transfer of this precious antibody, all endogenous Nup 205 blots were cut small, showing only regions between 100 kDa to 250 kDa.

PP2A-Bα. Monoclonal Anti-PP2A subunit B isoform PR55-α was a gift from Dr. Phil Branton (McGill University).

Adenoviral proteins. All antibodies against adenoviral proteins were obtained from Dr. Phil Branton (McGill University). These antibodies have been described in previous publications. E4orf6 rabbit polyclonal 1807 [152], E1A mouse monoclonal M73 [153], Ad5 capsid rabbit polyclonal L133 [154], and DBP (E2A) mouse monoclonal B6-8 [155].

Immunoprecipitation antibodies. For all immunoprecipitation experiments (except for the ones using primary antibody conjugated beads), Protein G agarose beads (Upstate) were added following incubations with primary antibodies. Unless otherwise specified in the result section (used Rabbit-anti-Flag followed by Protein G beads to pull down Flag-tagged Nup 205 in Nup 205-E4orf4-PP2A-Bα tri-molecular complex experiment), Flag affinity agarose beads (Sigma, M2) were used to pull down Flag-tagged proteins in all experiments.

Secondary antibodies. Following primary antibodies, appropriate horseradish peroxidase (HRP) conjugated secondary antibodies were used for detection in Western

blotting, and these included goat anti-mouse immunoglobulin G (IgG) and goat anti-rabbit IgG (Jackson ImmunoResearch Laboratories). For experiments where the size of the protein of interest was around 55 KDa, for example, PP2A-Bα, a special secondary antibody preferentially recognizing the non-reduced form of IgG, TrueBlot® anti-mouse (eBioscience), was used to avoid the heavy chains in Western blotting, following the manufacturer's instructions.

The dilutions of all antibodies used are tabulated in Table I-5.

Target	Species	Weight	Western Dilution	Western Diluted in	IP Dilution (µg Ab/µg Lysate)	Provider
FLAG	Mouse-Monoclonal	Epi-topes	1:1K	Skim Milk	1/2000	Sigma
FLAG	Rabbit-Polyclonal		1:1K		1/1000	Sigma
HA	Mouse-Monoclonal		1:3K		1/3000	Covance
V5	Mouse-Monoclonal		1:2K	TBS-T	1/2000	Invitrogen
FLAG-Agarose					20µL/2.5mg Lysate	Sigma
Protein G agarose					20µL/2.5mg Lysate	Upstate
Nup 205	Rabbit-Polyclonal	228KDa	1:0.5K	TBS-T		Dr. D. Forbes
PP2A-Bα	Mouse-Monoclonal	55KDa	1:1K	Skim Milk		Dr. P. Branton
Late Protein	Rabbit-Polyclonal	Whole Gel	1:2K	PBS-T		Dr. P. Branton
E1A (M73)	Mouse-Monoclonal	45KDa	1:0.5K			
E4orf6	Rabbit-Polyclonal	~34KDa	1:5K			
E4-E1B55K	Rabbit-Polyclonal	55KDa	1:20K			
DBP	Mouse-Monoclonal	72KDa	1:5K	5% BSA		
Mouse	Goat	Com-mon	1:10K	Skim Milk		Jackson
Rabbit			1:5K			
TrueBlot Mouse			1:1K			eBioscience

Table I-5. Antibodies and Dilutions.

Immunoprecipitation

H1299 cells were transfected with plasmids and incubated for 40 hours. Cells were harvested by scraping, washed in cold PBS and lysed on ice for 30 minutes in Buffer X (50 mM Tris [pH 8.5], 250 mM NaCl, 1mM EDTA, 1% NP40, Protease Inhibitor Mini Tablet [Roche]). The lysates were clarified at 13000 × g for 10 minutes, and the protein concentration of the supernatant was quantified by Bradford assay with Protein Assay Dye Reagent Concentrate (BioRad Laboratories). Equal protein amounts (usually 1.5 mg, unless otherwise specified) of lysates were subject to immunoprecipitation of the target protein with primary antibodies as specified in the result section, which included Monoclonal mouse anti-HA antibody (Covance, HA.11, 16B12), Polyclonal rabbit anti-Flag (Sigma, F7425), and Monoclonal mouse anti-V5 (Sigma, V5-10). They were followed by incubation with Protein G agarose beads (Upstate). Unless otherwise specified in the result section (used Rabbit-anti-Flag followed by Protein G beads to pull down Flag-tagged Nup 205 in Nup 205-E4orf4-PP2A-Bα tri-molecular complex experiment), Flag affinity agarose beads (Sigma, M2) were used to pull down Flag-tagged proteins in all experiments. Beads were washed in Buffer X, and the bound proteins were eluted by boiling for 5 minutes in 1X SDS sample buffer.

For all experiments requiring TrueBlot® anti-mouse (eBioscience) as the secondary antibody in Western blotting, fresh-made DTT was added to samples to a final concentration of 50mM DTT, before samples were boiled for elution and loading.

Two Dimensional Gel Electrophoresis

The protocol for 2-D gel electrophoresis used in our lab was established by Dr. Wissal El-Assad. It has been previously described by Karen Lefebvre in [156]. Briefly, the procedure was as follows.

First Dimension. H1299 cells were co-transfected with 3XFLAG-tagged Nup 205, together with either of Empty-HA vector, HA-E4orf4-WT, or HA-E4orf4-ARM-mutant, for 42 hours. They were then harvested by scraping, washed in cold PBS and lysed in Buffer X (50 mM Tris [pH 8.5], 250 mM NaCl, 1mM EDTA, 1% NP40, Protease Inhibitor Mini Tablet [Roche]) plus phosphatase inhibitors (4 mM NaF and 500 μM sodium vanadate) on ice for 30 minutes. The lysates were clarified at 13000 × g for 10 minutes, and the protein concentration of the supernatant was quantified by Bradford assay with Protein Assay Dye Reagent Concentrate (BioRad Laboratories). 2mg of the whole cell lysates were subject to enrichment/concentration of Flag-Nup 205 by immunoprecipitation with anti-Flag affinity agarose beads (Sigma, M2). The products were eluted using 90μL of Sample Urea Buffer (7M Urea, 2M Thiourea, 4% w/v CHAPS, 30mM Tris-Base). 80μL of the IP product was then combined with 4.5 μL of 1% immobilized pH gradient (IPG) buffer (GE Healthcare), 5.4 μL of DeStreak Reagent (GE Healthcare), and a variable volume of rehydration buffer (7M Urea, 2M Thiourea, 4% CHAPS, 0.002% Bromophenol blue), to bring the total volume for each IPG strip up to 450 μL. Samples were then loaded onto 7cm pH 3-11 non-linear Immobiline DryStrips (GE Healthcare, Immobiline DryStrip, #17-6003-73, Lot#: 10032316). Active rehydration and isoelectric focusing (IEF) were then performed using the Ettan IPGphor IEF system (GE Healthcare).

Second Dimension. Immediately following completion of the IEF protocol, the IPG strips were promptly removed from the strip holders and equilibrated them in two different equilibration buffers (100mM Tris, 6M Urea, 30% Glycerol, 2% SDS, 0.002% Bromophenol blue). First, each strip was equilibrated in 10 mL of Equilibration Buffer + 5 mg/mL DTT for 15 minutes. Next, the strips were equilibrated in Equilibration Buffer + 45 mg/mL iodoacetamide. Immediately following equilibration, the IPG strips were then

loaded into the wells of 6% SDS-PAGE gels, and sealed in place using a 1% agarose solution.

Standard SDS-PAGE and Western blotting procedure was followed hereafter.

Nuclear and Cytoplasmic extracts

Protein extracts. The following protocol, modified from [157], was used to isolate the protein content from both nuclear and cytoplasmic compartments. In short, cells were harvested by scraping, washed in cold PBS and lysed on ice for 15 minutes in Buffer A (10 mM HEPES [pH=8], 1.5 mM $MgCl_2$, 10 mM KCl, 5 mM DTT, 0.5% NP40, Protease Inhibitor Mini Tablet [Roche]). Upon centrifugation at 13000 × g for 10 minutes, the supernatant was collected as the cytoplasmic fraction. The pellet was washed twice with Buffer A and was then resuspended in Buffer C (20 mM HEPES [pH=8], 416.7 mM NaCl, 0.2 mM EDTA, 1mM DTT, 25% Glycerol, Protease Inhibitor Mini Tablet [Roche]) and kept on ice for 30 minutes. Cell debris was removed by centrifugation at 13000 × g for 10 minutes and the supernatant was collected as the nuclear fraction. Protein concentrations of nuclear and cytoplasmic extracts were determined by the Bio-Rad protein assay.

mRNA extracts. To isolate mRNAs from the nucleus and the cytoplasm, cells were harvested by scraping, washed in cold PBS and lysed on ice for 10 minutes in NP40 Buffer (10mM Hepes [pH=7.8], 10 mM KCl, 20% glycerol, 0,25% NP40, Protease Inhibitor Mini Tablet [Roche]). Upon centrifugation, the supernatant portion was added with TRIzol to form the cytoplasmic fraction. The pellet was washed twice with NP40 Buffer. Upon removal of supernatant after centrifugation, the pellet was lysed in TRIzol to form the nuclear fraction. The standard mRNA extraction protocol described above in *Reverse and Quantitative Real-Time PCR* was followed hereafter.

Mass Spectrometry

The products that co-immunoprecipitated with the infected Ad-E4orf4 were subject to Mass Spectrometry to identify the host factors that interact with E4orf4. This procedure was developed and carried out by Dr. Jose Teodoro, and the result was shown in Figure II-1. In short, H1299 cells were infected with either adenoviral vector expressing FLAG-tagged E4orf4 (Ad-FLAG-E4orf4) or control β-galactosidase (Ad-LacZ) at 35 M.O.I. for 24 hours. E4orf4 Interacting proteins were immunoprecipitated from cell extracts using a monoclonal FLAG antibody. The products from both conditions were purified by SDS-PAGE side-by-side. The gel was stained with a protein-binding dye, silver nitrate, and two lanes were compared to determine bands specific to Ad-E4orf4. The resulting bands were excised and digested in gel, and they were identified by Mass Spectrometry and listed in Table II-1. Specific protocol for the purification and analysis of phophopeptides by mass spectrometry, described in detail in [158-160], was developed by Dr. David Thomas (McGill University), following which, the phosphorylation sites on Nup 205 can be identified, as proposed in the future experiments in the Results and Discussion sections.

Size-Exclusion Chromatography/Gel Filtration

Gel Filtration protocol used in our lab was established by Dr. Jose Teodoro and described previously in [42]. H1299 cells were infected with either Ad-LacZ or Ad-E4orf4 for 24 hours. They were then washed in PBS, harvested by scraping and lysed in Lysis Buffer A (20 mM Tris at pH 7.5, 100 mM NaCl, 20 mM β-glycerophosphate, 0.2% NP-40, 10% glycerol, 0.5 mM DTT, Protease Inhibitor Mini Tablet [Roche]) on ice for 30 minutes. Lysates were clarified by centrifuging at 100000 × g for 1 hour. The protein concentration of the lysate supernatant was quantified by Bradford assay with Protein Assay Dye Reagent Concentrate (BioRad Laboratories). 550 μg of total protein

was injected into a Pharmacia FPLC apparatus and separated on a Superose 6 10/30 (Pharmacia) column. About 30 fractions (500 μL each) were collected and precipitated with anhydrous Ethanol at -20°C overnight. Precipitates were then centrifuged at 13000 × g for 30 minutes, washed with 75% Ethanol at -20°C and dried. They were resuspended in 1× SDS Laemmli buffer, and boiled for 5 minutes prior to loading. Proteins of known high molecular weight were used as markers for the size of the fractions, and they were Thyroglobulin of 669 kDa [161], Ferritin of 440 kDa [162], Catalase of 232 kDa [163], and BSA of 66 kDa [164].

Growth Curve

The growth curves of both Non-Silencing Control and Nup 205 siRNA treated H1299 cells were generated based on the following protocol modified from [165]. Given the fast growth of H1299 cells and the short period which the effect of siRNA could sustain, only the first four days following siRNA lipofection were examined. Briefly, 4×10^3 H1299 cells were seeded in each well of a 12-well plate, so that each well would have 9×10^3 H1299 cells 24 hours later at the time of siRNA lipofection. These cells were then treated with either type of the two siRNAs, Non-Silencing Control or Nup 205 siRNA#2, and the counting started by setting the transfection time as Day 0. Every 24 hours, samples were collected by trypsinization with 500μL of Trypsin-EDTA (Wisent, Catalogue Number 325-041-CL), followed by recovering with 1000μL of DMEM, and pelleted by centrifugation at 2500 × g. They were then resuspended in 1000μL DMEM and thoroughly mixed by gentle vortexing. 200uL of the cell suspension was collected and mixed it with 40uL of Trypan Blue (Wisent, Catalogue Number 609-130-EL) to stain dead cells; it was then mixed by gentle vortexing, and proceeded to Hemocytometer Counting. The counts of both living and dead cells were recorded, and the total amount of

cells was extrapolated based on dilution factors. Each sample point was averaged from 24 different counts, 8 counts from each of three independent replicates.

Statistics

Unless otherwise specified, results were expressed as the means ± standard deviations from three independent experiments. The data were analyzed by one-tail or two-tails Student's t test. P values less than 0.01 were considered statistically significant, and values less than 10^{-10} were expressed as $p<10^{-10}$.

References

1. Fields, B.N., D.M. Knipe, and P.M. Howley, *Fields' virology*, 2007, Wolters Kluwer Health/Lippincott Williams & Wilkins,: Philadelphia.
2. Nemerow, G.R., et al., *Insights into adenovirus host cell interactions from structural studies.* Virology, 2009. **384**(2): p. 380-8.
3. Endter, C. and T. Dobner, *Cell transformation by human adenoviruses.* Curr Top Microbiol Immunol, 2004. **273**: p. 163-214.
4. Estmer Nilsson, C., et al., *The adenovirus E4-ORF4 splicing enhancer protein interacts with a subset of phosphorylated SR proteins.* EMBO J, 2001. **20**(4): p. 864-71.
5. Boulanger, P.A. and G.E. Blair, *Expression and interactions of human adenovirus oncoproteins.* Biochem J, 1991. **275 (Pt 2)**: p. 281-99.
6. Perricaudet, M., et al., *Structure of two spliced mRNAs from the transforming region of human subgroup C adenoviruses.* Nature, 1979. **281**(5733): p. 694-6.
7. Stephens, C. and E. Harlow, *Differential splicing yields novel adenovirus 5 E1A mRNAs that encode 30 kd and 35 kd proteins.* EMBO J, 1987. **6**(7): p. 2027-35.
8. Ulfendahl, P.J., et al., *A novel adenovirus-2 E1A mRNA encoding a protein with transcription activation properties.* EMBO J, 1987. **6**(7): p. 2037-44.
9. van Ormondt, H., J. Maat, and R. Dijkema, *Comparison of nucleotide sequences of the early E1a regions for subgroups A, B and C of human adenoviruses.* Gene, 1980. **12**(1-2): p. 63-76.
10. van Ormondt, H., J. Maat, and C.P. van Beveren, *The nucleotide sequence of the transforming early region E1 of adenovirus type 5 DNA.* Gene, 1980. **11**(3-4): p. 299-309.
11. Berk, A.J., et al., *Pre-early adenovirus 5 gene product regulates synthesis of early viral messenger RNAs.* Cell, 1979. **17**(4): p. 935-44.
12. Jones, N. and T. Shenk, *An adenovirus type 5 early gene function regulates expression of other early viral genes.* Proc Natl Acad Sci U S A, 1979. **76**(8): p. 3665-9.
13. Gallimore, P.H. and A.S. Turnell, *Adenovirus E1A: remodelling the host cell, a life or death experience.* Oncogene, 2001. **20**(54): p. 7824-35.
14. Bondesson, M., et al., *Adenovirus E4 open reading frame 4 protein autoregulates E4 transcription by inhibiting E1A transactivation of the E4 promoter.* J Virol, 1996. **70**(6): p. 3844-51.
15. Whyte, P., et al., *Association between an oncogene and an anti-oncogene: the adenovirus E1A proteins bind to the retinoblastoma gene product.* Nature, 1988. **334**(6178): p. 124-9.

16. Bagchi, S., P. Raychaudhuri, and J.R. Nevins, *Adenovirus E1A proteins can dissociate heteromeric complexes involving the E2F transcription factor: a novel mechanism for E1A trans-activation.* Cell, 1990. **62**(4): p. 659-69.
17. Bandara, L.R. and N.B. La Thangue, *Adenovirus E1a prevents the retinoblastoma gene product from complexing with a cellular transcription factor.* Nature, 1991. **351**(6326): p. 494-7.
18. Tauber, B. and T. Dobner, *Molecular regulation and biological function of adenovirus early genes: the E4 ORFs.* Gene, 2001. **278**(1-2): p. 1-23.
19. Imperiale, M.J., G. Akusjnarvi, and K.N. Leppard, *Post-transcriptional control of adenovirus gene expression.* Curr Top Microbiol Immunol, 1995. **199 (Pt 2)**: p. 139-71.
20. Dobner, T. and J. Kzhyshkowska, *Nuclear export of adenovirus RNA.* Curr Top Microbiol Immunol, 2001. **259**: p. 25-54.
21. Leppard, K.N., *E4 gene function in adenovirus, adenovirus vector and adeno-associated virus infections.* J Gen Virol, 1997. **78 (Pt 9)**: p. 2131-8.
22. Weinberg, D.H. and G. Ketner, *Adenoviral early region 4 is required for efficient viral DNA replication and for late gene expression.* J Virol, 1986. **57**(3): p. 833-8.
23. Nevins, J.R., et al., *Regulation of the primary expression of the early adenovirus transcription units.* J Virol, 1979. **32**(3): p. 727-33.
24. Akusjarvi, G., *Proteins with transcription regulatory properties encoded by human adenoviruses.* Trends Microbiol, 1993. **1**(5): p. 163-70.
25. Whalen, S.G., et al., *Phosphorylation within the transactivation domain of adenovirus E1A protein by mitogen-activated protein kinase regulates expression of early region 4.* J Virol, 1997. **71**(5): p. 3545-53.
26. Kleinberger, T. and T. Shenk, *Adenovirus E4orf4 protein binds to protein phosphatase 2A, and the complex down regulates E1A-enhanced junB transcription.* J Virol, 1993. **67**(12): p. 7556-60.
27. Logan, J. and T. Shenk, *Adenovirus tripartite leader sequence enhances translation of mRNAs late after infection.* Proc Natl Acad Sci U S A, 1984. **81**(12): p. 3655-9.
28. Cuesta, R., Q. Xi, and R.J. Schneider, *Preferential translation of adenovirus mRNAs in infected cells.* Cold Spring Harb Symp Quant Biol, 2001. **66**: p. 259-67.
29. Babiss, L.E., H.S. Ginsberg, and J.E. Darnell, Jr., *Adenovirus E1B proteins are required for accumulation of late viral mRNA and for effects on cellular mRNA translation and transport.* Mol Cell Biol, 1985. **5**(10): p. 2552-8.
30. Halbert, D.N., J.R. Cutt, and T. Shenk, *Adenovirus early region 4 encodes functions required for efficient DNA replication, late gene expression, and host cell shutoff.* J Virol, 1985. **56**(1): p. 250-7.

31. Pilder, S., et al., *The adenovirus E1B-55K transforming polypeptide modulates transport or cytoplasmic stabilization of viral and host cell mRNAs.* Mol Cell Biol, 1986. **6**(2): p. 470-6.
32. Bridge, E. and G. Ketner, *Interaction of adenoviral E4 and E1b products in late gene expression.* Virology, 1990. **174**(2): p. 345-53.
33. Enders, J.F., *Cytopathology of virus infections: particular reference to tissue culture studies.* Annu Rev Microbiol, 1954. **8**: p. 473-502.
34. Shtrichman, R., et al., *Induction of apoptosis by adenovirus E4orf4 protein is specific to transformed cells and requires an interaction with protein phosphatase 2A.* Proc Natl Acad Sci U S A, 1999. **96**(18): p. 10080-5.
35. Marcellus, R.C., et al., *Induction of p53-independent apoptosis by the adenovirus E4orf4 protein requires binding to the Balpha subunit of protein phosphatase 2A.* J Virol, 2000. **74**(17): p. 7869-77.
36. Lavoie, J.N., et al., *E4orf4, a novel adenovirus death factor that induces p53-independent apoptosis by a pathway that is not inhibited by zVAD-fmk.* J Cell Biol, 1998. **140**(3): p. 637-45.
37. Miron, M.J., et al., *Localization and importance of the adenovirus E4orf4 protein during lytic infection.* J Virol, 2009. **83**(4): p. 1689-99.
38. O'Shea, C., et al., *Adenoviral proteins mimic nutrient/growth signals to activate the mTOR pathway for viral replication.* EMBO J, 2005. **24**(6): p. 1211-21.
39. Miron, M.J., et al., *Nuclear localization of the adenovirus E4orf4 protein is mediated through an arginine-rich motif and correlates with cell death.* Oncogene, 2004. **23**(45): p. 7458-68.
40. Gingras, M.C., et al., *Cytoplasmic death signal triggered by SRC-mediated phosphorylation of the adenovirus E4orf4 protein.* Mol Cell Biol, 2002. **22**(1): p. 41-56.
41. Heilman, D.W., J.G. Teodoro, and M.R. Green, *Apoptin nucleocytoplasmic shuttling is required for cell type-specific localization, apoptosis, and recruitment of the anaphase-promoting complex/cyclosome to PML bodies.* J Virol, 2006. **80**(15): p. 7535-45.
42. Teodoro, J.G., et al., *The viral protein Apoptin associates with the anaphase-promoting complex to induce G2/M arrest and apoptosis in the absence of p53.* Genes Dev, 2004. **18**(16): p. 1952-7.
43. Kuppuswamy, M., et al., *Multiple functional domains of Tat, the trans-activator of HIV-1, defined by mutational analysis.* Nucleic Acids Res, 1989. **17**(9): p. 3551-61.
44. Kubota, S., et al., *Functional similarity of HIV-I rev and HTLV-I rex proteins: identification of a new nucleolar-targeting signal in rev protein.* Biochem Biophys Res Commun, 1989. **162**(3): p. 963-70.

45. Malim, M.H., et al., *The HIV-1 rev trans-activator acts through a structured target sequence to activate nuclear export of unspliced viral mRNA.* Nature, 1989. **338**(6212): p. 254-7.
46. Marcellus, R.C., et al., *Adenovirus type 5 early region 4 is responsible for E1A-induced p53-independent apoptosis.* J Virol, 1996. **70**(9): p. 6207-15.
47. Shtrichman, R. and T. Kleinberger, *Adenovirus type 5 E4 open reading frame 4 protein induces apoptosis in transformed cells.* J Virol, 1998. **72**(4): p. 2975-82.
48. Kleinberger, T., *Induction of apoptosis by adenovirus E4orf4 protein.* Apoptosis, 2000. **5**(3): p. 211-5.
49. Roopchand, D.E., et al., *Toxicity of human adenovirus E4orf4 protein in Saccharomyces cerevisiae results from interactions with the Cdc55 regulatory B subunit of PP2A.* Oncogene, 2001. **20**(38): p. 5279-90.
50. Robert, A., et al., *Distinct cell death pathways triggered by the adenovirus early region 4 ORF 4 protein.* J Cell Biol, 2002. **158**(3): p. 519-28.
51. Brestovitsky, A., et al., *The adenovirus E4orf4 protein targets PP2A to the ACF chromatin-remodeling factor and induces cell death through regulation of SNF2h-containing complexes.* Nucleic Acids Res, 2011. **39**(15): p. 6414-27.
52. Zhang, Z., et al., *Genetic analysis of B55alpha/Cdc55 protein phosphatase 2A subunits: association with the adenovirus E4orf4 protein.* J Virol, 2011. **85**(1): p. 286-95.
53. Li, S., et al., *The adenovirus E4orf4 protein induces G2/M arrest and cell death by blocking protein phosphatase 2A activity regulated by the B55 subunit.* J Virol, 2009. **83**(17): p. 8340-52.
54. Li, S., et al., *The adenovirus E4orf4 protein induces growth arrest and mitotic catastrophe in H1299 human lung carcinoma cells.* Oncogene, 2009. **28**(3): p. 390-400.
55. Ben-Israel, H., et al., *Adenovirus E4orf4 protein downregulates MYC expression through interaction with the PP2A-B55 subunit.* J Virol, 2008. **82**(19): p. 9381-8.
56. Shtrichman, R., R. Sharf, and T. Kleinberger, *Adenovirus E4orf4 protein interacts with both Balpha and B' subunits of protein phosphatase 2A, but E4orf4-induced apoptosis is mediated only by the interaction with Balpha.* Oncogene, 2000. **19**(33): p. 3757-65.
57. Muller, U., T. Kleinberger, and T. Shenk, *Adenovirus E4orf4 protein reduces phosphorylation of c-Fos and E1A proteins while simultaneously reducing the level of AP-1.* J Virol, 1992. **66**(10): p. 5867-78.
58. Branton, P.E. and D.E. Roopchand, *The role of adenovirus E4orf4 protein in viral replication and cell killing.* Oncogene, 2001. **20**(54): p. 7855-65.

59. Kornitzer, D., R. Sharf, and T. Kleinberger, *Adenovirus E4orf4 protein induces PP2A-dependent growth arrest in Saccharomyces cerevisiae and interacts with the anaphase-promoting complex/cyclosome.* J Cell Biol, 2001. **154**(2): p. 331-44.
60. Mui, M.Z., et al., *Adenovirus protein E4orf4 induces premature APCCdc20 activation in Saccharomyces cerevisiae by a protein phosphatase 2A-dependent mechanism.* J Virol, 2010. **84**(9): p. 4798-809.
61. Muller, U., et al., *Induction of transcription factor AP-1 by adenovirus E1A protein and cAMP.* Genes Dev, 1989. **3**(12A): p. 1991-2002.
62. Mannervik, M., et al., *Adenovirus E4 open reading frame 4-induced dephosphorylation inhibits E1A activation of the E2 promoter and E2F-1-mediated transactivation independently of the retinoblastoma tumor suppressor protein.* Virology, 1999. **256**(2): p. 313-21.
63. Medghalchi, S., R. Padmanabhan, and G. Ketner, *Early region 4 modulates adenovirus DNA replication by two genetically separable mechanisms.* Virology, 1997. **236**(1): p. 8-17.
64. Bridge, E., et al., *Adenovirus early region 4 and viral DNA synthesis.* Virology, 1993. **193**(2): p. 794-801.
65. Kanopka, A., O. Muhlemann, and G. Akusjarvi, *Inhibition by SR proteins of splicing of a regulated adenovirus pre-mRNA.* Nature, 1996. **381**(6582): p. 535-8.
66. Kanopka, A., et al., *Regulation of adenovirus alternative RNA splicing by dephosphorylation of SR proteins.* Nature, 1998. **393**(6681): p. 185-7.
67. Lavoie, J.N., et al., *Adenovirus E4 open reading frame 4-induced apoptosis involves dysregulation of Src family kinases.* J Cell Biol, 2000. **150**(5): p. 1037-56.
68. Xu, Y., et al., *Structure of a protein phosphatase 2A holoenzyme: insights into B55-mediated Tau dephosphorylation.* Mol Cell, 2008. **31**(6): p. 873-85.
69. Hunter, T., *Protein kinases and phosphatases: the yin and yang of protein phosphorylation and signaling.* Cell, 1995. **80**(2): p. 225-36.
70. Virshup, D.M., *Protein phosphatase 2A: a panoply of enzymes.* Curr Opin Cell Biol, 2000. **12**(2): p. 180-5.
71. Janssens, V. and J. Goris, *Protein phosphatase 2A: a highly regulated family of serine/threonine phosphatases implicated in cell growth and signalling.* Biochem J, 2001. **353**(Pt 3): p. 417-39.
72. Lechward, K., et al., *Protein phosphatase 2A: variety of forms and diversity of functions.* Acta Biochim Pol, 2001. **48**(4): p. 921-33.
73. Zolnierowicz, S., et al., *Diversity in the regulatory B-subunits of protein phosphatase 2A: identification of a novel isoform highly expressed in brain.* Biochemistry, 1994. **33**(39): p. 11858-67.

74. Cohen, P., C.F. Holmes, and Y. Tsukitani, *Okadaic acid: a new probe for the study of cellular regulation.* Trends Biochem Sci, 1990. **15**(3): p. 98-102.
75. Morgan, D.O., *The cell cycle : principles of control*. Primers in biology2007, London; Sunderland, MA: Published by New Science Press in association with Oxford University Press; Distributed inside North America by Sinauer Associates, Publishers. xxvii, 297 p.
76. Boke, E. and I.M. Hagan, *Polo, greatwall, and protein phosphatase PP2A Jostle for pole position.* PLoS Genet, 2011. **7**(8): p. e1002213.
77. Doye, V., *Mitotic phosphorylation of nucleoporins: dismantling NPCs and beyond.* Dev Cell, 2011. **20**(3): p. 281-2.
78. Laurell, E., et al., *Phosphorylation of Nup98 by multiple kinases is crucial for NPC disassembly during mitotic entry.* Cell, 2011. **144**(4): p. 539-50.
79. Strambio-De-Castillia, C., M. Niepel, and M.P. Rout, *The nuclear pore complex: bridging nuclear transport and gene regulation.* Nat Rev Mol Cell Biol, 2010. **11**(7): p. 490-501.
80. Cronshaw, J.M., et al., *Proteomic analysis of the mammalian nuclear pore complex.* J Cell Biol, 2002. **158**(5): p. 915-27.
81. Alber, F., et al., *The molecular architecture of the nuclear pore complex.* Nature, 2007. **450**(7170): p. 695-701.
82. Alber, F., et al., *Determining the architectures of macromolecular assemblies.* Nature, 2007. **450**(7170): p. 683-94.
83. Walther, T.C., et al., *The conserved Nup107-160 complex is critical for nuclear pore complex assembly.* Cell, 2003. **113**(2): p. 195-206.
84. Grandi, P., et al., *Nup93, a vertebrate homologue of yeast Nic96p, forms a complex with a novel 205-kDa protein and is required for correct nuclear pore assembly.* Mol Biol Cell, 1997. **8**(10): p. 2017-38.
85. Hawryluk-Gara, L.A., E.K. Shibuya, and R.W. Wozniak, *Vertebrate Nup53 interacts with the nuclear lamina and is required for the assembly of a Nup93-containing complex.* Mol Biol Cell, 2005. **16**(5): p. 2382-94.
86. Miller, B.R., et al., *Identification of a new vertebrate nucleoporin, Nup188, with the use of a novel organelle trap assay.* Mol Biol Cell, 2000. **11**(10): p. 3381-96.
87. Fujitomo, T., et al., *Critical Function for Nuclear Envelope Protein TMEM209 in Human Pulmonary Carcinogenesis.* Cancer Res, 2012.
88. Chen, X. and L. Xu, *Specific nucleoporin requirement for Smad nuclear translocation.* Mol Cell Biol, 2010. **30**(16): p. 4022-34.
89. Akhtar, A. and S.M. Gasser, *The nuclear envelope and transcriptional control.* Nat Rev Genet, 2007. **8**(7): p. 507-17.
90. Kohler, A. and E. Hurt, *Gene regulation by nucleoporins and links to cancer.* Mol Cell, 2010. **38**(1): p. 6-15.

91. Tamura, K. and I. Hara-Nishimura, *The molecular architecture of the plant nuclear pore complex.* J Exp Bot, 2012.
92. Theerthagiri, G., et al., *The nucleoporin Nup188 controls passage of membrane proteins across the nuclear pore complex.* J Cell Biol, 2010. **189**(7): p. 1129-42.
93. Blom, N., S. Gammeltoft, and S. Brunak, *Sequence and structure-based prediction of eukaryotic protein phosphorylation sites.* J Mol Biol, 1999. **294**(5): p. 1351-62.
94. Hornbeck, P.V., et al., *PhosphoSite: A bioinformatics resource dedicated to physiological protein phosphorylation.* Proteomics, 2004. **4**(6): p. 1551-61.
95. Hornbeck, P.V., et al., *PhosphoSitePlus: a comprehensive resource for investigating the structure and function of experimentally determined post-translational modifications in man and mouse.* Nucleic Acids Res, 2012. **40**(Database issue): p. D261-70.
96. Blom, N., et al., *Prediction of post-translational glycosylation and phosphorylation of proteins from the amino acid sequence.* Proteomics, 2004. **4**(6): p. 1633-49.
97. Galy, V., I.W. Mattaj, and P. Askjaer, *Caenorhabditis elegans nucleoporins Nup93 and Nup205 determine the limit of nuclear pore complex size exclusion in vivo.* Mol Biol Cell, 2003. **14**(12): p. 5104-15.
98. Hachet, V., et al., *The nucleoporin Nup205/NPP-3 is lost near centrosomes at mitotic onset and can modulate the timing of this process in Caenorhabditis elegans embryos.* Mol Biol Cell, 2012. **23**(16): p. 3111-21.
99. Rodenas, E., et al., *Early embryonic requirement for nucleoporin Nup35/NPP-19 in nuclear assembly.* Dev Biol, 2009. **327**(2): p. 399-409.
100. Karlas, A., et al., *Genome-wide RNAi screen identifies human host factors crucial for influenza virus replication.* Nature, 2010. **463**(7282): p. 818-22.
101. Strom, A.C. and K. Weis, *Importin-beta-like nuclear transport receptors.* Genome Biol, 2001. **2**(6): p. REVIEWS3008.
102. Lange, A., et al., *Classical nuclear localization signals: definition, function, and interaction with importin alpha.* J Biol Chem, 2007. **282**(8): p. 5101-5.
103. Bayliss, R., et al., *GLFG and FxFG nucleoporins bind to overlapping sites on importin-beta.* J Biol Chem, 2002. **277**(52): p. 50597-606.
104. Truant, R. and B.R. Cullen, *The arginine-rich domains present in human immunodeficiency virus type 1 Tat and Rev function as direct importin beta-dependent nuclear localization signals.* Mol Cell Biol, 1999. **19**(2): p. 1210-7.
105. Pouton, C.W., et al., *Targeted delivery to the nucleus.* Adv Drug Deliv Rev, 2007. **59**(8): p. 698-717.

106. la Cour, T., et al., *Analysis and prediction of leucine-rich nuclear export signals.* Protein Eng Des Sel, 2004. **17**(6): p. 527-36.
107. Nakielny, S. and G. Dreyfuss, *Nuclear export of proteins and RNAs.* Curr Opin Cell Biol, 1997. **9**(3): p. 420-9.
108. Fischer, U., et al., *The HIV-1 Rev activation domain is a nuclear export signal that accesses an export pathway used by specific cellular RNAs.* Cell, 1995. **82**(3): p. 475-83.
109. Terry, L.J. and S.R. Wente, *Flexible gates: dynamic topologies and functions for FG nucleoporins in nucleocytoplasmic transport.* Eukaryot Cell, 2009. **8**(12): p. 1814-27.
110. Guttinger, S., E. Laurell, and U. Kutay, *Orchestrating nuclear envelope disassembly and reassembly during mitosis.* Nat Rev Mol Cell Biol, 2009. **10**(3): p. 178-91.
111. Lenart, P., et al., *Nuclear envelope breakdown in starfish oocytes proceeds by partial NPC disassembly followed by a rapidly spreading fenestration of nuclear membranes.* J Cell Biol, 2003. **160**(7): p. 1055-68.
112. Dultz, E. and J. Ellenberg, *Live imaging of single nuclear pores reveals unique assembly kinetics and mechanism in interphase.* J Cell Biol, 2010. **191**(1): p. 15-22.
113. Beaudouin, J., et al., *Nuclear envelope breakdown proceeds by microtubule-induced tearing of the lamina.* Cell, 2002. **108**(1): p. 83-96.
114. Dultz, E., et al., *Systematic kinetic analysis of mitotic dis- and reassembly of the nuclear pore in living cells.* J Cell Biol, 2008. **180**(5): p. 857-65.
115. Greber, U.F., et al., *The role of the nuclear pore complex in adenovirus DNA entry.* EMBO J, 1997. **16**(19): p. 5998-6007.
116. Harel, A. and D.J. Forbes, *Welcome to the nucleus: CAN I take your coat?* Nat Cell Biol, 2001. **3**(12): p. E267-9.
117. Greber, U.F. and A. Fassati, *Nuclear import of viral DNA genomes.* Traffic, 2003. **4**(3): p. 136-43.
118. Fontoura, B.M., P.A. Faria, and D.R. Nussenzveig, *Viral interactions with the nuclear transport machinery: discovering and disrupting pathways.* IUBMB Life, 2005. **57**(2): p. 65-72.
119. de Noronha, C.M., et al., *Dynamic disruptions in nuclear envelope architecture and integrity induced by HIV-1 Vpr.* Science, 2001. **294**(5544): p. 1105-8.
120. Burke, B. and J. Ellenberg, *Remodelling the walls of the nucleus.* Nat Rev Mol Cell Biol, 2002. **3**(7): p. 487-97.
121. Marcellus, R.C., et al., *The early region 4 orf4 protein of human adenovirus type 5 induces p53-independent cell death by apoptosis.* J Virol, 1998. **72**(9): p. 7144-53.

122. Siomi, H. and G. Dreyfuss, *A nuclear localization domain in the hnRNP A1 protein.* J Cell Biol, 1995. **129**(3): p. 551-60.
123. Bjellqvist, B., et al., *The focusing positions of polypeptides in immobilized pH gradients can be predicted from their amino acid sequences.* Electrophoresis, 1993. **14**(10): p. 1023-31.
124. Bjellqvist, B., et al., *Reference points for comparisons of two-dimensional maps of proteins from different human cell types defined in a pH scale where isoelectric points correlate with polypeptide compositions.* Electrophoresis, 1994. **15**(3-4): p. 529-39.
125. Wilkins, M.R., et al., *Protein identification and analysis tools in the ExPASy server.* Methods Mol Biol, 1999. **112**: p. 531-52.
126. Huang, W. and S.J. Flint, *The tripartite leader sequence of subgroup C adenovirus major late mRNAs can increase the efficiency of mRNA export.* J Virol, 1998. **72**(1): p. 225-35.
127. Zhang, Y., D. Feigenblum, and R.J. Schneider, *A late adenovirus factor induces eIF-4E dephosphorylation and inhibition of cell protein synthesis.* J Virol, 1994. **68**(11): p. 7040-50.
128. Konarska, M.M., et al., *Characterization of the branch site in lariat RNAs produced by splicing of mRNA precursors.* Nature, 1985. **313**(6003): p. 552-7.
129. Pereira, H.G., *The cytopathic effect of animal viruses.* Adv Virus Res, 1961. **8**: p. 245-85.
130. Armstrong, J.A. and H.G. Pereira, *Significance of cytopathic effects observed during the growth of adenovirus.* Exp Cell Res, 1960. **21**: p. 144-50.
131. Pereira, H.G., *A protein factor responsible for the early cytopathic effect of adenoviruses.* Virology, 1958. **6**(3): p. 601-11.
132. Groitl, P. and T. Dobner, *Construction of adenovirus type 5 early region 1 and 4 virus mutants.* Methods Mol Med, 2007. **130**: p. 29-39.
133. Philipson, L., *Adenovirus assay by the fluorescent cell-counting procedure.* Virology, 1961. **15**: p. 263-8.
134. Boer, J., J. Bonten-Surtel, and G. Grosveld, *Overexpression of the nucleoporin CAN/NUP214 induces growth arrest, nucleocytoplasmic transport defects, and apoptosis.* Mol Cell Biol, 1998. **18**(3): p. 1236-47.
135. Ikegami, K. and J.D. Lieb, *Nucleoporins and transcription: new connections, new questions.* PLoS Genet, 2010. **6**(2): p. e1000861.
136. Kasper, L.H., et al., *CREB binding protein interacts with nucleoporin-specific FG repeats that activate transcription and mediate NUP98-HOXA9 oncogenicity.* Mol Cell Biol, 1999. **19**(1): p. 764-76.
137. Fields, B.N., D.M. Knipe, and P.M. Howley, *Fields virology*. 3rd ed1995, New York: Lippincott-Raven Press.

138. Fujitomo, T., et al., *Critical function for nuclear envelope protein TMEM209 in human pulmonary carcinogenesis.* Cancer Res, 2012. **72**(16): p. 4110-8.
139. Trotman, L.C., et al., *Import of adenovirus DNA involves the nuclear pore complex receptor CAN/Nup214 and histone H1.* Nat Cell Biol, 2001. **3**(12): p. 1092-100.
140. Schmitz, M.H., et al., *Live-cell imaging RNAi screen identifies PP2A-B55alpha and importin-beta1 as key mitotic exit regulators in human cells.* Nat Cell Biol, 2010. **12**(9): p. 886-93.
141. Gautier, V.W., et al., *In vitro nuclear interactome of the HIV-1 Tat protein.* Retrovirology, 2009. **6**: p. 47.
142. Xiao, Z., et al., *Nucleocytoplasmic shuttling of Smad1 conferred by its nuclear localization and nuclear export signals.* J Biol Chem, 2001. **276**(42): p. 39404-10.
143. Dang, C.V. and W.M. Lee, *Identification of the human c-myc protein nuclear translocation signal.* Mol Cell Biol, 1988. **8**(10): p. 4048-54.
144. Henderson, B.R. and P. Percipalle, *Interactions between HIV Rev and nuclear import and export factors: the Rev nuclear localisation signal mediates specific binding to human importin-beta.* J Mol Biol, 1997. **274**(5): p. 693-707.
145. Fontes, M.R., T. Teh, and B. Kobe, *Structural basis of recognition of monopartite and bipartite nuclear localization sequences by mammalian importin-alpha.* J Mol Biol, 2000. **297**(5): p. 1183-94.
146. Strebel, K., *Virus-host interactions: role of HIV proteins Vif, Tat, and Rev.* AIDS, 2003. **17 Suppl 4**: p. S25-34.
147. Frankel, A.D. and J.A. Young, *HIV-1: fifteen proteins and an RNA.* Annu Rev Biochem, 1998. **67**: p. 1-25.
148. Pollard, V.W. and M.H. Malim, *The HIV-1 Rev protein.* Annu Rev Microbiol, 1998. **52**: p. 491-532.
149. Tollefson, A.E., et al., *Preparation and titration of CsCl-banded adenovirus stocks.* Methods Mol Med, 2007. **130**: p. 223-35.
150. Bacchetti, S. and F. Graham, *Inhibition of cell-proliferation by an adenovirus vector expressing the human wild type-p53 protein.* Int J Oncol, 1993. **3**(5): p. 781-8.
151. Cujec, T.P., et al., *The HIV transactivator TAT binds to the CDK-activating kinase and activates the phosphorylation of the carboxy-terminal domain of RNA polymerase II.* Genes Dev, 1997. **11**(20): p. 2645-57.
152. Boivin, D., et al., *Analysis of synthesis, stability, phosphorylation, and interacting polypeptides of the 34-kilodalton product of open reading frame 6 of the early region 4 protein of human adenovirus type 5.* J Virol, 1999. **73**(2): p. 1245-53.

153. Harlow, E., B.R. Franza, Jr., and C. Schley, *Monoclonal antibodies specific for adenovirus early region 1A proteins: extensive heterogeneity in early region 1A products.* J Virol, 1985. **55**(3): p. 533-46.
154. Kindsmuller, K., et al., *Intranuclear targeting and nuclear export of the adenovirus E1B-55K protein are regulated by SUMO1 conjugation.* Proc Natl Acad Sci U S A, 2007. **104**(16): p. 6684-9.
155. Reich, N.C., et al., *Monoclonal antibodies which recognize native and denatured forms of the adenovirus DNA-binding protein.* Virology, 1983. **128**(2): p. 480-4.
156. Lefebvre, K.J., *Identification of novel PTEN-regulated secreted factors*, in *McGill theses*2010, McGill University Library,: Montreal.
157. Dignam, J.D., R.M. Lebovitz, and R.G. Roeder, *Accurate transcription initiation by RNA polymerase II in a soluble extract from isolated mammalian nuclei.* Nucleic Acids Res, 1983. **11**(5): p. 1475-89.
158. Boersema, P.J., S. Mohammed, and A.J. Heck, *Phosphopeptide fragmentation and analysis by mass spectrometry.* J Mass Spectrom, 2009. **44**(6): p. 861-78.
159. Dunn, J.D., G.E. Reid, and M.L. Bruening, *Techniques for phosphopeptide enrichment prior to analysis by mass spectrometry.* Mass Spectrom Rev, 2010. **29**(1): p. 29-54.
160. Aryal, U.K. and A.R. Ross, *Enrichment and analysis of phosphopeptides under different experimental conditions using titanium dioxide affinity chromatography and mass spectrometry.* Rapid Commun Mass Spectrom, 2010. **24**(2): p. 219-31.
161. Spiro, M.J., *Subunit heterogeneity of thyroglobulin.* J Biol Chem, 1973. **248**(12): p. 4446-60.
162. Bryce, C.F. and R.R. Crichton, *The subunit structure of horse spleen apoferritin. I. The molecular weight of the subunit.* J Biol Chem, 1971. **246**(13): p. 4198-205.
163. Takeda, A., et al., *Effect of sodium dodecyl fulfate on the dissociation of bovine liver catalase.* J Biochem, 1975. **78**(5): p. 911-24.
164. Hirayama, K., et al., *Rapid confirmation and revision of the primary structure of bovine serum albumin by ESIMS and Frit-FAB LC/MS.* Biochem Biophys Res Commun, 1990. **173**(2): p. 639-46.
165. Mather, J.P. and P.E. Roberts, *Introduction to cell and tissue culture : theory and technique*. Introductory cell and molecular biology techniques1998, New York: Plenum Press. xv, 241 p.

Appendix I

Site	Kinase
T-3	p38MAPK
S-9	PKG
S-52	PKC
T-83	cdc2
S-98	CKII
S-145	PKC
S-152	PKC
T-157	PKA
S-163	CKI
S-163	GSK3
T-183	PKC
S-191	ATM
S-210	PKC
S-218	CKII
S-227	DNAPK
S-227	PKA
S-231	cdc2
S-239	p38MAPK
S-239	cdc2
S-263	DNAPK
S-282	CKII
S-287	CKII
T-288	CKII
T-302	PKC
T-309	PKC
S-317	ATM
S-341	ATM
S-341	PKA
T-353	CKII
T-353	CKI
S-379	CKII
Y-381	EGFR
T-472	p38MAPK
T-472	cdk5
S-478	cdc2
S-495	PKC
S-532	PKC
S-551	p38MAPK
S-551	cdc2
S-551	GSK3
S-561	PKA
T-590	PKG

Site	Kinase
T-609	CKII
S-611	PKC
S-637	cdc2
T-649	PKC
S-666	DNAPK
T-675	PKC
S-680	DNAPK
S-680	ATM
S-680	PKC
S-696	CKII
S-712	cdc2
T-713	cdc2
S-718	CKI
S-718	cdc2
S-742	PKA
T-749	PKA
T-749	PKG
S-804	PKA
S-813	cdc2
S-821	CKII
S-821	cdc2
T-832	PKC
Y-833	INSR
S-870	DNAPK
S-870	ATM
S-870	PKA
T-890	PKC
S-927	PKC
S-944	ATM
S-970	CKII
T-983	PKG
S-994	DNAPK
S-1016	PKA
T-1048	cdc2
S-1056	p38MAPK
Y-1064	SRC
S-1074	cdc2
S-1077	cdc2
T-1086	PKC
S-1087	RSK
S-1087	DNAPK
S-1087	ATM

Site	Kinase
S-1093	cdc2
S-1101	CKII
S-1101	cdc2
S-1114	cdc2
S-1121	PKA
S-1134	PKA
T-1136	DNAPK
Y-1152	INSR
S-1153	CKII
T-1176	PKC
S-1192	DNAPK
S-1192	ATM
T-1225	PKA
S-1260	cdc2
T-1261	PKC
S-1285	PKC
T-1341	PKC
T-1343	PKC
S-1347	DNAPK
S-1347	ATM
T-1352	PKC
S-1358	CKI
S-1377	CKII
S-1377	GSK3
S-1377	cdk5
S-1395	DNAPK
T-1410	PKC
S-1424	PKC
S-1424	PKA
S-1424	cdc2
T-1447	PKG
T-1453	CKII
S-1505	RSK
S-1505	PKC
S-1517	cdc2
S-1519	cdc2
Y-1521	EGFR
S-1528	CKII
S-1538	PKC
S-1538	cdc2
T-1541	p38MAPK
T-1552	PKC

Site	Kinase
S-1555	PKC
T-1561	PKC
T-1611	p38MAPK
T-1611	cdk5
T-1632	PKC
S-1633	PKC
S-1634	DNAPK
S-1634	PKC
S-1651	cdc2
S-1653	cdc2
S-1669	CKII
T-1677	PKC
T-1677	cdc2
S-1690	CKII
S-1700	CKII
S-1700	CKI
S-1725	PKC
S-1744	CKII
S-1744	CKI
S-1744	PKC
S-1772	cdc2
T-1774	cdc2
T-1783	p38MAPK
S-1785	DNAPK
S-1785	PKA
T-1799	DNAPK
S-1822	PKG
S-1828	PKC
S-1832	PKC
S-1836	RSK
S-1836	PKC
S-1836	PKA
S-1838	PKC
S-1867	PKG
S-1891	PKA
S-1920	DNAPK
S-1920	ATM
S-1920	cdc2
S-1923	CKI
T-1929	PKC
S-1956	DNAPK

Table VI-1. Predicted phosphorylation sites and kinases.

Nup 205 phosphorylation sites and associated specific kinases predicted using *NetPhosK 1.0* [96]. One site can fall into the consensuses of multiple kinases.

Site	Sequence
T-3	MA*T*PLAVNSA
T-328	KLPGLQA*T*VRLAWAL
S-434	MGNEPPI*S*LRRDLEH
Y-450	MLLIGEL*Y*KKNPFHL
S-575	HLRKDLP*S*ADSVQYR
S-578	KDLPSAD*S*VQYRHLP
Y-581	PSADSVQ*Y*RHLPSRG
S-1153	DMPVKPY*S*DGEGGIE
S-1165	GIEDENR*S*VSGFLHF
S-1167	EDENRSV*S*GFLHFDT
S-1505	ALLDRIV*S*VDKQQQW
T-1799	RDGPRQD*T*QAPVVPY
T-1868	AGVDKIS*T*AQKYVLA
S-1939	KSRRLQD*S*FASETNL
S-1942	RLQDSFA*S*ETNLDFR

Table VI-2. Mass Spectrometry confirmed Nup 205 Phosphorylation sites.

The above 13 phosphorylation sites have been confirmed using Mass Spectrometry (PhosphoSitePlus®, [95]). Nup 205 phosphorylation sites and associated specific kinases predicted using *NetPhosK 1.0* [96]. One site can fall into the consensuses of multiple kinases.